Molecular Mechanisms of $G\alpha_i$ Signaling Selectivity

by

Tyler Jacob Lefevre

A dissertation submitted in partial fulfillment
of the requirements for the degree of
Doctor of Philosophy
(Chemical Biology)
in the University of Michigan
2023

Doctoral Committee:

Professor Alan V. Smrcka, Chair
Associate Professor Amanda Garner
Professor Carole Parent
Associate Professor Gregory Tall

Tyler J. Lefevre

tlefevre@umich.edu

ORCID iD: 0000-0002-7665-3353

Dedication

I dedicate this dissertation to my family, friends, and mentors whose patience and support have made this work possible.

Acknowledgements

I offer my sincere gratitude to the many bright minds of the Smrcka laboratory, past and present. To our specialists Michael Burroughs and Saji Abraham, for their unwavering, steadfast support of the laboratory and its mission. To my early mentors, Isaac Fisher, Craig Nash, Naincy Chandan, Hoa Phan, Richard Ransom, Adrian Campbell, and Loren Brown, from whom I learned the power of knowledge, perspective, and perseverance. To my current colleagues, Wenhui Wei, Gissell Sanchez, Nathalie Momplaisir, Joseph Loomis, and Sai Pranathi Meda Venkata, from whom I learned the importance of enthusiasm, patience, and camaraderie. And most importantly, to my advisor Professor Alan Smrcka, from whom I learned the necessity of focus, discipline, and intention, among many other lessons. Dr. Smrcka has a scintillating passion for science and discovery that resonates across the laboratory and shines bright with the news of any progress. More importantly, he has offered steady guidance in the wake of many nebulous or discouraging results. Thank you, Alan, for pushing me to realize my scientific potential.

I would also like to thank the members of my dissertation committee, Professor Amanda Garner, Professor Carole Parent, Professor Greg Tall, and Professor Manoj Puthenveedu for their valuable insight and guidance through the years.

I must thank my influences along the way to graduate school. Mr. Joe Bruessow, who first showed me what a real scientist looked like through his tactical curiosity for the world and contagious enthusiasm for the sciences. Professor Tami Sivy, for introducing me to the world of biochemistry and her support through the entirety of my undergraduate degree.

Thanks to my friends and classmates in Ann Arbor, Anthony, Fabienne, Lara, Meredith, and Sydney, for the support and community we built through this challenging time in our lives. I wouldn't have wanted to do it with anyone else.

I thank my family and my lifelong friends for all of their continuous support from afar. Your immeasurable love, patience, and understanding have made this work possible and kept me grounded during challenging times.

Finally, thank you Alaina, the brightest light on the darkest days. I complete this work for you, and I am here because of you.

Table of Contents

List of Figures

Abstract

Nearly all of human physiology is under the control of G protein-coupled receptors (GPCRs), which transmit signals from extracellular stimuli to affect intracellular processes. The heterotrimeric G proteins that these receptors are coupled to transduce signals from the GPCR and pass it on to intracellular effector proteins, which have diverse functions. The α subunit of heterotrimeric G proteins acts as a molecular switch, binding different guanine nucleotides which control its functional state. Sixteen human Gα subunits form four distinct families: $G\alpha_s$, $G\alpha_{i/o}$, $G\alpha_{q/11}$, and $G\alpha_{12/13}$. Each of these families are highly similar in sequence and function, resulting in highly unique signaling patterns between families. While seemingly functionally redundant, members of these families differ in tissue distribution and cellular function. The $G\alpha_{i/o}$ family consists of $G\alpha_{i1-3}$, $G\alpha_o$, $G\alpha_{T1-3}$, and $G\alpha_z$. These subunits vary widely in tissue expression, but $G\alpha_{i1-3}$ are expressed relatively ubiquitously. They are nearly identical in their canonical function: $G\alpha_{i1}$, $G\alpha_{i2}$, and $G\alpha_{i3}$ equipotently inhibit the membrane enzyme adenylyl cyclase. They also have similar binding and hydrolysis rates of guanosine-5'-diphosphate (GDP) and guanosine-5'-triphosphate (GTP), respectively.

Without downstream signaling partners which display specificity for interaction with $G\alpha_i$ subtypes, investigators have turned to studies *in vivo* to parse their functional differences. These studies have revealed important, non-overlapping roles for $G\alpha_i$ subtypes in different tissues and systems, but have not revealed any molecular details of the interactions responsible for such effects. Some differences in $G\alpha_i$ subtype interactions with other proteins have been demonstrated at the molecular level, but the mechanism for this selectivity is not well understood. Recently, our

laboratory used proximity labeling proteomics to discover a novel effector of $G\alpha_i$: PDZ-RhoGEF (PRG), a guanine nucleotide exchange factor for the monomeric G protein Rho. Remarkably, this downstream effector is activated strongly by $G\alpha_{i1}$ and $G\alpha_{i3}$, but activation by $G\alpha_{i2}$ in cells is significantly weaker.

Here, I outline our investigation into the molecular basis for this stark difference in selectivity of PRG for $G\alpha_i$ subtypes using $G\alpha_{i1}$ and $G\alpha_{i2}$. Using cell-based functional assays and molecular dynamics simulations, we demonstrated that nucleotide-dependent activation of PRG by $G\alpha_{i1}$ is controlled by interactions at the interface of the two domains of Gα, the Ras-like domain (RLD) and the helical domain (HD). In particular, one amino acid in the Switch III loop of $G\alpha_{i1,}$ D229, makes an interaction with R144 in the helical domain, permitting an array of other interdomain interactions and stabilizing the Switch III loop. The corresponding residue of $G\alpha_{i1}$ D229 is $G\alpha_{i2}$ A230, which does not interact with the cognate arginine in the HD, and does not support these additional interdomain interactions. Substitution of the whole $G\alpha_{i1}$ HD into $G\alpha_{i2}$ also confers the ability to activate PRG in this manner. Finally, using unbiased proximity labeling in cells coupled to tandem mass spectrometry proteomics, we show that this mechanism of Switch III stabilization, which confers $G\alpha_i$ nucleotide-dependent interaction with and activation of PRG, also increases interaction of $G\alpha_i$ subtypes with other novel effector proteins.

These results describe a novel mechanism which may also extend to other Gα protein families, modulating their selectivity for effector proteins and determining their signaling. Elucidating such molecular processes is key to our understanding of the nature of G protein-effector interactions. This has clear implications for signaling downstream of all GPCRs, the most prevalent protein target for the treatment of human disease.

Chapter 1 - General Introduction

1.1 Cellular signaling

Cells communicate with their environment and with one another through vastly complex and calibrated signals. These signals can consist of chemical compounds, temperature changes, light, ionic charge, or physical force. In functional cellular communication, a signal must be detected, transduced, and responded to. Cells use these signals to grow, reproduce, adapt to their environment, or perform other specific functions to maintain the organism. Dysregulation or exploitation of the detection, transduction, or response to a signal can result in harmful effects for the organism. Such dysregulation and its consequences form the basis of human pathophysiology.

In humans, several classes of receptors serve to receive information on the outside of a cell. These cell surface receptors have evolved to receive specific signals or subsets of signals for transduction into the cell. Such receptors include ion channels, receptor tyrosine kinases (RTKs), and G protein-coupled receptors (GPCRs), among others. Upon signal reception, these receptors differ in how the signal is transduced into the cell, and this downstream signal transduction in turn determines the cell's response (Figure 1.1). Transduced signals can, for example, cause the release of intracellular ions, initiation of protein phosphorylation cascades, or generation of second messenger molecules to cause changes in cell structure, nutrient metabolism, or release of chemical signals to other cells, among many other functions.

Studying the nature of cell signal transduction continues to be a challenging but rewarding effort, for the progress made in understanding these pathways has enabled the hypothesis-driven development of therapeutic treatments for a variety of human diseases. An important target in

mammalian therapeutics is the GPCR: a key receptor in all cell types and biological systems. These receptors and their signaling will be discussed as they pertain to the work herein.

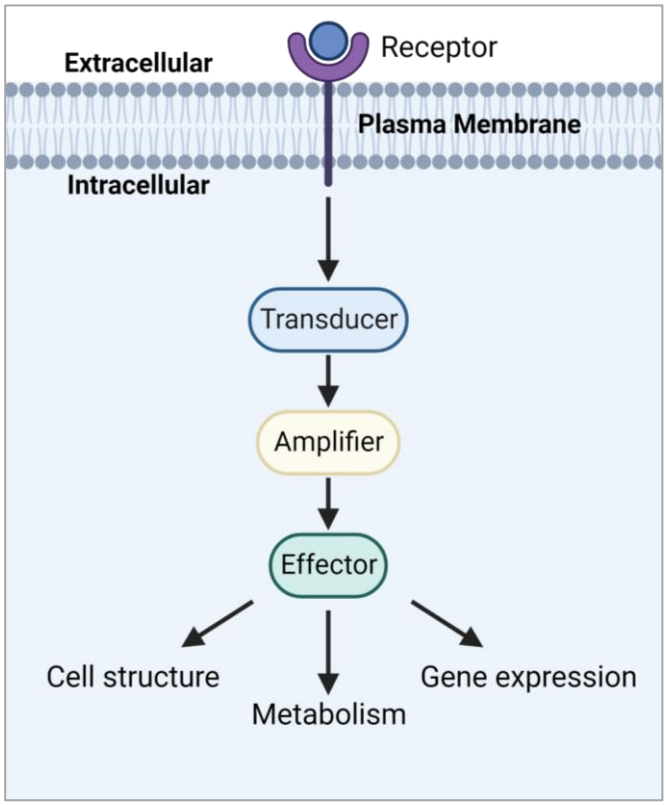

Figure 1.1: Principles of cellular signaling
An extracellular signal interacts with a receptor at the plasma membrane, beginning an intracellular signaling cascade which has various downstream cellular and physiological effects. Created with BioRender.

1.2 G protein-coupled receptors (GPCRs)

1.2.1 GPCRs – structure and function

G protein-coupled receptors, or GPCRs, are critically important signal receivers that are ubiquitous in mammalian biology. These receptors are phylogenetically classified into six families: Class A, the Rhodopsin-like receptors; Class B, secretin receptors and adhesion receptors; Class C, which consists of metabotropic glutamate receptors, γ-aminobutyric $acid_B$ ($GABA_B$ receptors), taste and odorant receptors, and calcium-sensing receptors; Class D, the fungal mating receptors; Class E, cAMP receptors; and Class F, Frizzled/Taste2 receptors. Classes A, B, C, and F are present in humans, constituting the largest protein superfamily and representing over 800 members [5]. GPCRs consist of a single polypeptide, including seven transmembrane α-helical segments connected by six interhelical loops. The N- and C-termini extend into the extracellular and intracellular space, respectively. The transmembrane helices pack together into a bundle in the phospholipid membrane, forming a defined central cavity, which is often the orthosteric site in Rhodopsin-like GPCRs, and accommodates specific ligands. Endogenous ligands can come in many chemical forms, including steroid hormones, neurotransmitters, peptides, lipids, nucleotides, amino acids, or sugars. Some GPCRs can even be activated by shear force or light.

The expression of the various families and types of receptors throughout the systems of the body crossed with the range of ligands and receptor-ligand selectivity begets a ubiquitous role of GPCRs in human biology. As such, GPCRs are a common node of influence on physiological function, whether causing disease or serving as a pharmacological target to treat disease. In fact, today, over 30% of approved drugs target GPCRs [5], while GPCRs and their protein signaling partners account for approximately 17% of protein targets for approved drugs [6].

Whether endogenous or exogenous, GPCR ligands can have differential effects on receptor function and signaling by stabilizing different receptor conformations. Agonists stabilize the active state, while inverse agonists stabilize the inactive state upon binding to the receptor. Antagonists do not stabilize a specific state; they bind to the orthosteric site and competitively occlude the binding of other ligands. Allosteric modulators, both positive and negative, bind to sites other than the receptor's orthosteric site. These molecules, primarily synthetic small molecules, allosterically enhance or inhibit the functional response to orthosteric ligands [7].

1.2.2 GPCR signal transduction

Once an agonist binds to a GPCR and stabilizes its active state, the receptor passes the signal into the cell via heterotrimeric G proteins. These signal transducers consist of two main components: the Gα GTPase and the obligate heterodimer Gβγ. Interaction with the active-state receptor facilitates the exchange of guanosine-5'-diphosphate (GDP) for guanosine-5'-triphosphate (GTP) in the Gα subunit, activating these G proteins and allowing them to dissociate from this ternary complex and begin signaling to other downstream effector proteins (Figure 1.2). Activation of GPCRs occurs on the order of milliseconds, while the G protein activation/deactivation cycle spans several seconds [8]. Downstream effector signaling including second messenger generation varies widely in time scale, but often takes place for up to minutes or hours [9].

G protein activation allows the recruitment of GPCR kinases (GRKs) to the receptor membrane locale. These kinases phosphorylate the intracellular c-terminal tail of the GPCR, creating an interaction site for β-arrestin proteins. β-arrestins are known as signal terminators that bind to the phosphorylated GPCR, blocking activation of additional heterotrimeric G proteins and acting as a scaffold for additional receptor internalization machinery. While the initial G protein-

mediated signal from activated GPCRs is blocked primarily by β-arrestins, receptors are also internalized into endosomes, which alters their signaling. The fate of receptors in these endosomes varies; some are recycled back to cell lipid membranes for additional signaling, some are sent to the proteosome for destruction, and some continue to signal away from major membranes as residents of endosomes [10]. Compartmentalized GPCR signaling away from the plasma membrane, including endosomal signaling, is an area of concentration in current GPCR research [11-17]. Signaling from these compartments encodes an additional layer of signaling specificity for GPCRs conferred by the differential availability of GPCR ligands and downstream effectors.

1.3 Heterotrimeric G proteins

1.3.1 Gβγ

The Gβ subunit consists of an N-terminal α-helix followed by a seven-bladed β-propeller structure, creating a toroid shape with a central hole. Each β-propeller is a WD40 repeat made of four anti-parallel β-sheets. The Gβ subunit forms a coiled-coil interaction with the α-helical Gγ subunit during biosynthesis, facilitating its folding and stability. Gγ is post-translationally modified with farnesyl or geranyl lipids, facilitating robust interaction and localization with lipid membranes in the cell. Gβγ therefore plays a large role in interacting with membrane-associated proteins or recruiting cytosolic proteins to the membrane for signaling and/or activation. There are multiple genes which encode for Gβ and Gγ, allowing for 48 different combinations of Gβγ subunits. Gβ has 5 isoforms ($G\beta_{1\text{-}5}$) which, except $G\beta_5$, are ~80% similar in sequence and function very similarly. $G\beta_5$ does not couple to a Gα or Gγ; instead it binds and regulates RGS7 function [18-20]. Twelve Gγ are available to pair with Gβ and are thought to provide diversity in function through unique lipidation patterns leading to differential localization [21-23]. The broad surfaces of Gβ provide abundant space for protein-protein interactions with a wide range of effectors across

signaling paradigms, including phospholipase Cs, GRK2/3, adenylyl cyclases, G protein-gated inwardly-rectifying potassium (GIRK) channels, voltage-gated calcium channels, phosphatidylinositol 3-kinase (PI3K), and SNARE complex proteins, among others [24, 25].

While the binding "signature" of each Gβγ effector utilizes a unique set of amino acid contacts across the Gβ surface, many of these effectors bind overlapping residues near a central "hotspot" over the central cavity. This combination of binding modes allows for significant inhibition of Gβγ signaling using peptides or small molecules that bind over this hotspot, which has been a useful method for studying Gβγ signaling. Gβγ effector-specific inhibition by blocking interaction with the binding residues on the Gβγ surface is also possible, but challenging due to the broad distribution of protein-protein interaction sites across the Gβ surface [26]. All G protein heterotrimers contain Gβγ subunits, however only signaling downstream of G_i-coupled receptors has been known to initiate significant Gβγ signaling. The main reason for this has not been definitively determined, however local scaffolding of Gi-coupled receptors with effectors or differences in Gα-Gβγ affinity have been suggested [27].

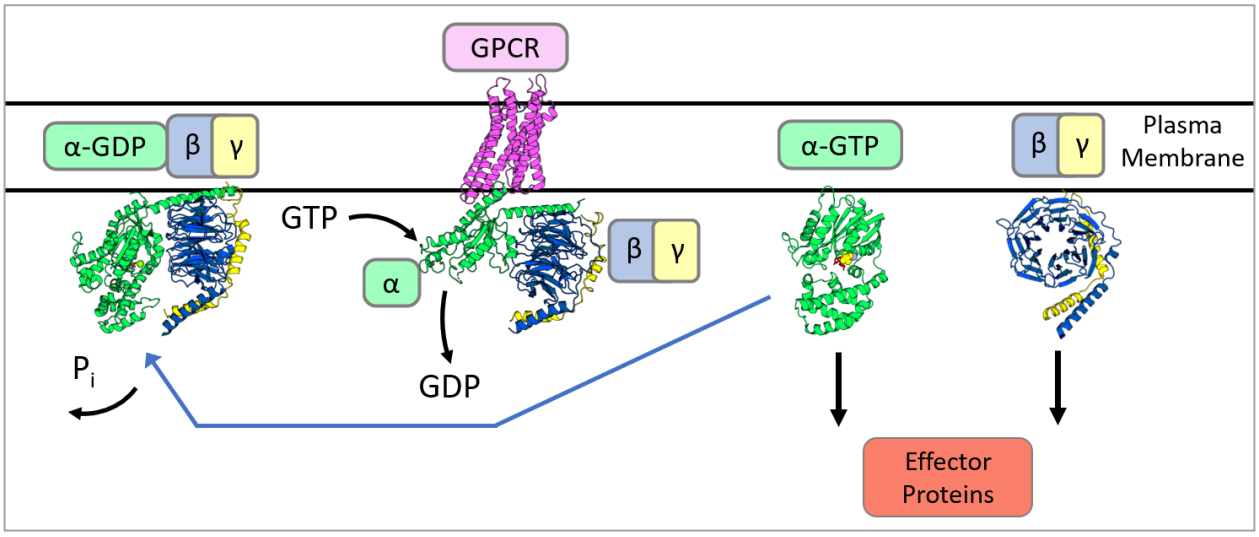

Figure 1.2: GPCR-G protein signal transduction cycle
An active-state GPCR interacts with a G protein heterotrimer, enhancing the rate of dissociation of GDP from the nucleotide-binding Gα subunit. GTP-bound, active Gα subunits and Gβγ dimers signal to downstream effectors until the intrinsic GTPase activity of the α subunit hydrolyzes the terminal phosphate of GTP, allowing the reunification of the G protein heterotrimer, which sits poised for another round of signaling.

1.3.2 Gα – Molecular switches

Gα acts as a molecular switch, with guanine nucleotide binding acting as an 'On' or 'Off' signal that is reflected in conformational state of the G protein. Gα-GDP is considered the inactive state which is capable of binding Gβγ to form the G protein heterotrimer. This heterotrimer interacts with GPCRs, which when activated act as a GEF, enhancing the dissociation of GDP from Gα. GTP binds to nucleotide-free Gα in its binding site rather than GDP due to its relatively high intracellular concentration [28]. Gα in turn changes conformation, dissociating from Gβγ and the GPCR and signaling to effector proteins. All Gα possess intrinsic GTPase activity, allowing them to eventually hydrolyze the γ-phosphate from GTP. The γ-phosphate dissociates freely and Gα returns to its inactive conformation as the newly produced GDP occupies the nucleotide binding site, concluding the G protein activation cycle (Figure 1.2). The secondary and tertiary structure of all heterotrimeric Gα proteins is highly conserved, which preserves the GDP-GTP cycling capabilities across all Gα families.

Gα subunits are organized into two domains: the GTPase domain, and the α-helical domain, or HD (Figure 1.5). The GTPase domain is highly conserved throughout all G proteins, including elongation factors and monomeric G proteins of the Ras superfamily. For this reason, this domain is commonly known as the Ras-like domain or RLD for its homology to the Ras small GTPase. The RLD consists of five α-helices and six β-sheets which fold to create a nucleotide binding pocket surrounded by an effector binding surface [29]. This binding surface includes three "Switch" regions, or short stretches of amino acids which change conformation upon GTP binding in the nucleotide binding pocket [30] (Figure 1.5).

The N-terminus of Gα folds into an α-helix which interacts with the outer edge of the Gβ torus while the heterotrimer is intact. Additionally, this N-terminal helix is post-translationally

modified by lipid transferases. Lipid modifications for Gα include myristate and palmitate, which are permanent or reversible covalent modifications, respectively. N-myristoylation is performed by N-myristoyl transferases (NMT), and involves the addition of a saturated, 14-carbon myristate to a glycine amide. Palmitoylation represents the attachment of a saturated, 16-carbon palmitate through a thioester bond to cysteine. All Gα subunits are palmitoylated except $G\alpha_T$, while only members of the $G\alpha_{i/o}$ family are myristoylated. Myristoylation is understood to confer transient association with lipid membranes in the cell, allowing partial membrane association. This, combined with Gα·GDP association with membrane-associated Gβγ, position $G\alpha_{i/o}$ subunits to be palmitoylated, further increasing membrane binding [31, 32].

Sixteen total genes code for Gα in humans which are spread between four different Gα families (Figure 1.3). The G_s family contains $G\alpha_s$ and $G\alpha_{olf}$, while the $G_{12/13}$ family contains $G\alpha_{12}$ and $G\alpha_{13}$. $G_{q/11}$ contains the second-most members: $G\alpha_q$, $G\alpha_{11}$, $G\alpha_{14}$, and $G\alpha_{15}$ (or $G\alpha_{16}$). $G\alpha_{i/o}$ is the largest family, consisting of $G\alpha_{i1}$, $G\alpha_{i2}$, $G\alpha_{i3}$, $G\alpha_{T1}$, $G\alpha_{T2}$, $G\alpha_{T3}$ (or $G\alpha_g$), $G\alpha_o$, and $G\alpha_z$. Each family has at least two subunits that are widely expressed across human tissues, so signaling from each G protein family is intact in each cell type. Expression of some subunits, for example $G\alpha_{T1}$ and $G\alpha_{T2}$ in retinal rods and cones respectively, are tightly restricted to one tissue, suggesting that they play a vital role in the function of the cell type. As these proteins are classified phylogenetically, each family is at least 60% identical in sequence (Figure 1.3), leading to significant overlap in function and protein-protein interactions among each family [1]. Despite this restricted expression of some subtypes, combinatorial expression of multiple Gα from the same family suggest some amount of non-overlapping function among Gα subunit families.

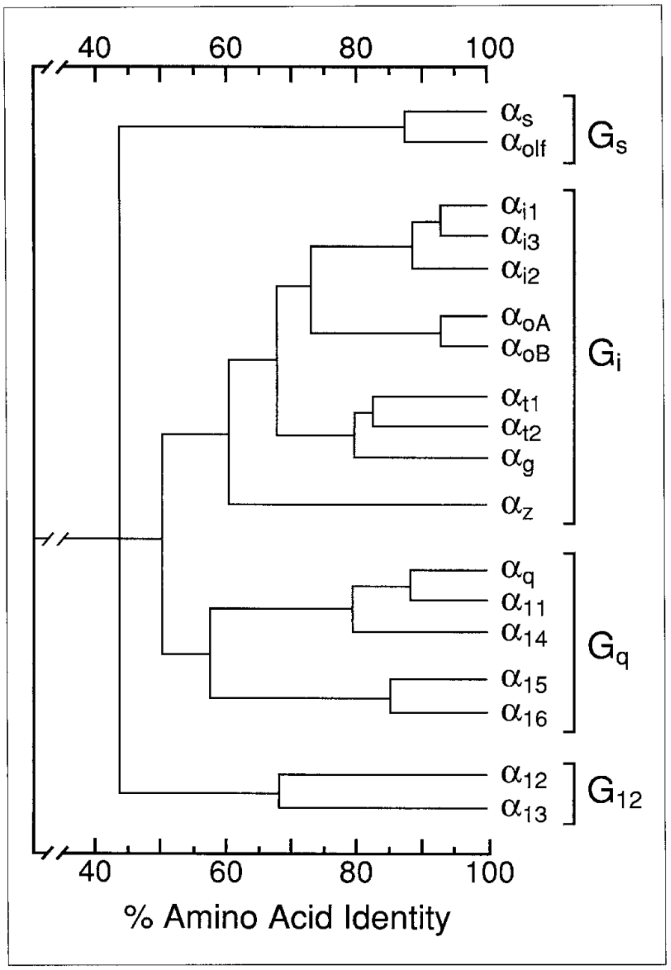

Figure 1.3: Gα phylogenetic tree
Graphical representation of the genetic similarity of human Gα subunits by amino acid identity. Adapted from [1].

Even with the similarities in structure, intrinsic function, and modification, great divergence exists between the target proteins of each Gα family. Canonically, $G\alpha_s$ activates adenylyl cyclase (AC) which generates the second messenger 3'-5'-cyclic adenosine monophosphate (cAMP). $G\alpha_{i/o}$ family subunits act in the opposite manner, inhibiting AC. $G\alpha_{q/11}$ activates phospholipase C enzymes, which hydrolyze membrane lipids phosphatidylinositol 4,5-bisphosphate (PIP_2) and phosphatidylinositol 4-phosphate (PI4P) to produce second messengers inositol triphosphate (IP_3) and membrane-embedded diacylglycerol (DAG). $G\alpha_{12/13}$ are known to activate GEFs for the small GTPase Rho (RhoGEFs) (Figure 1.4) [1]. This short list of classical effectors is not exhaustive, and the full known Gα interactome has continued to grow at a steady rate for over three decades.

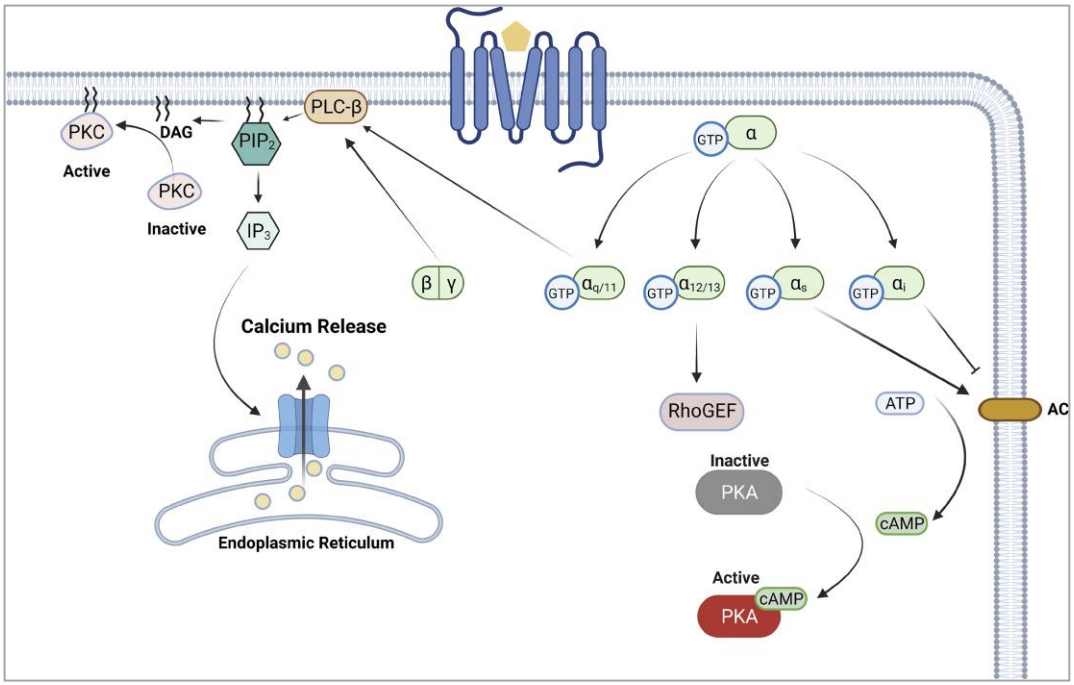

Figure 1.4: Gα subunit signaling
Cartoon representation of Gα signaling downstream of GPCRs. $G\alpha_s$ and $G\alpha_i$ subunits activate and inhibit adenylyl cyclase respectively, while $G\alpha_{12/13}$ subunits activate RhoGEFs, and $G\alpha_{q/11}$ subunits activate phospholipase C beta (PLCβ). Adapted from [3].

1.3.3 Regulators of Gα signaling

Regulation of the nucleotide binding state of Gα subunits is key to the action of these transducers on their downstream effector proteins. Some signals received and transduced into the cell, such as hormones regulating ion channel function, must be tightly temporally regulated to deliver the signal to effectors for the right duration at the proper time. Although Gα proteins have intrinsic GTPase activity allowing them to cycle GDP and GTP independently, the hydrolysis and GDP exchange rates are slow. Tight modulation of GDP release and GTP hydrolysis allow for diversity of temporal signaling from one Gα protein. Such modulation is performed by accessory proteins termed guanine nucleotide exchange factors (GEFs) or GTPase activating proteins (GAPs). GEFs bind to Gα-GDP and cause conformational change that catalyzes GDP dissociation from Gα, which is the rate-limiting step of guanine nucleotide cycling in Gα. The most common GEF by far for Gα subunits is the GPCR itself. Upon GPCR activation by an agonist, the Gαβγ heterotrimer binds via the c-terminal α5 helix of Gα. Conformational change in the receptor transmembrane helices is communicated down the α5 helix of Gα, causing a concomitant conformational change in Gα that reduces its affinity for GDP. This α5 helix has significant influence on the coupling specificity of G protein heterotrimers to different GPCRs [33], however other Gα interaction surfaces have also been characterized to contribute to this selectivity [34, 35].

Nonreceptor GEFs for Gα subunits also exist for $G\alpha_{i/o}$, $G\alpha_{q/11}$, and $G\alpha_{12/13}$ families, which serve to further regulate Gα signaling independent of the GPCR. These proteins have a common motif that binds Gα subunits known as the G protein regulatory (GPR) motif, or GoLoco motif [36]. One example of these GEFs include Activators of G protein Signaling, or AGS proteins, which were first characterized in genetic screens in yeast [37-39]. Resistance to inhibitors of cholinesterase (Ric8) or synembryn is a non-receptor GEF that activates monomeric Gα proteins

but does not act on the G protein heterotrimer. In addition to its GEF activity, it acts as a chaperone for Gα proteins during biosynthesis and folding [40-43]. GIV/Girdin has also been identified as a GEF for $G\alpha_{i/o}$ proteins, however acts as a guanine nucleotide dissociation inhibitor (GDI) to inhibit GDP dissociation from $G\alpha_s$, stabilizing $G\alpha_s$ in the 'Off' state [44, 45]. Proteins with differential effects on nucleotide binding or exchange activity on different targets have come to be known as guanine nucleotide exchange modulators (GEMs) [46].

RGS proteins terminate signaling from active Gα by binding Gα-GTP and stabilizing the transition state of GTP hydrolysis [47]. This accelerates the GTP hydrolysis rate, returning Gα to its inactive GDP-bound state. There are 20 RGS proteins in total, spanning four families (R4, RZ, R12, and R7). Each family except the R7 family shows some specificity toward $G\alpha_{i/o}$ and $G\alpha_{q/11}$ proteins, but none of these RGS have shown any ability to act on $G\alpha_s$ or $G\alpha_{12/13}$ family [48]. However, some RhoGEFs which are activated by $G\alpha_{12/13}$ have interestingly been shown to have GAP activity on $G\alpha_{12/13}$ [49, 50].

1.4 Gα structure and function

1.4.1 Switch regions

Switch regions I, II, and III are found in the Ras-like domain, while Switch IV is between the αB and αC loops of the helical domain (Figure 1.5). Switch I is an 11-residue flexible loop which interacts with the ribose and phosphate groups of GDP and GTP. Importantly, it contains an arginine conserved in all Ras-like GTPases which is required for hydrolysis of the γ-phosphate of GTP. Switch I also forms part of the flexible hinge which covalently connects the RLD to the HD.

Switch II constitutes the α2 helix and its flanking flexible linker regions (Figure 1.5) and contains residues that serve as contacts for effector binding, including Gβγ. Also residing in Switch

II is the catalytic Glu (Q204 in $G\alpha_{i1}$). This residue, along with a catalytic Arg in Switch I (R178 in $G\alpha_{i1}$) stabilize the pentavalent transition state during hydrolysis of the terminal phosphate of GTP. It is not likely that either residue facilitates the catalysis through a general base mechanism, but the catalytic Glu may help position a local water molecule for hydrolysis [51]. As mentioned, Switch II is also heavily involved in Gβγ binding. In the Gα-GDP state, Gβγ is able to bind directly to Switch II which contacts the Gβ interaction hotspot. Upon GDP dissociation from Gα, GTP enters the nucleotide-free active site and is stabilized by a G-R-E polar interaction network. At the same time, these "triad" residues put torsional strain on Switch II residues, causing conformation change in Switch II and dissociation of Gβγ [52]. Due to these critical functional roles, residues in the nucleotide binding pocket and Switch II are highly conserved across all Gα subunits.

Switch III comprises the loop between β-sheet 4 and helix 3 (Figure 1.5). In addition to conformational change upon GTP binding, Switch III communicates to the HD through direct interactions at the domain interface [53-56]. Mutations to residues at this interdomain interface are known to enhance the dissociation of GDP from Gα subunits, as measured by GTPγS binding rates [57]. Despite higher rates of nucleotide exchange, binding and activation of effectors downstream of Gα is not affected, indicating the inability to assume an active conformation downstream of an active receptor, as demonstrated by Berlot and colleagues. Mutations at the domain interface of $G\alpha_s$ resulted in intact ability to activate AC in GTPγS-bound or GTPase-deficient forms, but loss of isoproterenol-dependent activation of AC downstream of the β2-adrenergic receptor [53, 56].

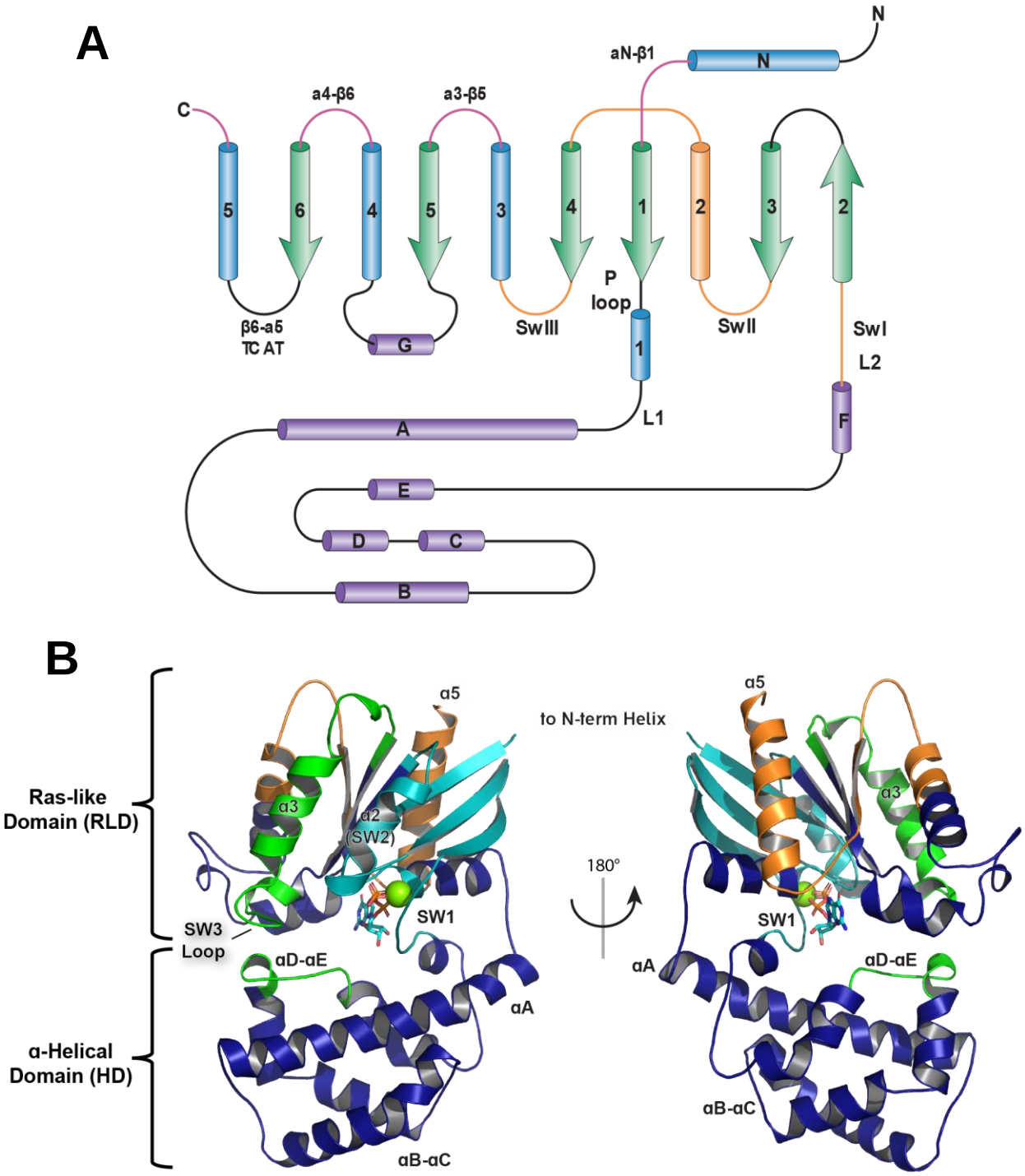

Figure 1.5: Gα molecular structure

A) Secondary structure of Gα. Arrows represent β-sheets, while cylinders are α-helices. Lines are interconnecting loops. Secondary structure elements are placed in approximate two-dimensional layout with respect to three-dimensional orientation. **B)** Labeled three-dimensional structure of Gα. Elements of the helical domain are dark blue, as are the α1 and α4 helices and β4 and β5 sheets. The loop between β6-α5 (orange) containing the TCAT motif is crucial for binding guanine nucleotides, while the α5 helix binds directly to the receptor's intracellular face. Switch III and the αD-αE helix (green) are important for interdomain communication, while Switches I-II and β1-3 are cyan. Adapted from [4]. PDB: 1CIP.

1.4.2 Helical domain function and interdomain interaction

The Ras superfamily of monomeric GTPases share significant structural homology with Gα, differing in sequence but still functioning similarly to Gα. These G proteins only harbor the GTPase domain, but still act as guanine nucleotide-controlled molecular switches, have intrinsic GTPase activity, interact specifically with certain GEFs and GAPs, and signal directly to downstream effector proteins. Like the Ras superfamily, Gα have Switch I and II. Switch III and Switch IV are unique to Gα – suggesting that they may work in concert with the other main difference from monomeric GTPases: the helical domain [51]. The Gα helical domain is made up of six tightly-packed α-helices (αA – αF) and the five loops that connect them (Figure 1.5) [29, 30]. The domain exists as a rigid body, with the exception of the Switch IV region which rearranges upon binding GTP [58]. The functional role of the HD has remained somewhat elusive, however modern methods of real-time structural analysis have enabled advances in understanding the role of the HD in Gα function.

Even prior to the first crystal structure of a Gα protein [29] and discovery of the first mammalian RGS proteins [59-61], initial reports and speculation on HD focused on its contributions to nucleotide binding and hydrolysis. Bourne and colleagues showed that the HD of $G\alpha_s$ could be purified and remained stably folded *in vitro*, and combining purified $G\alpha_s$ HD with purified RLD was sufficient for GTP hydrolysis and activation of membrane-bound adenylyl cyclase [62, 63]. The suggested role of a GAP was quickly confirmed by Codina and Birnbaumer, who demonstrated that a lysine conserved in Gα (K293 in $G\alpha_s$, K270 in $G\alpha_{i1}$) in the RLD and a conserved aspartate in the HD ($G\alpha_s$ D173, $G\alpha_{i1}$ D150) interact in the nucleotide binding pocket. Mutations abolishing this binding still allowed for GTPγS binding and activation of AC, but did not allow for AlF_4^--mediated activation, indicating that interdomain interaction is required for the

inactive – active transition in Gα [64]. Recent studies have reinforced the HD's role in nucleotide binding, exchange, and hydrolysis. Several differences are found between residues in the αA helices of $G\alpha_i$ subtypes and $G\alpha_o$. $G\alpha_o$ also has a higher rate of GDP dissociation, resulting in a higher rate of GTPγS binding than $G\alpha_i$ subtypes. Substitution of the entire HD of $G\alpha_o$ into $G\alpha_{i3}$ was shown to increase the rate of GTPγS binding and maximum GTPγS binding to that of $G\alpha_o$, while substitution of multiple separate clusters of these residues in the αA helix increased both rate and maximum binding in a stepwise manner [65].

Not only does the amino acid composition of the HD modulate nucleotide binding and exchange, but its movement is key to these functions. In many co-crystal structures of active ternary complexes (that is, active-state GPCR bound to G protein heterotrimers), the Gα HD is not resolved, suggesting that in the Gα nucleotide-free state, the HD is not in one stable position. However, in some structures, including the first GPCR-G protein heterotrimer (the β_2-AR bound to a Gs heterotrimer), the $G\alpha_s$ HD is observed to be stabilized swung out from its normal position within interacting distance of Gβγ [66]. This movement was confirmed in cryo-EM [67] and hydrogen-deuterium exchange (HDX) [68] studies on these complexes, which revealed this motion of the HD as multiple non-uniform populations can be observed and analyzed via these structural methods. In the nucleotide-free state of Gα, the HD moves dynamically as a rigid body, opening with a "clamshell" motion along the flexible hinge comprised of Loop 1 and Switch I which connect the RLD and the HD. Furthermore, molecular dynamics (MD) simulations and double electron-electron resonance (DEER) spectroscopy studies on Gα show that the RLD and HD separate spontaneously without receptor binding, and that this separation is necessary but not sufficient for GDP dissociation, and therefore nucleotide exchange [69].

Of all of the non-receptor effector co-structures with Gα, all non-receptor effectors bind Switch II, and all non-RGS effectors bind between the α2 (Switch II) and α3 helices in the RLD. Despite this conserved binding site, the HD is also involved in Gα-effector interactions for every Gα family, either through direct contact with effectors or indirectly through communication with the RLD. This concept will be explored at length in Chapter 2 and Chapter 3.

1.5 Differentiation in $G\alpha_i$ function and signaling

1.5.1 Sequence, structure, and biochemistry

$G\alpha_i$ subunits are highly homologous in primary, secondary, and tertiary structure. $G\alpha_{i1}$ and $G\alpha_{i3}$ are each 354 amino acids in length, while $G\alpha_{i2}$ is 355 amino acids in length, including an additional glutamine inserted in the Switch IV region of the HD. Alignment of each protein's human sequence shows that $G\alpha_{i1}$ and $G\alpha_{i2}$ are 86% identical, $G\alpha_{i2}$ and $G\alpha_{i3}$ are 88% identical, and $G\alpha_{i1}$ and $G\alpha_{i3}$ are 94% identical (Figure 1.6). Considering such identity, it is perhaps unsurprising that the $G\alpha_i$ subfamily is very similar biochemically. $G\alpha_{i1}$, $G\alpha_{i2}$, and $G\alpha_{i3}$ have equal rates of steady state GTP hydrolysis *in vitro* [70]. $G\alpha_{i2}$ has a higher rate of single turnover GTP hydrolysis, which is determined by a higher GDP dissociation rate *in vitro* [70, 71]. All are myristoylated and palmitoylated in cells [31], and all are susceptible to pertussis toxin (PTX) inactivation. Interaction with their classical effector, adenylyl cyclase, is also conserved. Myristoylated $G\alpha_{i1}$, $G\alpha_{i2}$, and $G\alpha_{i3}$ inhibit the activity of adenylyl cyclase V and VI with the same efficacy and potency *in vitro*, whether AC was activated by $G\alpha_s$ or by the direct AC agonist forskolin [72].

Due to their astounding structural and functional similarity combined with limited molecular information on effector specificity, high resolution structural analyses are not available for all of the $G\alpha_i$ subtypes. The first high-resolution x-ray crystal structure of $G\alpha_i$ was that of $G\alpha_{i1}$, solved in 1994 by Sprang and colleagues [30]. Illustratively, no high-resolution structure of $G\alpha_{i2}$

had been reported until 24 years later in 2018, when the structure of the human adenosine A_1 receptor was solved via cryo-EM in complex with adenosine and a $G\alpha_{i2}$-$G\beta_1\gamma_2$ heterotrimer [73]. Several other receptor-$G\alpha_{i2}$ heterotrimer cryo-EM structures quickly followed [74-77], however none of these represent an active-state G protein or resolve the helical domain. $G\alpha_{i3}$ structures were first available as GDP-AlF_4^--bound co-crystal structures with RGS8, RGS10, [78] and RGS2 [79], followed by GDP-bound $G\alpha_{i3}$ with the GIV GoLoco peptide [80]. As expected, none of these structures show significant differences in structure of the RLD, however the HD and domain interface between $G\alpha_{i2}$ and $G\alpha_{i1/3}$ clearly cannot be compared.

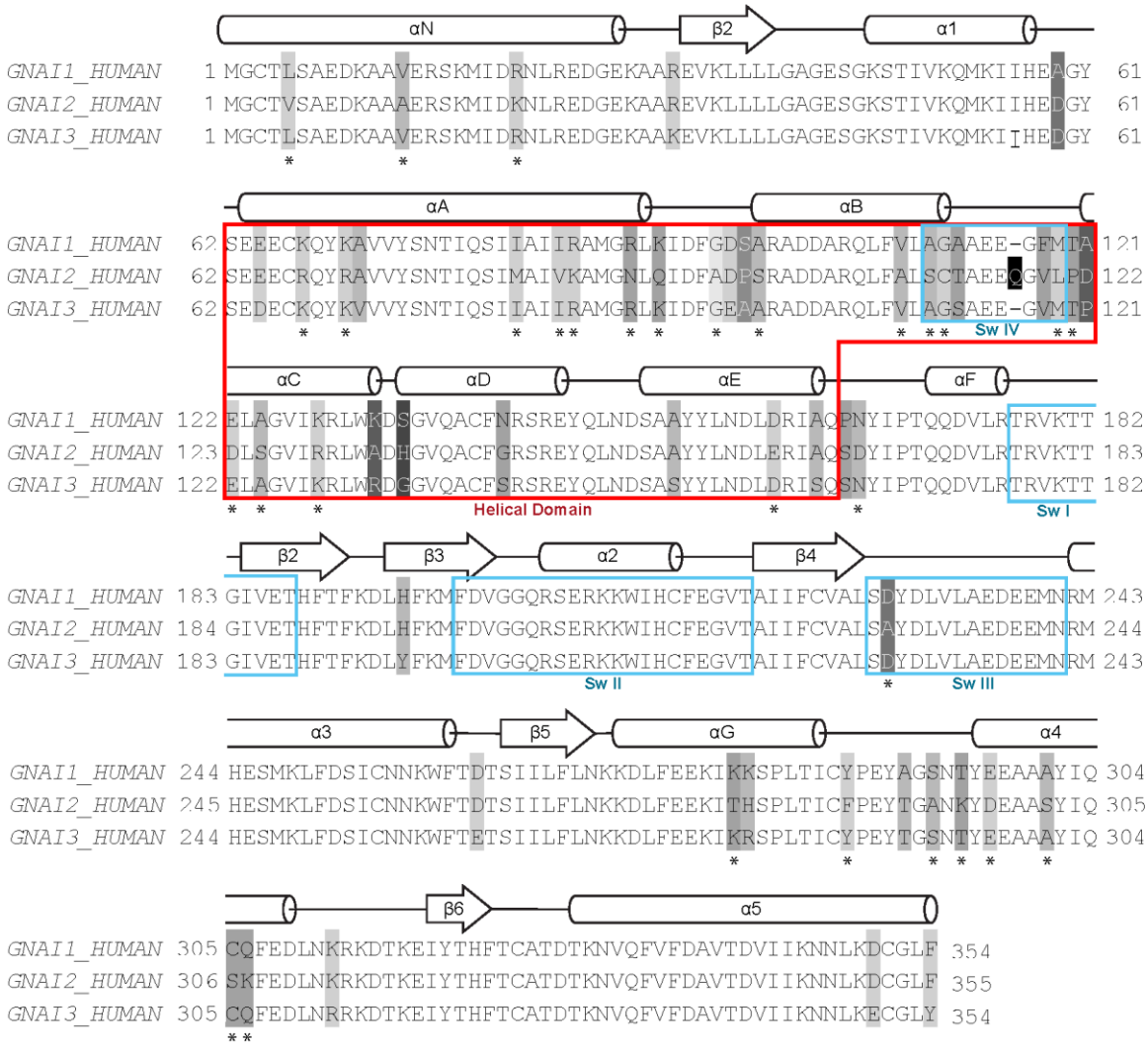

Figure 1.6: Gα$_i$ sequence alignment.
Shade of grey represents degree of similarity across Gα$_i$ subunits, with black being most dissimilar and white being identical. The helical domain is outlined in red. Switch regions are outlined in blue. Above the sequences, arrows signify β-sheets and cylinders represent α-helices.

1.5.2 *Molecular interactions*

GIRK channels

Examples of direct $G\alpha_i$-effector interaction beyond AC have been few and far between, with any selective interactors displaying a preference for $G\alpha_{i1}$ and $G\alpha_{i3}$ over $G\alpha_{i2}$. In *Xenopus* oocytes, $G\alpha_{i3}$-GDP has been shown to regulate GIRK1/2 by binding to the cytosolic portion of GIRK1 [81], suppressing basal current while priming the channel to enhance $G\beta\gamma$-mediated channel stimulation [82, 83]. $G\alpha_{i1}$-GDP performs a similar function, albeit with a lower affinity for GIRK [84]. $G\alpha_{i2}$ has been considered primarily a $G\beta\gamma$ donor for GIRK activation upon Gi-coupled receptor activation. Nuclear magnetic resonance (NMR) studies have suggested that that the GIRK binding site on $G\alpha_{i3}$-GTP is at the conserved α2-α3 binding site in the RLD [85], while a $G\alpha_{i3}\beta\gamma$ heterotrimer was found to bind to GIRK via a section of the $G\alpha_{i3}$ αA helix [86]. Importantly, the $G\alpha_{i3}$ HD was shown to be required for agonist-stimulated $G\alpha_{i3}\beta\gamma$-GIRK binding. Differences in sequence of the αA helix across $G\alpha_i$ subtypes could underlie the observed specificity of $G\alpha_i$ for GIRK.

EGFR signaling

$G\alpha_i$ involvement in RTK signaling is an interesting recent paradigm, involving both $G\alpha_i$ mediation of RTK signaling as well as transactivation of $G\alpha_i$ by RTKs. These interactions appear to be highly selective for $G\alpha_i$ subtypes. Specifically, $G\alpha_{i1}$ and $G\alpha_{i3}$ have been found to be important for epidermal growth factor receptor (EGFR) signaling. $G\alpha_{i1}/G\alpha_{i3}$ double knockout mouse embryonic fibroblasts displayed significantly ablated epidermal growth factor (EGF)-induced Akt phosphorylation, while $G\alpha_{i2}$ knockout had no effect. Additionally, upon treatment with EGF, $G\alpha_{i1}$ and $G\alpha_{i3}$ co-immunoprecipitated with growth factor receptor binding 2–associated binding protein 1 (Gab1), which is necessary for EGF-induced Akt phosphorylation, and $G\alpha_{i3}$ co-

immunoprecipitated with EGFR [87]. EGFR and cSrc can phosphorylate tyrosine residues at the $G\alpha_i$ domain interface, impacting protein stability and enhancing $G\alpha_i$ activation [88]. This phosphorylation was highly specific for $G\alpha_{i1}$ and $G\alpha_{i3}$ over $G\alpha_{i2}$, indicating a unique role for different $G\alpha_i$ subtypes in these signaling pathways.

RGS14

RGS14 exhibits a highly unique binding mode for any Gα binding protein. The RGS14 GoLoco motif binds deep in the α2-α3 cleft of $G\alpha_{i1}$, extends down over the HD αA helix, and contacts the αB helix [89]. This cross-domain engagement results in a high degree of specificity, as $G\alpha_{i1}$ and $G\alpha_{i3}$, but not $G\alpha_{i2}$, have been reported to bind and regulate localization of RGS14 [90]. Others have reported that RGS14 has both GAP and GDI activity on $G\alpha_{i1}$ and $G\alpha_{i3}$, but only GDI activity on $G\alpha_{i2}$. Importantly, GDI activity of RGS14 can be conferred to $G\alpha_{i2}$ by substituting clusters of cognate residues from the $G\alpha_{i1}$ αA, αB, and αC helices into $G\alpha_{i2}$ [91].

RGS19

RGS19, or G alpha interacting protein (GAIP), was discovered in a yeast two-hybrid screen to interact with $G\alpha_i$ in yeast [61]. Later, in a similar assay, RGS19 was found to interact preferentially with $G\alpha_{i1}$ and $G\alpha_{i3}$ over $G\alpha_{i2}$**,** and to interact with GTP-bound $G\alpha_{i3}$ over GDP-bound $G\alpha_{i3}$ [92]. These results were confirmed by Woulfe and Stadel, who demonstrated that RGS19 has GAP activity on purified $G\alpha_{i1}$, but not $G\alpha_{i2}$. Further, they identified a single amino acid substitution in Switch III, $G\alpha_{i2}$ A230 to its cognate D229 in $G\alpha_{i1}$, conferred to $G\alpha_{i2}$ the ability to interact with RGS19 in yeast and susceptibility to RGS19 GAP activity *in vitro* [93]. The opposite selectivity of RGS19 for $G\alpha_i$ subtypes was recently observed in an investigation of a panel of all human RGS proteins with all human Gα subunits [48], however this approach utilized the dopamine D2 receptor for $G\alpha_{i/o}$ activation, which has been noted to differentially associate with and activate

$G\alpha_{i/o}$ subunits [94, 95]. While there are no structures of $G\alpha_i$ bound to RGS19, RGS19 does contain an RGS domain. Additionally, the C-terminus of $G\alpha_{i1}$, which includes much of the RLD, is sufficient to confer interaction with RGS19 in $G\alpha_{i2}$. Hence, it would be reasonable to infer that RGS19 binds to $G\alpha_i$ similarly to other RGS proteins: across the RLD, spanning Switch I-III.

PDZ-RhoGEF

PRG is a dbl-family RhoGEF which includes a RhoGEF-RGS (rgRGS) domain, a type of RGS Homology (RH) domain, and a tandem Dbl-homology/Pleckstrin-homology (DH/PH) domain which activate downstream signals from Rho family GTPases [96]. Recently, our laboratory has reported the direct activation of PRG by the $G\alpha_i$ subfamily, specifically strong activation by the $G\alpha_{i1}$ and $G\alpha_{i3}$ subunits [97]. Strikingly, the $G\alpha_{i2}$ subunit only weakly activates PRG, despite the many similarities among the $G\alpha_i$ subfamily in sequence homology and known function. This intriguing selectivity for $G\alpha_i$ subunits is the impetus and the focus of Chapter 2.

1.5.3 Signaling in vivo

$G\alpha_i$ in cardiac biology

β-adrenergic receptors, or βARs, are highly prevalent in the cardiovascular system and have long been known to signal through the Gs family of heterotrimeric G proteins. Excessive and prolonged signaling through this pathway is a known cause of heart failure and pathological hypertrophy [98, 99]. However, it was later established that βARs, or the β2AR in particular, signals through both the G_s and G_i families of G proteins [100-105].

$G\alpha_{i2}$ is generally understood to be cardioprotective, as determined in several studies enabled by a $G\alpha_{i2}$ global knockout model generated by Lutz Birnbaumer and colleagues [106, 107]. In this murine model lacking $G\alpha_{i2}$, mice saw exacerbated ischemic injury and cardiac infarction, while homozygous knockout of $G\alpha_{i3}$ resulted in a slight upregulation in $G\alpha_{i2}$ and

reduced injury. [108-112]. In a domestic swine model, overexpression of constitutively active $G\alpha_{i2}$ Q205L and WT $G\alpha_{i2}$ via adenoviral gene transfer normalized heart rate and stimulated cardiac remodeling in a model of atrial fibrillation [113]**.** Dizayee et al. observed that $G\alpha_{i2}$ deletion caused a defect in L-type voltage-dependent calcium channels in mouse cardiomyocytes while $G\alpha_{i3}$ deletion had no such effect. However, this result is complicated by a 5-fold compensatory increase in $G\alpha_{i3}$ protein levels in $G\alpha_{i2}$ -/- mice [109].

$G\alpha_i$ in platelets

Platelets from mice lacking $G\alpha_{i2}$ showed a loss of ADP-dependent Rap1B activation downstream of the P2Y12 receptor. Rap1B activation was also PI3K dependent, but knockout of PI3Kγ largely reduced Gi-mediated Rap1B activation by epinephrine or ADP stimulation, indicating that activation of PI3Kγ (likely by Gβγ) plays an important role in Rap1B activation [114]. $G\alpha_{i2}$ and $G\alpha_{i3}$ differentially regulate basal and agonist-stimulated cAMP production in platelets, with $G\alpha_{i2}$ deletion reducing inhibition and $G\alpha_{i3}$ deletion having no effect. These effects were also agonist-dependent, suggesting potential preferential receptor coupling for different $G\alpha_i$ subtypes [115] $G\alpha_{i2}$ whole body knockout mice as well as platelet-specific $G\alpha_{i2}$ knockout resulted in prolonged bleeding, impaired thrombus formation, and reduced development of ischemia reperfusion injury [116]. Interestingly, in a study using a hyperactive $G\alpha_{i2}$ mutant insensitive to RGS protein regulation [117, 118], increases in Rap1B activation were not observed in $G\alpha_{i2}$ G184S global knock-in mice or in platelet-specific knock-in, however these genetic alterations did result in enhanced cAMP inhibition, platelet aggregation *in vitro*, and accumulation of platelets to injury sites *in vivo* [119].

$G\alpha_i$ regulation of cell migration and cancer

Chemokine receptors are involved in regulating chemotaxis, a form of cell migration. Chemotaxis is primarily regulated through Gi signaling downstream of chemokine receptors [120], and almost all chemokine receptors in hematopoietic cells are coupled to $G_{i/o}$ proteins [121]. $G\beta\gamma$ has been well-characterized as a required component for chemotaxis [25, 122-124]. Recently, our laboratory has demonstrated the requirement for both $G\alpha_i$ and $G\beta\gamma$ for proper adhesion and chemotaxis in neutrophils and neutrophil-like cells [125, 126]. Interestingly, receptor-independent activation of both $G\alpha_i$ and $G\beta\gamma$ signaling restored some aspects of migration [125], suggesting that these pathways account for a large portion of chemotactic signaling.

Like studies on $G\alpha_i$ function in other systems, roles *in vivo* for $G\alpha_{i2}$ and $G\alpha_{i3}$ in chemotaxis have also relied heavily on ablation of signaling via gene knockout. In one study, neutrophils from $G\alpha_{i2}$-knockout mice showed reduced arrest in response to CXCL1 and LTB4, as well as reduced neutrophil recruitment to sites of inflammation in mice lacking $G\alpha_{i2}$ in hematopoietic cells [127]. In murine T cell lymphocytes lacking either $G\alpha_{i2}$ or $G\alpha_{i3}$, $G\alpha_{i2}$ deletion was found to reduce migration in response to CXCR3 agonists CXCL10 and CXCL11, while $G\alpha_{i3}$ deletion enhanced CXCL9, CXCL10, and CXCL11-induced cell migration downstream of CXCR3 [128]. In mouse neutrophils from $G\alpha_{i2}$ -/- or $G\alpha_{i3}$ -/- mice, differential effects were reported for each population downstream of CXCR2 activation by CXCL1. $G\alpha_{i2}$ knockout neutrophils showed a decrease in intracellular calcium and an increase in Akt phosphorylation, while $G\alpha_{i3}$ knockout cells saw a decrease in Akt phosphorylation and importantly, a decrease in both transwell migration and chemotaxis on ICAM-coated plates [129]. Combined with a previous study of CXCL1-mediated $G\alpha_i$ function in neutrophils [127], these experiments with whole-body $G\alpha_i$ knockout suggest that

$G\alpha_{i2}$ is responsible for neutrophil arrest while $G\alpha_{i3}$ is important for proper CXCL1-induced migration.

RGS-insensitive $G\alpha_{i2}$ has also been used to investigate $G\alpha_i$ function in animal models. B cell lymphocytes from whole body knock-in $G\alpha_{i2}$ G184S mice harbor higher nonspecific migration but lower response to chemokine-induced chemotaxis [130]. In mouse neutrophils, RGS insensitive $G\alpha_{i2}$ causes neutrophil accumulation in the bone marrow and reduced migration to sites of inflammation [131].

None of the studies cited above identify direct $G\alpha_i$ interactions with effectors involved in cell migration, but a limited number have been reported. In human breast cancer cell lines, $G\alpha_{i2}$ was found to interact with engulfment and cell motility protein 1 (ELMO1), which activates Rac1/2 signaling via its RacGEF binding partner Dock180. ELMO1/Dock180 therefore localizes to the plasma membrane, where it activates Rac1/2 and promotes actin polymerization and cell migration. The interaction between $G\alpha_{i2}$ and ELMO1 was dependent on activation of CXCR4 by its ligand CXCL12, and ELMO2 had an identical role as ELMO1. $G\alpha_{i1}$, and $G\alpha_{i3}$ are also present in breast cancer cells, but were not tested as siRNA knockdown of $G\alpha_{i2}$ completely abolished Rac activation by ELMO/Dock [132]. $G\alpha_{i2}$ was similarly found to coimmunoprecipitate with ELMO2 in PANC1 pancreatic cancer cells, and was CXCR4/CXCL12 dependent [133]. While active $G\alpha_i$ as well as free $G\beta\gamma$ are necessary for proper chemotaxis, inactive $G\alpha_i$ may also play a role in leukocyte migration. Kamakura et al. showed that $G\alpha_{i1}$-GDP and $G\alpha_{i2}$-GDP interact with AGS3 (LGN) at the leading edge of fMLP-stimulated chemotaxis in mouse neutrophils. This complex was required for concomitant scaffolding of mammalian homologue of Inscuteable (mInsc) at the leading edge, and thus recruitment of the Par3-Par6-aPKC complex which is important for

directionality of chemotaxis [134]. While these important studies identify direct protein targets of $G\alpha_i$ in cells, they do not describe any molecular details of $G\alpha_i$ binding or specificity.

1.6 **Thesis overview**

Despite over three decades of broad and deep studies on G protein function and signaling, no clear intramolecular differences between the $G\alpha_i$ subtypes have been defined which adequately explain their target selectivity. *In vivo* approaches have consistently described significant nonoverlapping $G\alpha_i$ subtype function in several systems including cardiovascular function, immune cell migration, and platelet aggregation. These studies have often failed to determine the identity of $G\alpha_i$ protein interactors or molecular features of $G\alpha_i$ responsible for these observed subtype differences. $G\alpha_i$ subtype-specific effectors that have been described at the molecular level are few but include RGS proteins and inwardly-rectifying potassium channels. While they use different binding modes, the subtype selectivity displayed by each of these effectors is influenced by interactions that involve $G\alpha_i$ Switch III, the HD, or both. While the HD has been robustly characterized for its influence on nucleotide exchange and hydrolysis, it has also been postulated as a region of effector selectivity due to its heterogeneity in sequence among Gα families. Interdomain interaction has been shown to be a critical determinant for nucleotide binding and receptor-mediated activation of Gα, but this has not been demonstrated as a mechanism for determination of effector selectivity for Gα subunits.

In Chapter 1, I have cited examples which provide a basis for principles of selective interaction with effector proteins among $G\alpha_i$ protein subtypes. In Chapter 2, I focus on our efforts to establish the molecular determinants of specificity of $G\alpha_i$ subtypes for their effectors. Through extensive mutagenesis, in-cell reporter assays, and molecular dynamics simulations, we demonstrate that stabilization of Switch III via interaction with the HD is responsible for regulating

differential interactions with protein targets of $G\alpha_{i1}$ and $G\alpha_{i2}$. We first demonstrate this with the recently-discovered effector of $G\alpha_i$, PDZ-RhoGEF, and then extend this principle to multiple novel $G\alpha_i$-interacting proteins in a proximity labeling proteomic screen. In Chapter 3, I discuss the implications of our findings on $G\alpha_i$ subtype signaling and $G\alpha$ signaling at large, followed by highlighting the importance of technical approaches to accelerate discovery of novel $G\alpha$ signaling at the molecular level.

Chapter 2 - Interdomain Interactions Determine $G\alpha_i$ Subfamily Effector Specificity

2.1 Abstract

Highly homologous members of the $G\alpha_i$ family, $G\alpha_{i1-3}$, have distinct tissue distributions and physiological functions, yet the functional properties of these proteins are nearly indistinguishable. $G\alpha_i$ subtypes identically regulate their canonical effector adenylate cyclase, while guanine nucleotide binding and hydrolysis by these proteins is also very similar. In a recent proteomic screen, we identified PDZ-RhoGEF (PRG) as a novel effector for $G\alpha_{i1}$. Surprisingly, PRG was poorly activated by $G\alpha_{i2}$. Here, we find that this difference between these two subtypes extends to interaction with other targets, and we investigate the mechanistic basis for these differences using PRG as a model target. We find that substitution of either the helical domain (HD) from $G\alpha_{i1}$ into $G\alpha_{i2}$ or substitution of a single amino acid, A230 in $G\alpha_{i2}$ to the corresponding D in $G\alpha_{i1}$, largely rescues PRG activation and interactions with other targets. Molecular dynamics simulations reveal that in the GTP bound state, opening of the HD with respect to the Ras-like domain (RLD) is prevalent in $G\alpha_{i2}$ relative to $G\alpha_{i1}$, and that mutation of A230 to D in $G\alpha_{i2}$ stabilizes HD-RLD interactions. In turn, these interactions modify the conformation of Switch III which we show to be required for PRG activation. These data support a model where, although Switch III amino acids are identical between $G\alpha_{i1}$ and $G\alpha_{i2}$, D229 in $G\alpha_{i1}$ stabilizes a network of interactions between HD and RLD that in turn stabilize Switch III to promote protein target recognition. The corresponding A230 in $G\alpha_{i2}$ is unable to stabilize this network resulting in conformations of Switch III that lead to an overall lower efficacy with respect to target interactions.

This reveals significant distinct mechanistic properties that could underly differential biological and physiological consequences of activation of $G\alpha_{i1}$ or $G\alpha_{i2}$ by GPCRs.

2.2 Introduction

Many physiologically important hormones and neurotransmitters signal through G protein-coupled receptors (GPCRs), rendering these membrane-spanning receptors highly clinically significant in the development of drugs. Upon binding an extracellular ligand, GPCRs transduce this signal into the cell via heterotrimeric G proteins, consisting of the Gα subunit and the Gβγ constitutive heterodimer. Signaling diversity from GPCRs is primarily achieved via an array of Gα subunit protein families which harbor distinct downstream signaling capabilities, including the G_s, $G_{i/o}$, $G_{q/11}$, and $G_{12/13}$ families of Gα. Though their coupling to GPCRs and their downstream signaling to effector proteins are highly selective between families, Gα proteins have significant similarity in tertiary and quaternary structure and function.

Gα consist of a Ras-like domain (Ras), which binds and hydrolyzes guanine nucleotides, and an all-helical domain (HD), connected by a flexible hinge region (Figure 2.3A). Much of the investigative focus on Gα protein function has been on the Ras domain, which harbors three "Switch" regions (Switch I-III). An additional switch region, Switch IV, is found in the HD, connecting the αB and αC helices. Upon binding GTP, each of these Switch regions collapse in toward the bound nucleotide in a conformational rearrangement that permits Gα·GTP-effector interaction after dissociation from Gβγ and the receptor. In contrast, the HD is relatively rigid and opens along the interdomain cleft via the flexible hinge. Evidence suggests that this opening enhances the rate of GDP dissociation from Gα independent of receptor activation. Mutation of residues along the Ras-HD interface has been shown to further increase the rate of GDP

dissociation in $G\alpha_i$ [57], which is the rate-limiting step in nucleotide exchange and results in faster rates of GTP binding.

Switch II rearrangement upon binding GTP allows each family of Gα subunit to dissociate from Gβγ and its associated GPCR and signal to downstream effector proteins. Generally, the $G\alpha_s$ family activates adenylyl cyclases (ACs) to produce 3',5'-cyclic adenosine monophosphate (cAMP), the $G\alpha_i$ family inhibits ACs, the $G\alpha_{q/11}$ family activates phospholipase C enzymes, and the $G\alpha_{12/13}$ family activates Rho guanine nucleotide exchange factors (RhoGEFs). The $G\alpha_{i/o}$ family consists of $G\alpha_{i1}$, $G\alpha_{i2}$, $G\alpha_{i3}$, $G\alpha_o$**,** $G\alpha_{T1,}$ $G\alpha_{T2,}$ $G\alpha_{T3}$, and $G\alpha_z$. $G\alpha_o$ is prominent in the brain, $G\alpha_T$ in the visual and taste systems, and $G\alpha_z$ in the brain and prostate. $G\alpha_{i2}$ protein expression is more widespread and more abundant than any other protein in the $G\alpha_{i/o}$ family, except for $G\alpha_o$ which is most abundant in the brain [135]. $G\alpha_{i1\text{-}3}$ are expressed broadly in humans, with $G\alpha_{i2}$ often being expressed alongside $G\alpha_{i3}$ and/or $G\alpha_{i1}$. $G\alpha_i$ subunits have strong sequence conservation, with 94% identity between $G\alpha_{i1}$ and $G\alpha_{i3}$, 86% between $G\alpha_{i1}$ and $G\alpha_{i2}$, and 88% between $G\alpha_{i2}$ and $G\alpha_{i3}$ (Figure 2.7A) [136]. The $G\alpha_i$ subfamily has identical rates of single turnover GTP hydrolysis, but the GDP dissociation rate from $G\alpha_{i2}$ is faster than for the other two isoforms [70].

In terms of signaling specificity for the most well understood effector of $G\alpha_i$, AC, all $G\alpha_i$ subtypes inhibit various AC isoforms with similar potency and efficacy [72]. For decades, AC was the only known effector of $G\alpha_i$. Since, a small number of protein effectors have been characterized as targets of $G\alpha_i$ isoforms: G protein-activated inwardly-rectifying potassium channels (GIRK) [82-84, 137], epidermal growth factor receptor (EGFR), and growth factor receptor binding 2–associated binding protein 1 (Gab1) in mTOR signaling [87], although the biochemical and biological significance of these interactions is less well understood.

Importantly, genetic deletion or inactivation of endogenous individual $G\alpha_i$ isoforms have yielded evidence for differential function in primary tissues and organisms. For example, knockout of $G\alpha_{i2}$ in mice results in exacerbated ischemic injury and cardiac infarction, while mice lacking $G\alpha_{i3}$ saw an upregulation in $G\alpha_{i2}$ and reduced injury [108-112]. Additionally, $G\alpha_{i2}$ primarily promotes arrest and $G\alpha_{i3}$ is required for transmigration and chemotaxis in mouse neutrophils [129], while $G\alpha_{i3}$ activation downstream of CXCR3 has been shown to inhibit $G\alpha_{i2}$ activation in murine activated T cells [128]. These data strongly suggest that these isoforms serve non-redundant, unique functions, yet the biochemical basis for driving selective functionality has yet to be determined despite nearly three decades of research.

Recently, our laboratory identified PDZ-RhoGEF (PRG) as a novel, direct effector of $G\alpha_i$ in an unbiased proximity interaction screen. $G\alpha_{i1}$ binds and activates PRG in a nucleotide-dependent and receptor-dependent manner in cells, while $G\alpha_{i3}$ also activates PRG and $G\alpha_{i2}$ only weakly stimulates PRG. Here, we have interrogated the nature of the specificity of $G\alpha_i$ subfamily members for PRG at the molecular level. In doing so, we have uncovered an atomic-level mechanism for differences between $G\alpha_{i1}$ and $G\alpha_{i2}$ in downstream signaling interactions, revealing differences in the ability to stabilize interactions between the HD and the Switch III region of the RLD. Follow-up with unbiased proximity labeling coupled to tandem MS proteomics supports the idea that this mechanism extends beyond PRG interactions to multiple additional $G\alpha_i$ targets. Overall, our studies support a model in which the strength and frequency of interactions between $G\alpha_i$ Switch III and helical domain residues determine the ability to bind and activate PRG and other proteins, differentiating $G\alpha_i$ subfamily structure and function.

2.3 Materials and methods

Plasmid cDNA constructs

BioID2 fused N-terminally with c-Myc tag and C-terminally with mVenus, followed by CaaX PM targeting motif (KKKKKKSKTKCVIM, derived from the C terminus of KRas), was a gift from S. Malik of the University of Rochester. C-terminally c-Myc–tagged full-length PRG cDNA construct in mammalian expression vector was a gift from J. Tesmer of Purdue University. The following plasmids were obtained from Addgene: mEmerald-parvin-C-14 (#54214), EGFP-vimentin-7 (#56439).

HA-Gα_i-BioID2 plasmids in pcDNA3.1+ were constructed as described previously [97]. All WT Gα clones in pcDNA3.1+ were obtained from the cDNA Resource Center. The sequences of the clones are available upon request. All mutagenesis to Gα_i DNA constructs was accomplished using reagents, protocols, and guidelines from New England Biolabs Q5® Site-Directed Mutagenesis Kit (E0554S). Gαi2-1HD, all Gα_{i1} HD subdivision constructs, and Gα_i N- and C-terminal substitutions were generated using reagents, protocols, and guidelines from New England Biolabs HiFi DNA Assembly Master Mix (E2621) and Cloning Kit (E5520).

Cell Culture

A293 and HT1080 cells were obtained from the American Type Culture Collection. A293 and HT1080 cells were grown supplemented in DMEM (Dulbecco's modified Eagle medium) with 10% fetal bovine serum (FBS) (10437028, Gibco) and 100 U of penicillin/streptomycin (15140122, Gibco) at 37°C with 5% CO2. Trypsin-EDTA (25200056, Gibco) was used for cell passage.

Reagents

The following primary and secondary antibodies were used: $G\alpha_{i1/2}$ (anti-sera) [138], c-Myc (13-2500, Invitrogen), GFP (A11122, Invitrogen), HA (C29F4, Cell Signaling), FLAG (PA1-984B, Invitrogen). Streptavidin-IRDye800 was from LI-COR (925-32230). Primary antibodies were diluted in 3% bovine serum albumin (BSA) and 0.1% sodium azide and incubated with blots overnight at 4°C. Streptavidin-IRDye800 was incubated for 1 hour at room temperature. For secondary antibodies, goat anti-rabbit DyLight 800 (SA535571, Invitrogen) and goat anti-mouse IRDye 800CW (926-32210, LI-COR) were used at 1:10,000.

NanoBiT Luciferase Complementation Assay

6.0×10^5 HEK293A cells were seeded in poly-D-lysine coated 6-well plates (Fisher FB012927). Immediately after plating, HA-Gα-LgBiT constructs and SmB-cmyc-PDZ-RhoGEF were cotransfected using a 1:3 mass to volume ratio of DNA to Lipofectamine 2000 (Invitrogen). After 24 hours, transfection media was aspirated and cells were gently washed once with 1 mL warm PBS. The PBS was discarded, 200 μL trypsin solution was added, and the plate was incubated at 37°C and 5% CO_2 for 5 mins. Following incubation, 800 μL of warm 1X HBSS was added to each well, and the detached cells were aspirated and dispensed into new 15 mL conical tubes. Cells were then pelleted by centrifugation at 250 x g for 5 mins at RT. After carefully aspirating the supernatant, each pellet was resuspended in 1 mL warm HBSS, and cell number in each suspension counted. Cell suspensions were centrifuged once more at 250 x g for 5 mins at RT and resuspended in warm 10 μM furimazine in HBSS, 1% DMSO. 5×10^4 cells were distributed to each well in a 96-well plate; samples were analyzed with six technical replicates.

The sample plate was incubated at 37°C for 15 mins, followed by a luminescence measurement in each well.

SRE-Luciferase Reporter Assay

96-well format

4.5 x 10^4 HEK293A cells were seeded in poly-D-lysine coated 96-well plates (Greiner 655983). Cells were transfected with the following plasmids and amounts per well: 25 ng SRE-Luc reporter (E134A, Promega), 75 ng $G\alpha_i$ or $G\alpha_i$ QL in pcDNA3.1+, 2.5 ng cmyc-PRG. Minor adjustments in added DNA were made to equalize expression of $G\alpha_i$ subunits. In these cases, empty pcDNA3.1+ vector supplemented to equalize total DNA added per well. Transfection took place immediately after seeding with a 1:3 mass to volume ratio of DNA to Lipofectamine 2000 (Invitrogen). Twelve hours after transfection, the media was replaced with 75 µL of serum-free media. Twenty-four hours after transfection, 75 µL (1:1 volume) of One-Glo reagent (E6110, Promega) was added to each well and incubated for 10 min at room temperature. The luminescence signal was measured using Varioskan LUX multimode microplate reader (Thermo Fisher Scientific).

24-well format

The SRE-Luc reporter assay was also performed nearly identically in 24-well plates (Thermo 142475), which offered better well-to-well consistency for technical replicates. 1 x 10^5 HEK293A cells were seeded in poly-D-lysine coated 24-well plates. One hundred ng SRE-Luc reporter (E134A, Promega), 300 ng $G\alpha_i$ or $G\alpha_i$ QL in pcDNA3.1+, and 5 ng cmyc-PRG DNA were transfected into each well except in $G\alpha_i$ titration experiments, where reduced $G\alpha_i$ DNA was substituted with empty pcDNA3.1+. Transfection took place immediately after seeding with a 1:3

mass to volume ratio of DNA to Lipofectamine 2000 (Invitrogen). Twelve hours after transfection, the media was replaced with 250 µL of serum-free media. Twenty-four hours after transfection, 250 µL (1:1 volume) of One-Glo reagent (E6110, Promega) was added to each well and incubated for 10 min at room temperature. The luminescence signal was measured using Varioskan LUX multimode microplate reader (Thermo Fisher Scientific).

GloSensor cAMP Assay

4.5 x 10^4 HEK293A cells were seeded in poly-D-lysine coated 96-well plates (Greiner 655983). Cells were transfected with the following plasmids and amounts per well: 50 ng GloSensor -20F cAMP plasmid (E1171, Promega), 125 ng $G\alpha_i$ or $G\alpha_i$ QL in pcDNA3.1+. In $G\alpha_i$ titration experiments, DNA was supplemented with empty pcDNA3.1+ vector. Transfection took place immediately after seeding with a 1:3 mass to volume ratio of DNA to Lipofectamine 2000 (Invitrogen). Twenty four hours post-transfection, the media was discarded and the cells were loaded with 75 µL 0.5 mg/mL D-Luciferin (L2916, Sigma Aldrich) in Leibowitz's L-15, incubating for 2 hours at 37°C and 5% CO_2.

Western blotting

Samples in 1X Laemmli sample buffer were resolved on 4-20% gradient Mini-PROTEAN TGX gels (4561094, Bio-Rad), transferred to nitrocellulose membranes (Pall 66485), and stained with Ponceau S (141194, Sigma Aldrich). Membranes were blocked with 3% bovine serum albumin (Fisher BP1600) in TBST (0.1% Tween-20 in 20 mM Tris pH 7.5 + 150 mM NaCl) at room temperature (RT) for 30 min with constant agitation. Primary antibodies were applied for 2 hours at RT or overnight at 4°C. After three RT washes with TBST at 5 min each, secondary

antibodies were applied for 1 hour. Membranes were imaged on an Odyssey Infrared Imaging System (LI-COR Biosciences).

BioID2 proximity labeling and tandem mass spectrometry analysis

HT1080 cells at passage number up to 15 were used for proximity labeling experiments. Cells were plated into 175 cm^2 flasks at a density of 5.5×10^6 cells per flask. The next day, media was replaced with 35 mL of DMEM containing 50 µM biotin and 10% FBS. Each flask was transfected with 8 µg of plasmid encoding BioID2-fused $G\alpha_i$ construct and 4 µg of YFP cDNA. A total of 0.6 µL of Viromer Red (VR-01LB-00, Lipocalyx, Germany) reagent was used per 2 µg of cDNA for transfection, resulting in ~80 to 85% transfection efficiency. Twenty-four hours after labeling and transfection, the labeling medium was decanted, cells were washed twice with 1× PBS, and harvested at 4000 x g for 10 min. This step was repeated twice using 1× PBS to recover the maximum number of cells. The supernatant was aspirated, and pellets were flash-frozen and stored at −80°C until further use.

All stock solutions used for streptavidin pulldown were freshly prepared, except lysis buffer. Low protein binding tubes (022431081, Eppendorf) were used for sample preparation. Frozen pellets were lysed in 1 mL of ice-cold lysis solution (composition described above) for 10 min on ice and incubated with 125 U of benzonase with end over-end rotation at 4°C for 20 min. A total of 0.3% SDS was added to lysates, which were incubated for another 10 min at 4°C. Lysates were centrifuged at 15,000 x g for 15 min. The supernatant was transferred to fresh tubes, and the total protein concentration was measured using Pierce 660 nm protein assay reagent. A total of 5% of lysates, adjusted for protein concentration, was reserved to analyze the biotinylation in inputs. The remaining lysates were incubated with 500 µL of Pierce streptavidin magnetic beads slurry

per sample in an end-over-end rotator at 4°C overnight. Beads were washed twice with modRIPA buffer [modRIPA: 50 mM tris, 150 mM NaCl, 0.1% SDS, 0.5% sodium deoxycholate, and 1% Triton X-100 (final pH 7.5)] and once with four different solutions: 1 M KCl, 0.1 M Na_2CO_3, 2% SDS [in 50 mM tris (pH 7.5)], and 2 M urea [in 10 mM tris (pH 8.0)]. Beads were washed twice with 1× PBS and were flash-frozen and stored at -80°C until further processed for MS.

BioID2 proximity labeling and immunoblot analysis

1.5 x 10^6 HEK293A cells were seeded in a poly-D-lysine coated 10 cm plate. The next day, media was replaced with 10 mL DMEM +10% FBS and biotin was added to 50 µM. Cells were transfected with 3 µg of either BioID-CAAX or one of the $G\alpha_i$-BioID2-HA constructs in pcDNA3.1+, in addition to 3 µg of one of the effectors of interest (cmyc-PRG, V5-ADNP, RASA2-FLAG, mEmerald-Parvin, RSK1-HA, or GFP-Vimentin). DNA complexes were added to Lipofectamine 2000 solutions with a 1:3 mass:volume ratio (18 µL per plate). After 24 hours of expression and labeling, the medium was decanted, cells were rinsed twice with 5 mL of ice cold 1X PBS, scraped off of the plate, and pelleted at 4°C and 4000 x g for 10 min. The supernatant was aspirated and the cell pellets were flash-frozen with liquid N_2 and stored at -80°C until processed via IP.

For the IP, 500 µL ice cold modRIPA was used to resuspend cell pellets. Lysis using benzonase and SDS proceeded as above. Lysates were centrifuged for 15,000 x g for 15 min at 4°C, and protein concentration was measured using Pierce 660 nm protein assay reagent. After equalizing for protein concentration, 20 µL of each sample volume was retained as an input sample. Five hundred µL of each equalized sample was added to 170 µL of Pierce streptavidin magnetic bead slurry and rotated end-over-end at 4°C for at least 2 hours to capture biotinylated

proteins. Beads were washed three times with ice cold modRIPA and once more with cold 1X PBS. Beads were then resuspended in 100 µL 1X PBS, and 4X Laemmli sample buffer was added to 1X final concentration. Beads were boiled for 10 min at 95°C, and the supernatant was analyzed by western blot using anti-HA (1:2000) for $G\alpha_i$-BioID2-HA and the corresponding antibody for each protein of interest [cmyc-PRG – anti-cmyc (1:2000), V5-ADNP – anti-V5 (1:1000), RASA2-FLAG – anti-FLAG (1:1000), mEmerald-Parvin – anti-GFP (1:1000), RSK1-HA – anti-HA (1:2000), or GFP-Vimentin – anti-GFP (1:1000)].

Protein digestion and TMT labeling

On-bead digestion followed by liquid chromatography–tandem MS (LC-MS/MS) analysis was performed at the MS-based Proteomics Resource Facility of the Department of Pathology at the University of Michigan. Samples were reduced [10 mM dithiothreitol in 0.1 M triethylammonium bicarbonate (TEAB) at 45°C for 30 min], alkylated (55 mM 2-chloroacetamide at room temperature for 30 min in the dark), and subsequently digested using a 1:25 ratio of trypsin (V5113, Promega):protein at 37°C with constant mixing. A total of 0.2% trifluoroacetic acid was added to stop the proteolysis, and peptides were desalted using a Sep-Pak C18 cartridge (WAT036945, Waters Corp). The desalted peptides were dried in a vacufuge and reconstituted in 100 µL of 0.1 M TEAB. A TMT10plex Isobaric Label Reagent Set plus TMT11-131C Label Reagent kit (A37725, Thermo Fisher Scientific) was used to label each sample per the manufacturer's protocol. The samples were labeled with TMT 11-plex reagents at room temperature for 1 hour. The reaction was quenched by adding 8 µL of 5% hydroxylamine for 15 min and dried. An offline fractionation of the combined sample into eight fractions was performed using a high pH reverse-phase peptide fractionation kit, as per the manufacturer's protocol (84868,

Pierce). Fractions were dried and reconstituted in 12 µL of 0.1% formic acid/2% acetonitrile for LC-MS/MS analysis.

LC-MS analysis

An Orbitrap Fusion (Thermo Fisher Scientific) and RSLC Ultimate 3000 nano-UPLC (Dionex) were used to acquire the data. For superior quantitation accuracy, we used multinotch-MS3 [139]. Two microliters of each fraction was resolved on a nanocapillary reverse-phase column (75 µm internal diameter by 50 cm; PepMap RSLC C18 column, Thermo Fisher Scientific) at a flowrate of 300 nL/min using 0.1% formic acid/acetonitrile gradient system (2 to 22% acetonitrile in 110 min; 22 to 40% acetonitrile in 25 min; 6-min wash at 90% acetonitrile; 25 min re-equilibration) and directly sprayed onto the Orbitrap Fusion using EasySpray source (Thermo Fisher Scientific). The mass spectrometer was set to collect one MS1 scan [Orbitrap; 120,000 resolution; AGC target 2 × 105; max IT (maximum ionization time) 50 ms] and data-dependent, "Top Speed" (3 s) MS2 scans [collision-induced dissociation; ion trap; NCE (normalized collision energy) 35; AGC (automatic gain control) 5 × 103; max IT 100 ms]. For multinotch-MS3, the top 10 precursors from each MS2 were fragmented by high energy collisional dissociation (HCD), followed by Orbitrap analysis (NCE 55; 60,000 resolution; AGC 5 × 104; max IT 120 ms, 100 to 500 mass/charge ratio scan range).

2.4 Results

2.4.1 $G\alpha_{i1}$ activates and interacts with PRG more effectively than $G\alpha_{i2}$

We have previously shown [97] that $G\alpha_{i1}$ stimulates PRG and subsequent RhoA activation dependent on the activation state of $G\alpha_i$. To mimic that GTP bound state of $G\alpha_i$, a catalytic glutamine was substituted with leucine which strongly inhibits GTP hydrolysis leading to constitutive GTP binding and activation [30, 140-142]. As shown in Figure 2.1B, transient coexpression of $G\alpha_{i1}$ Q204L ($G\alpha_{i1}$ QL), PRG, and an SRE-luciferase plasmid that reports on RhoA activation in HEK293 cells results in significant PRG activation, indicating $G\alpha_{i1}$-mediated RhoA activation through PRG as we previously published.. $G\alpha_{i2}$ Q205L ($G\alpha_{i2}$ QL) only weakly activates PRG activity in the same assay. Concentration-response experiments show a significant difference in the efficacy of PRG activation by $G\alpha_{i1}$ QL and $G\alpha_{i2}$ QL (Figure 2.1C).

To validate PRG-$G\alpha_i$ interactions in cells, we performed a NanoBiT nanoluciferase complementation assay [143], in which the NanoLuc LgBiT was inserted after the αA helix in Gα subunits [144], and NanoLuc SmBiT was appended to the N-terminus of myc-PRG (Figure 2.1D). Coexpressing $G\alpha_{i1}$ QL-LgBiT constructs with SmBiT-PRG in HEK293 cells resulted in an increase in luminescent signal over that for $G\alpha_{i1}$ WT-LgBiT, indicating a nucleotide state-dependent interaction with PRG. This was not observed for QL variants in $G\alpha_{i2}$, $G\alpha_s$, or $G\alpha_q$ (Figure 2.1E). Together, these results show that $G\alpha_{i1}$ interacts with and activates PRG in a GTP-dependent manner, while $G\alpha_{i2}$ is much less efficient in this interaction.

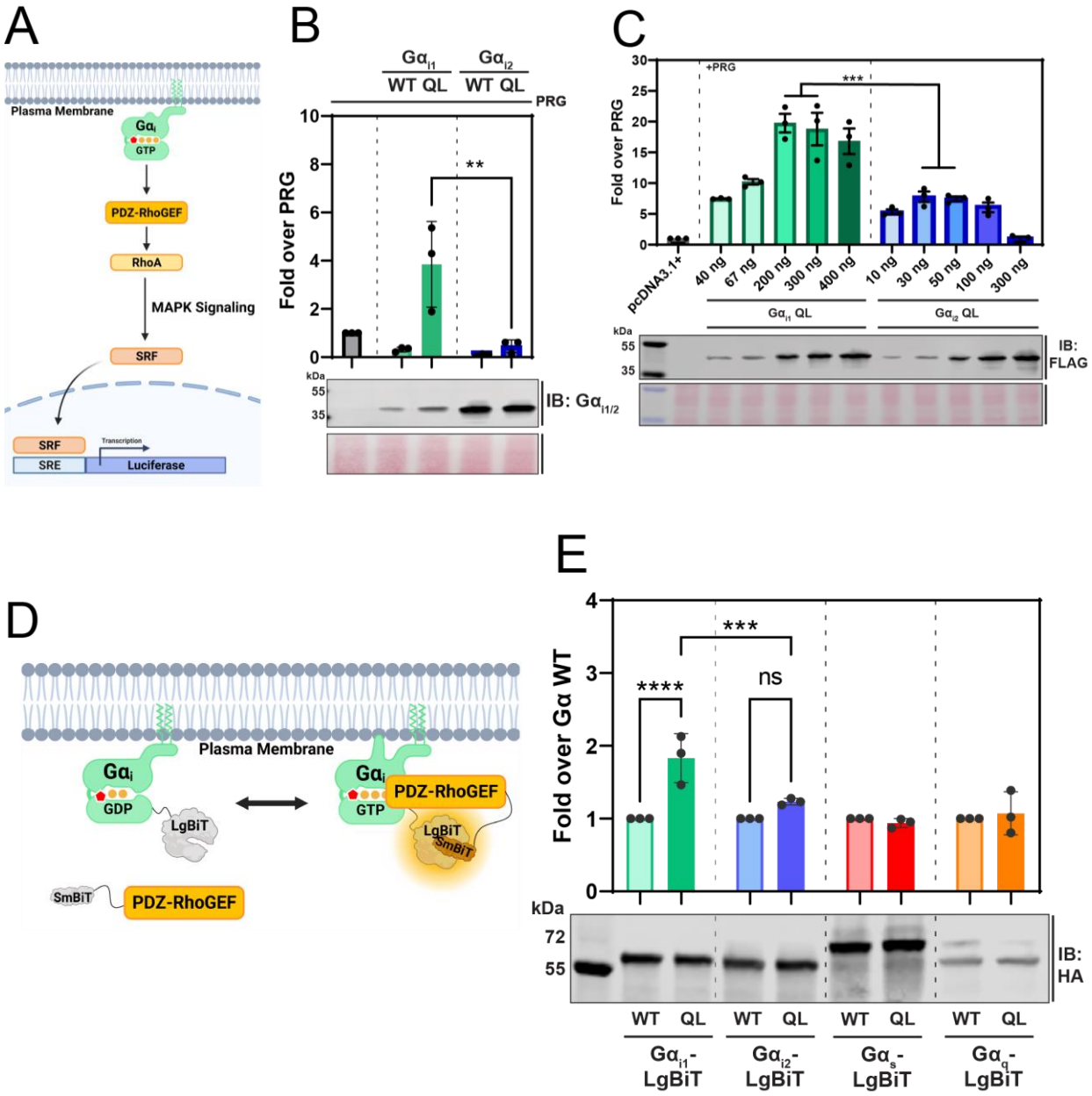
A
Plasma Membrane
Gαi
GTP
PDZ-RhoGEF
RhoA
MAPK Signaling
SRF
SRF
SRE
Transcription
Luciferase
B
Gαi1 WT QL
Gαi2 WT QL
PRG
Fold over PRG
**
kDa
55
35
IB: Gαi1/2
C
+PRG
***
Fold over PRG
pcDNA3.1+
40 ng
67 ng
200 ng
300 ng
400 ng
10 ng
30 ng
50 ng
100 ng
300 ng
Gαi1 QL
Gαi2 QL
kDa
55
35
IB: FLAG
D
Plasma Membrane
Gαi
GDP
LgBiT
Gαi
GTP
PDZ-RhoGEF
LgBiT
SmBiT
SmBiT
PDZ-RhoGEF
E
Fold over Gα WT
****
***
ns
kDa
72
55
IB: HA
WT QL WT QL WT QL WT QL
Gαi1-LgBiT
Gαi2-LgBiT
Gαs-LgBiT
Gαq-LgBiT

Figure 2.1: $G\alpha_{i1}$ more efficiently interacts with PRG than $G\alpha_{i2}$.
A) Diagram of the SRE luciferase used to assess Gα regulation of PRG. HEK293 cells were co-transfected with control plasmid pcDNA3.1+ or Gα plasmids as indicated, PRG, and an SRE luciferase reporter plasmid. 24 h after transfection, One-Glo luciferase reagent was added and luminescence was measured using a plate reader. **B)** Comparison of $G\alpha_{i1}$ and $G\alpha_{i2}$ which were transfected as indicated. All wells were transfected with PRG. Fold over PRG was calculated as the luminescent signal with Gα subunits co-transfected with PRG divided by the signal with PRG co transfected with control pcDNA3.1+ plasmid. Data were analyzed with a one-way ANOVA with Šídák post-test. **C)** Cells were transfected with the indicated amount of FLAG-$G\alpha_{i1}$ QL or FLAG-$G\alpha_{i2}$ QL adjusted to achieve equivalent expression as shown in the FLAG western blot shown in the bottom panel. To calculate the significance in the difference in maximal stimulation, the values for 200 and 300 ng of $G\alpha_{i1}$ plasmid were averaged and compared to the average of the 30 and 50 ng values for $G\alpha_{i2}$. T-test $P<0.001$. **D)** Diagram of the $G\alpha_{i}$-LgBiT complementation assay used with $G\alpha_{i}$ fused to LgBiT and PRG with N-terminal fusion of SmBiT peptide natural peptide sequence (SmBiT-PRG). **E)** The indicated plasmids were co-transfected into HEK293 cells with SmBiT-PRG. 24 h after transfection, cells were transferred into a 96-well plate and furimazine substrate was added for 15 min prior to measurement of luminescence in a plate reader. All experiments were performed with at least three biological replicates of assays performed in triplicate (duplicate technical replicates in C). Unless otherwise indicated, data was analyzed with a one-way ANOVA with a Šídák post-test. ** $P< 0.01$ and **** $P < 0.0001$.

2.4.2 Active $G\alpha_{i2}$ QL BioID weakly engages the proximal interactome relative to $G\alpha_{i1}$ QL BioID

Given their previously known functional overlap, the stark disparity between $G\alpha_{i1}$ and $G\alpha_{i2}$ in their ability to activate PRG prompted us to probe for further examples of selectivity between $G\alpha_i$ subtypes. PRG was initially identified as a novel target of $G\alpha_{i1}$ using unbiased BioID2 proximity labeling coupled to mass spectrometry. BioID2 functionalizes biotin releasing reactive biotinoyl-5'-AMP, which biotinylates proximal lysines within 20 nm [145]. By comparing relative biotinylation by BioID2 fused to either $G\alpha_i$ WT or $G\alpha_i$ QL, we revealed the activated $G\alpha_i$ proximity interactome (Figure 2.2A). Here, we applied this approach to probe the relative interactomes of $G\alpha_{i1}$ and $G\alpha_{i2}$.

Briefly, HA-$G\alpha_{i1}$ Q204L-BioID2 ($G\alpha_{i1}$ QL-BioID), HA-$G\alpha_{i2}$-BioID2 ($G\alpha_{i2}$-BioID), and HA-$G\alpha_{i2}$ Q205L-BioID2 ($G\alpha_{i2}$ QL-BioID) were transiently transfected into HT1080 fibrosarcoma cells and incubated with biotin to allow labeling of proximal proteins by $G\alpha_i$-BioID. After 24 hours of protein expression and biotin labeling, cells were lysed, biotinylated proteins were captured with streptavidin beads, and labeled with isobaric tandem mass tag (TMT) labels. Samples from all experimental groups were then analyzed via LC MS/MS in a single run. Proteins that are statistically significantly enriched in QL vs WT samples are considered proximal interactors. In Figure 2.2B are volcano plots of all the proteins identified with the statistical cutoffs for significance from two different comparisons, $G\alpha_{i1}$ QL/$G\alpha_{i2}$ WT (upper panel) and $G\alpha_{i2}$ QL/$G\alpha_{i2}$ WT (lower panel). We assumed that the WT interactions would be similar between the two subtypes thus $G\alpha_{i2}$ was used as a baseline for both plots. Validation of this assumption is discussed below.

The identities and fold QL/WT enrichment levels for many hits for active $G\alpha_{i1}$-BioID were consistent with those found in our previous screen [97]. Notably, there are no significant observable differences in identity of most of the proteins enriched for interaction with active $G\alpha_{i1}$ QL-BioID vs $G\alpha_{i2}$ QL-BioID. However, the number of proteins identified that reached statistical significance [-log(abundance ratio p-value) $\geq$ 2.0] were markedly fewer in $G\alpha_{i2}$ QL-BioID2 samples than in $G\alpha_{i1}$ QL-BioID2 samples. This is largely because the $G\alpha_{i2}$ QL-BioID2 / $G\alpha_{i2}$ WT-BioID2 fold enrichment was generally lower than for $G\alpha_{i1}$ QL BioID2 (Compare x-axes in Figure 2.2B). These data seem to indicate a difference in overall signaling activity of GTP-bound $G\alpha_{i1}$ compared to GTP-$G\alpha_{i2}$.

To confirm that these observations are not an artifact of the mass spectrometry analysis and that using $G\alpha_{i2}$ WT as a baseline in both plots is valid, verification assays were performed on selected "hits" that showed significant differences between $G\alpha_{i1}$ QL and $G\alpha_{i2}$ QL engagement. Epitope-tagged mammalian expression constructs were transiently coexpressed in HEK293 cells with either $G\alpha_{i1}$-BioID, $G\alpha_{i1}$ QL-BioID2, $G\alpha_{i2}$-BioID2, $G\alpha_{i2}$ QL-BioID2, or membrane-targeted BioID2 (BioID2-CAAX). Exogenous biotin was added for 24 hours, followed by a lysis and streptavidin bead purification. Captured biotinylated protein samples were run on SDS-PAGE and analyzed for pulldown via western blotting using antibodies against the respective affinity tags for the target proteins.

Proteins selected for analysis included several targets that were found in our previous report [97] and represent diverse signaling pathways: PDZ-RhoGEF, α-Parvin (Parvin), Vimentin, Ribosomal protein S6 Kinase A1 (RSK1), Neurofibromin 1 (NF1), and Ras p21 protein activator 2 (RASA2). Proteins including NF1, PRG, and Parvin showed selective enrichment in $G\alpha_{i1}$ QL/WT over $G\alpha_{i2}$ QL/WT (Figure 2.2C). Vimentin and RASA2 showed only a slight preference

for interaction with $G\alpha_{i1}$ QL-BioID over $G\alpha_{i2}$ QL-BioID, while RSK1 did not preferentially interact with either $G\alpha_{i1}$ QL-BioID or $G\alpha_{i2}$ QL-BioID over the WT-BioID variants. These results indicate that many of the proximal interactors found in the proteomic screen are reproducible in an orthogonal assay and are suitable for further analysis in their relationship to $G\alpha_i$. Importantly, the results confirm that nucleotide-dependent interaction with these targets by $G\alpha_{i2}$ is weaker than for $G\alpha_{i1}$.

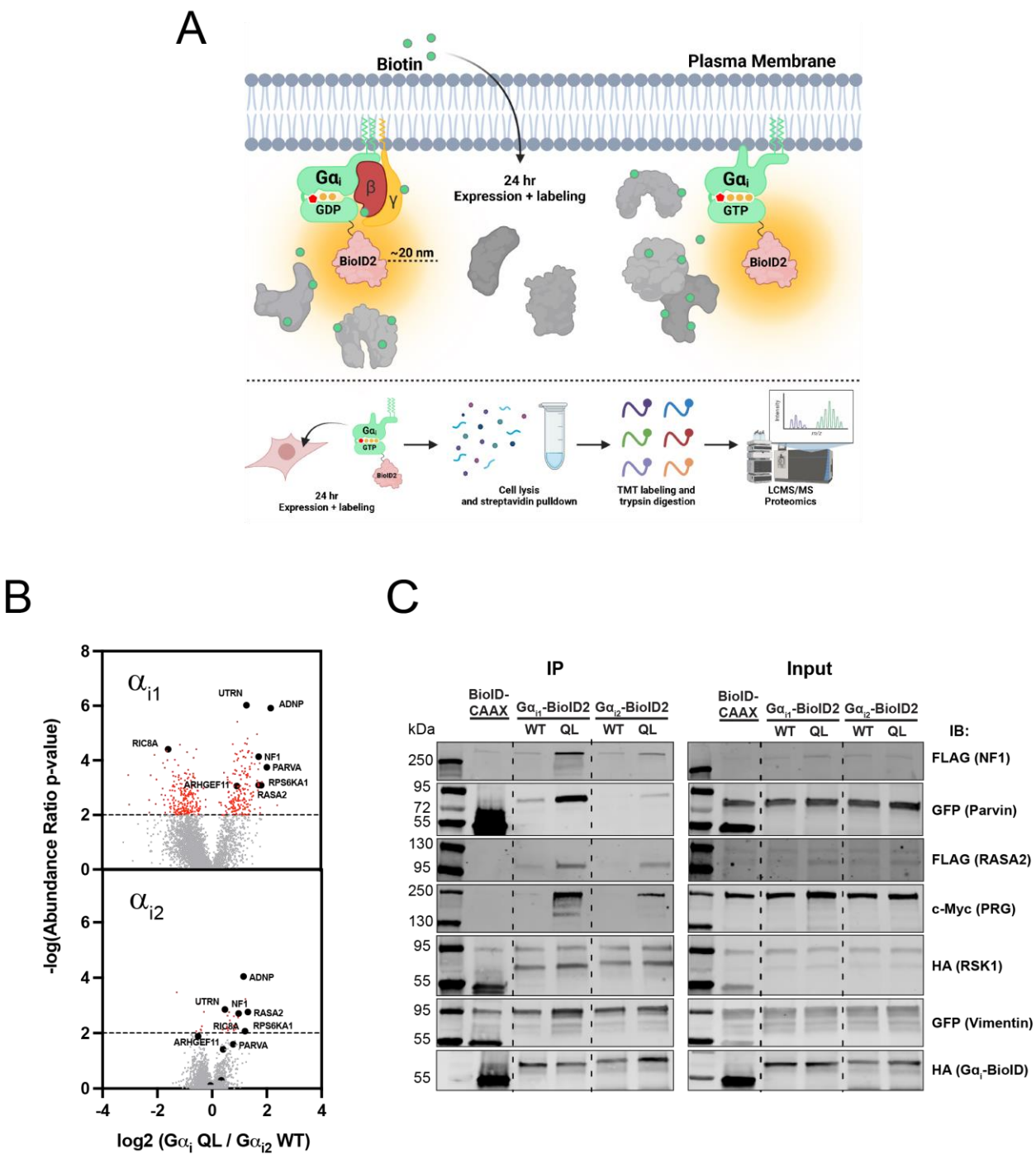

Figure 2.2: Gα$_{i2}$ weakly engages its active state interactome relative to Gα$_{i1}$.
A) Experimental scheme for biotin proximity labeling assays. B) The indicated HA-Gα$_i$-BioID2, or BioID-CAAX constructs were transiently transfected into HT1080 cells, in triplicate for each condition for 24 h followed by isolation of biotinylated proteins and analysis by TMT Mass Spectrometry. Spectral counts were analyzed as the ratio of samples transfected with the Gα$_i$-QL plasmids relative to samples transfected with Gα$_{i2}$ WT. The dashed line indicates a p value of 0.05 and all statistically significant proteins are colored in red. C) The indicated Gα$_i$-BioID2 constructs were co-transfected with the indicated epitope-tagged protein into HEK293 cells. 24 h after transfection biotinylated proteins were isolated with streptavidin beads and the followed by western blotting to determine the amount of biotinylated target protein pulled down. Shown is a representative western blot of an experiment performed twice.

2.4.3 Substitution of the $G\alpha_{i1}$ helical domain (HD) into $G\alpha_{i2}$ is sufficient for activation of PRG

To understand the molecular determinants that drive specificity of activation of PRG by $G\alpha_{i1}$, and perhaps by extension other targets, we first mapped the amino acid differences between the $G\alpha_i$ subfamily onto a crystal structure of $G\alpha_{i1}$ bound to a GTP analogue, GPPNHP (PDB 1CIP). There are 44 non-identical residues between $G\alpha_{i1}$ and $G\alpha_{i2}$, with 33 of these residues being common between $G\alpha_{i1}$ and $G\alpha_{i3}$. We identified the helical domain (HD) of $G\alpha_i$ as the region of greatest divergence between $G\alpha_i$ subtypes (Figure 2.7A), containing 21 of the differences between $G\alpha_{i1}$/$G\alpha_{i3}$ and $G\alpha_{i2}$. As an initial approach, we substituted the entire HD of $G\alpha_{i1}$ (residues 62-167) into the corresponding position in $G\alpha_{i2}$, resulting in the chimeric $G\alpha_i$ protein Gαi2-1HD (Figure 2.3A). This chimera is expressed in HEK293 cells and functionally inhibits forskolin-dependent cAMP generation by adenylyl cyclase (Figure 2.3C and 2.3D). Gαi2-1HD or Gαi2-1HD Q205L (QL) were then transfected into HEK293 cells in the SRE-luciferase reporter assay to examine their ability to activate PRG. Strikingly, Gαi2-1HD QL expression results in strong activation of PRG as compared to $G\alpha_{i2}$ QL (Figure 2.3B), indicating that the HD of $G\alpha_{i1}$, when substituted into $G\alpha_{i2}$, is sufficient to confer nucleotide-dependent activation of PRG.

The striking increase in PRG activation observed with substitution of the $G\alpha_{i1}$ HD into $G\alpha_{i2}$ prompted us to test the interaction of these $G\alpha_{i2}$ variants with other protein targets from the BioID proximity labeling screen. We tested multiple targets for activation-dependent labeling using the proximity labeling-dependent western blotting assay with the WT and QL versions of $G\alpha_{i1}$, $G\alpha_{i2}$ and Gαi2-1HD (Figure 2.3E). The western blots comparing $G\alpha_{i1}$-BioID2 and $G\alpha_{i2}$-BioID2 are the same as in Figure 2.2C but here we included Gαi2-1HD-BioID2. Substitution of the $G\alpha_{i1}$ HD into $G\alpha_{i2}$ partially rescues the QL-dependent labeling of some of these targets. Parvin shows the most striking rescue while NF1, PRG and vimentin show some degree of rescue. RASA2, which does

not show a preference for $G\alpha_{i1}$ vs. $G\alpha_{i2}$, is not affected by the HD substitution. These data support the idea that the structural differences conferred by the HD of the $G\alpha_i$ subunits are important for differences in general target engagement beyond PRG.

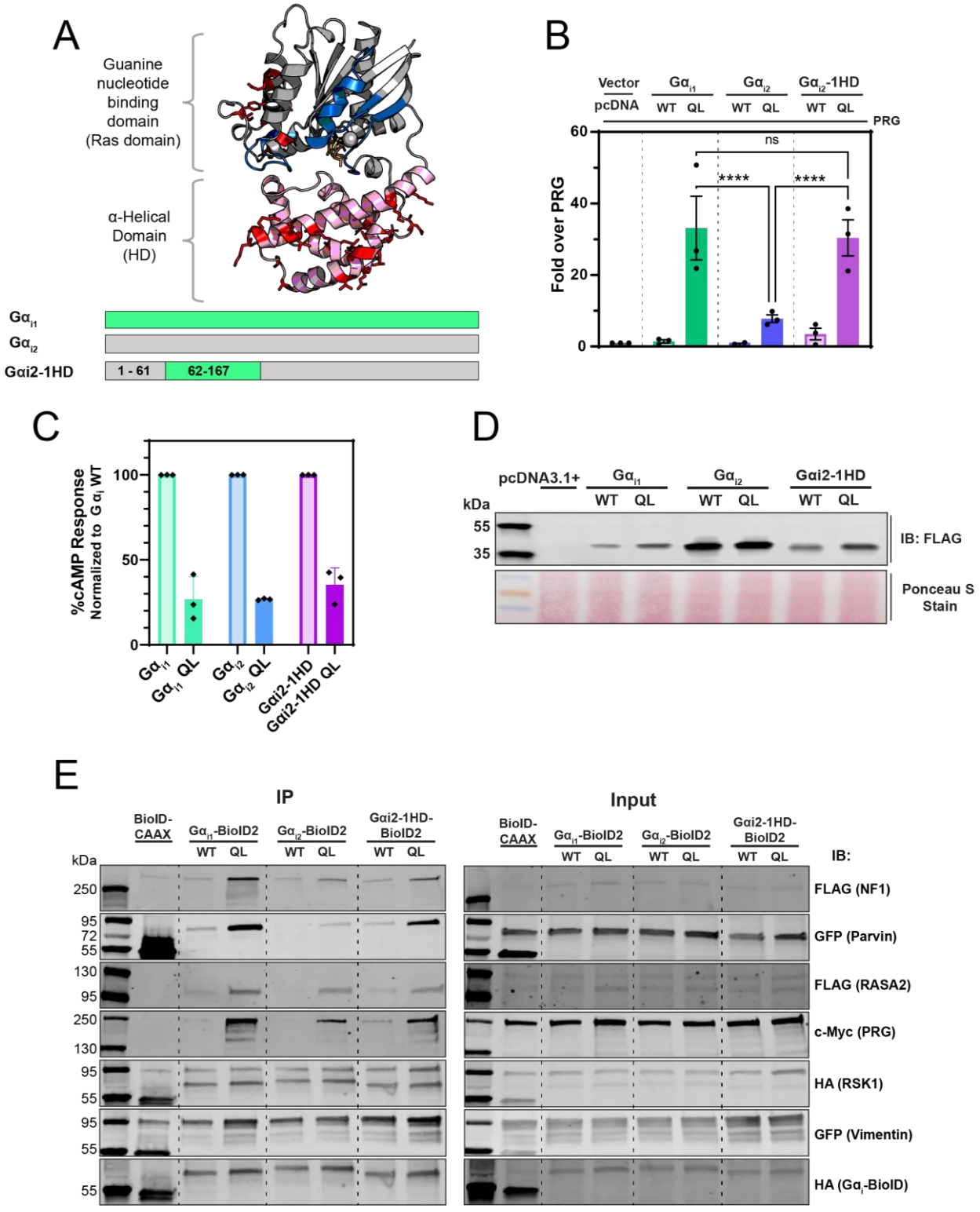
A
Guanine nucleotide binding domain (Ras domain)
α-Helical Domain (HD)
Gαi1
Gαi2
Gαi2-1HD
1 - 61
62-167
B
Vector pcDNA
Gαi1 WT QL
Gαi2 WT QL
Gαi2-1HD WT QL
PRG
Fold over PRG
ns
****
****
C
%cAMP Response Normalized to Gαi WT
Gαi1
Gαi1 QL
Gαi2
Gαi2 QL
Gαi2-1HD
Gαi2-1HD QL
D
pcDNA3.1+
Gαi1 WT QL
Gαi2 WT QL
Gαi2-1HD WT QL
kDa
IB: FLAG
Ponceau S Stain
E
IP
Input
BioID-CAAX
Gαi1-BioID2 WT QL
Gαi2-BioID2 WT QL
Gαi2-1HD-BioID2 WT QL
kDa
IB:
FLAG (NF1)
GFP (Parvin)
FLAG (RASA2)
c-Myc (PRG)
HA (RSK1)
GFP (Vimentin)
HA (Gαi-BioID)

Figure 2.3: Substitution of the $G\alpha_{i1}$ helical domain into $G\alpha_{i2}$ partially restores activation of PRG and active state proteome engagement.
A) Diagrammatic representation of the $G\alpha_{i1}$ structure. In light pink is the helical domain. Switch I-III are in blue. Red stick amino acids are amino acids conserved between $G\alpha_{i1}$ and $G\alpha_{i3}$ but not $G\alpha_{i2}$. PDB: 1CIP. In the domain schematic below, $G\alpha_{i1}$ is green, while $G\alpha_{i2}$ is grey. **B)** The indicated constructs were co-transfected with PRG and SRE-Luc and the assay was performed as in Fig. 2.1. **C)** cAMP assay measuring forskolin-stimulated AC inhibition. HEK293 cells were seeded in a 96-well plate and transfected with $G\alpha_i$ WT or QL and GloSensor -20F cAMP sensor (Promega). D-luciferin is added and forskolin-stimulated cAMP generation is measured via luminescence from the GloSensor. Plotted is the percent activity of each $G\alpha_i$ QL sample signal relative to its own $G\alpha_i$ WT variant signal after 20 mins. **D)** Western blot for expression of $G\alpha_i$ in B) and C). **E)** The indicated $G\alpha_i$ constructs were co-transfected into HEK293 cells with the indicated epitope-tagged constructs and analyzed as in Fig. 2.2C. The $G\alpha_{i1}$ and $G\alpha_{i2}$ two western blots are the same as in Fig. 2.3E with Gαi2-1HD added for comparison. Shown is a representative western blot of an experiment performed twice. All SRE-Luc experiments were performed with 3 biological replicates performed in triplicate. Data are +/-SEM analyzed by One-way ANOVA with Šídák post-test. **** P<0.0001.

2.4.4 PRG activation by $G\alpha_{i1}$ is conferred by an intact helical domain

To identify structural elements within the $G\alpha_{i1}$ HD that confer PRG activation, the domain was subdivided into three segments consisting of 1) The Gα αA helix, 2) αB – αC helices, and 3) αD – αE helices (Figure 2.4A and 2.4B). Each of these subdivisions of the $G\alpha_{i1}$ HD were then substituted into their cognate positions in $G\alpha_{i2}$ as done previously. None of these subdivisions of $G\alpha_{i1}$, when substituted into $G\alpha_{i2}$, activate PRG in cells more than $G\alpha_{i2}$ Q205L (Figure 2.4C), but were expressed and able to inhibit cAMP generation by adenylyl cyclase (Figure 2.4D and 2.4E). We also substituted the N and C-terminal domains of $G\alpha_{i1}$ flanking the HD into $G\alpha_{i2}$, creating Gαi1N-2HDC and Gαi2NHD-1C (Figure 2.5A and 2.5B). Despite being able to inhibit Fsk-dependent cAMP production (Figure 2.5C and 2.5D), neither of the QL variants of these constructs were able to activate PRG when coexpressed in HEK293 cells as measured in the SRE-luc reporter assay (Figure 2.5A and 2.5B).

These data suggest that $G\alpha_{i1}$-mediated activation of PRG relies on some intrinsic property of the intact $G\alpha_{i1}$ HD rather than one residue or a subset of residues within the $G\alpha_{i1}$ HD. It is possible that the $G\alpha_{i1}$ HD does participate in direct binding interactions with PRG, but also confers specificity through regulation of some other region of $G\alpha_i$.

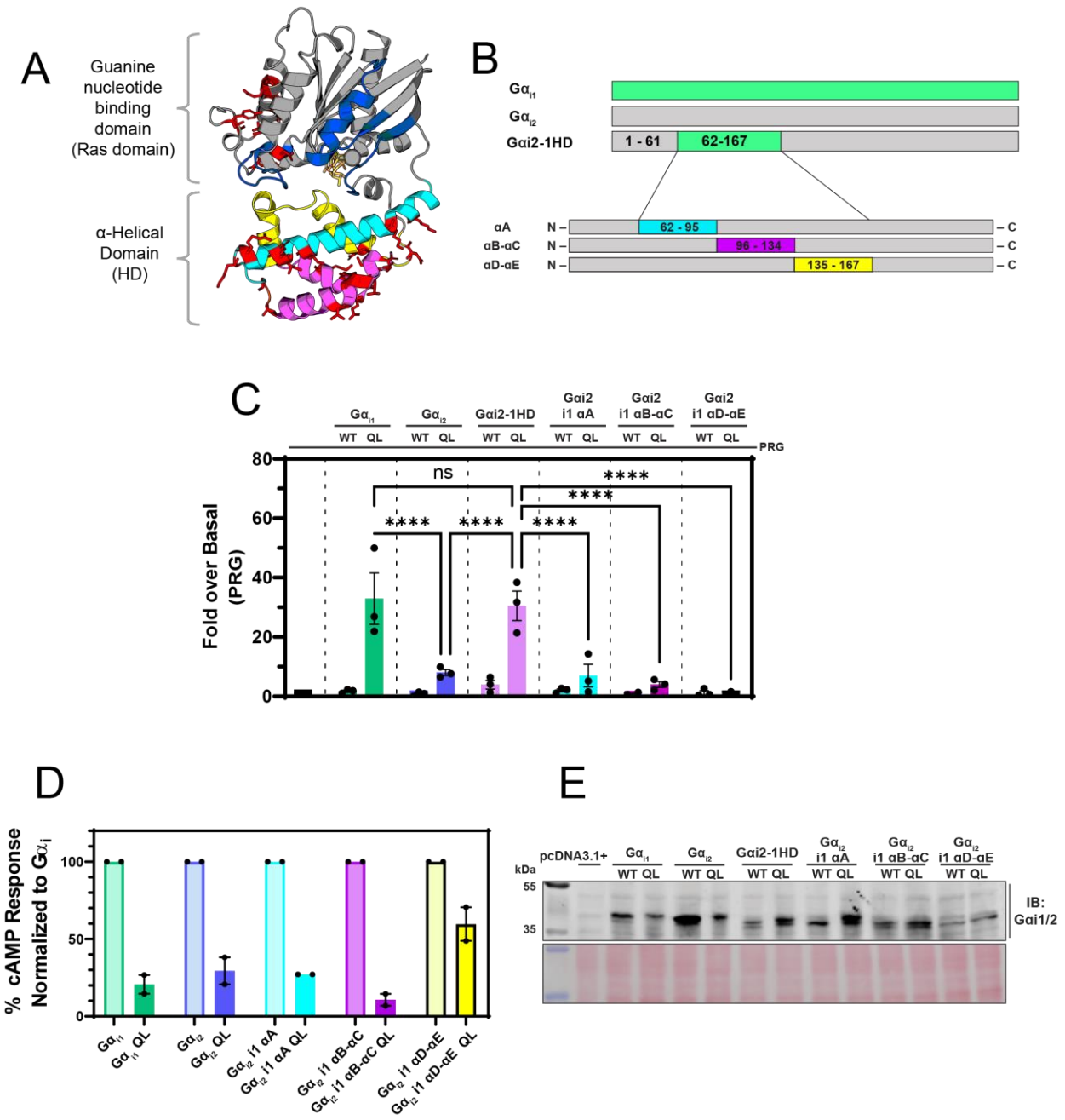

Figure 2.4: $G\alpha_{i1}$ helical domain subdivisions are not sufficient for PRG activation when substituted in to $G\alpha_{i2}$. **A)** Diagrammatic representation of the $G\alpha_{i1}$ structure. In cyan, magenta, and yellow are subdivisions of the helical domain. Switch I-III are in blue. Red stick amino acids are amino acids conserved between $G\alpha_{i1}$ and $G\alpha_{i3}$ but not $G\alpha_{i2}$. PDB: 1CIP. **B)** Diagram of the constructs used in these experiments. **C)** The indicated constructs were co-transfected with PRG and SRE-Luc and the assay was performed as in Fig. 2.1. Shown is the mean +/- SEM form three separate biological replicates, at least three technical replicates each. **D)** The constructs in B) transfected in the cAMP assay performed as in Fig. 2.3C. Data are mean +/- SEM from two biological replicates, three technical replicates each. **E)** Representative western blot showing expression of HD subdivision constructs. All data were analyzed by One-way ANOVA with Šídák post-test. **** P<0.0001.

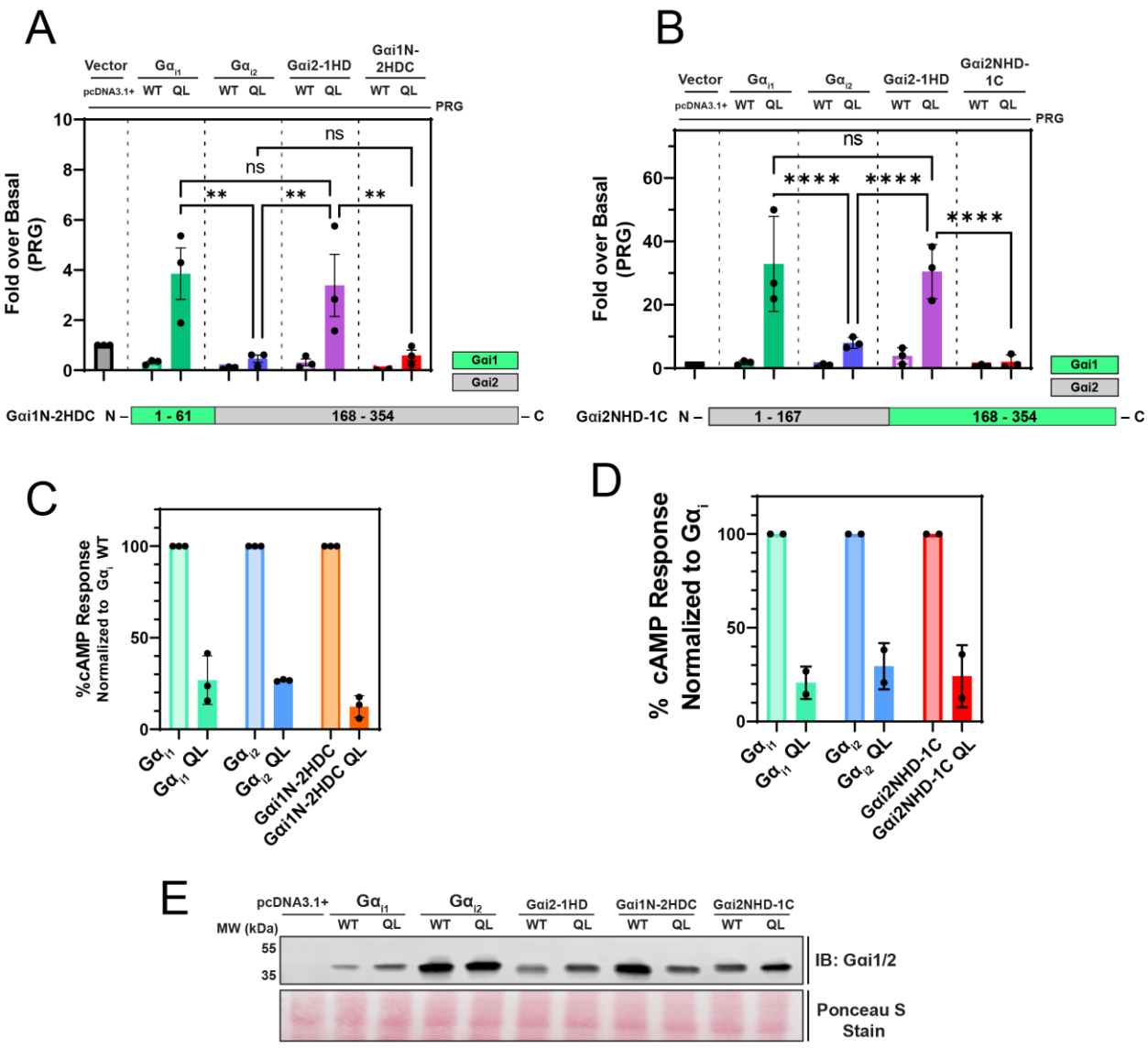

Figure 2.5: Gα$_{i1}$ terminal sections are not sufficient for PRG activation when substituted into Gα$_{i2}$.
Asdf **A)** and **B)** The indicated N- or C-terminal Gα$_{i1}$ regions were substituted into Gα$_{i2}$ and co-transfected with PRG and SRE-Luc and the assay was performed as in Fig. 2.1. Shown is the mean +/- SEM form three separate biological replicates, at least three technical replicates each. Diagrams of substitutions are displayed below each graph, regions from Gαi1 are green and from Gαi2 are grey. **C)** and **D)** The constructs in A) and B) transfected in the cAMP assay performed as in Fig. 2.3C. Data are mean +/- SEM from at least two biological replicates, three technical replicates each. **E)** Representative western blot showing expression of Gα$_i$ constructs. Data were analyzed by One-way ANOVA with Šídák post-test. ** P < 0.01, **** P < 0.0001.

2.4.5 Amino Acid Substitutions at the Domain Interface Impact PRG Activation by $G\alpha_i$

Since we were not able to find a specific region of the HD involved in PRG regulation, we considered that the HD may be cooperating with the RLD to confer PRG activation. In an existing co-crystal structure of $G\alpha_{13}$ bound to the rgRGS domain of PRG [146], a sequence of PRG amino acids is bound at the $G\alpha_{13}$ HD-RLD domain interface. We hypothesized that this paradigm may extend to PRG interactions with $G\alpha_{i1}$ as well. We substituted the various subdivisions of the $G\alpha_{i1}$ HD described in Figure 2.4B and the C-terminal portion of the Ras-like domain of $G\alpha_{i1}$ into $G\alpha_{i2}$ and tested them for PRG activation. Interestingly, one chimera, Gαi2-i1 αA+CT, showed levels of PRG activation consistent with $G\alpha_{i1}$ QL and above that of Gαi2-i1 αA (Figure 2.6D). This suggests that the HD may cooperate with the RLD to confer the ability to interact with PRG.

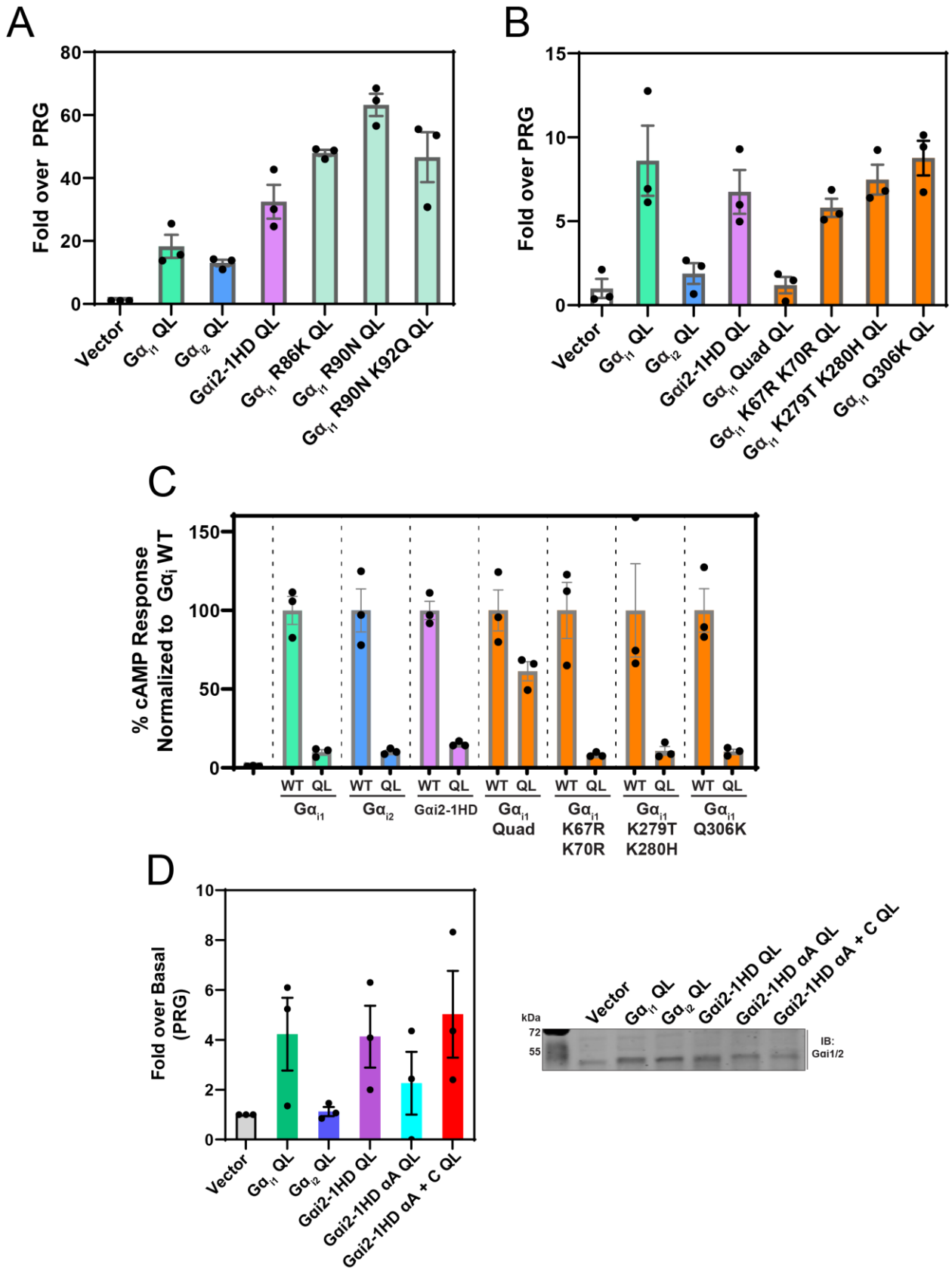
A
Fold over PRG
80
60
40
20
0
Vector
Gαi1 QL
Gαi2 QL
Gαi2-1HD QL
Gαi1 R86K QL
Gαi1 R90N QL
Gαi1 R90N K92Q QL
B
Fold over PRG
15
10
5
0
Vector
Gαi1 QL
Gαi2 QL
Gαi2-1HD QL
Gαi1 Quad QL
Gαi1 K67R K70R QL
Gαi1 K279T K280H QL
Gαi1 Q306K QL
C
% cAMP Response Normalized to Gαi WT
150
100
50
0
WT QL
Gαi1
Gαi2
Gαi2-1HD
Gαi1 Quad
Gαi1 K67R K70R
Gαi1 K279T K280H
Gαi1 Q306K
D
Fold over Basal (PRG)
10
8
6
4
2
0
Vector
Gαi1 QL
Gαi2 QL
Gαi2-1HD QL
Gαi2-1HD αA QL
Gαi2-1HD αA + C QL
kDa
72
55
IB: Gαi1/2

Figure 2.6: **Substitution of $G\alpha_{i1}$ Ras-like domain and helical domain elements into $G\alpha_{i2}$ confers the ability to activate PRG.**
$G\alpha_i$ constructs with substitutions of $G\alpha_{i2}$ residues into $G\alpha_{i1}$ in the **A)** αA helix and **B)** C-terminus were co-transfected with PRG and SRE-Luc in HEK293 cells and assayed as in Fig. 2.1. Data shown are representative of two biological replicates with three technical replicates each. Signal for each sample is ratio normalized to signal from pcDNA3.1 + PRG co-transfected samples. **C)** C-terminal $G\alpha i_1$ point mutants were co-transfected with GloSensor -20F and assayed as in Fig. 2.3. **D)** $G\alpha_{i1}$ αA helix and C-terminal segment were substituted into $G\alpha_{i2}$ and co-transfected in the SRE-Luc reporter assay as previously described. Mean +/- SEM for three separate biological replicates is shown, three technical replicates each. Western blot shown is representative of expression in assays performed.

2.4.6 Residue A230 in $G\alpha_{i2}$ controls PRG activation and leads to enhanced proximity interactome engagement

Based on the idea that the RLD may also contribute to PDZ-RhoGEF by $G\alpha_{i1}$, we selected various point substitutions to make in $G\alpha_{i1}$ that were similar in $G\alpha_{i3}$ but different in $G\alpha_{i2}$ with the expectation that these may reduce PRG activation. Substitutions along the αA helix included R86K, R90N, R92Q, K67R, and K70R, while additional substitutions in the C-terminal portion of the RLD included K279T, K280H, Q306K, and four local simultaneous substitutions denoted as "Quad": A291T, S293A, T295K, and E297D. None of the αA subsitutions caused a decrease in PRG activity via the SRE-Luc assay (Figure 2.6A and 2.6B). Neither did the K67R/K70R double mutant, the K279T/K280H double mutant, or the Q306K mutant, despite inhibiting Fsk-dependent cAMP generation (Figure 2.6C).

However, substitution of $G\alpha_{i2}$ A230 with Asp surprisingly confers $G\alpha_{i2}$ QL the ability to activate PRG (Figure 2.7C), while the reverse substitution of D229 to Ala in $G\alpha_{i1}$ blunts PRG activation (Figure 2.7B). This residue position is also known as s4h3.3 in the common Gα numbering system (CGN) proposed by Flock et al. [147], and will be used interchangeably henceforth. The $G\alpha_{i2}$ A230D substitution also confers to $G\alpha_{i2}$ the ability to interact with PRG in a nucleotide-dependent manner in the NanoBiT complementation assay (Figure 2.7D). From these data, it appears that both the A230D and the $G\alpha_{i1}$ HD substitutions confer nearly full rescue of the

ability to activate PRG. To examine the relative contributions of these substitutions more closely, we reduced the concentrations of the transfected Gα subunit plasmids to the EC_{50} concentration for $G\alpha_{i1}$ shown in Figure 2.1C. At these concentrations, neither $G\alpha_{i2}$ A230D QL nor Gai2-1HD QL significantly activate PRG over that seen for $G\alpha_{i2}$, but when combined in the same construct, strongly activate PRG (Figure 2.7G). This provides evidence that these two regions cooperate to confer PRG activation.

Next, we chose two of the other targets that show differential $G\alpha_{i1}$ and $G\alpha_{i2}$ engagement in the proximity labeling western blot assay, NF1 and Parvin, and performed the same assay comparing $G\alpha_{i1}$-BioID2, $G\alpha_{i2}$-BioID2 and $G\alpha_{i2}$ A230D-BioID2 (Figure 2.7H). The A230D substitution enhances the engagement of Ga_{i2} with these other targets. These data support the idea that the structural differences conferred by either the HD or $G\alpha_{i2}$ $A230^{s4h3.3}$ / $G\alpha_{i1}$ $D229^{s4h3.3}$ of the $G\alpha_{i}$ subunits are important for differences in general target engagement beyond PRG.

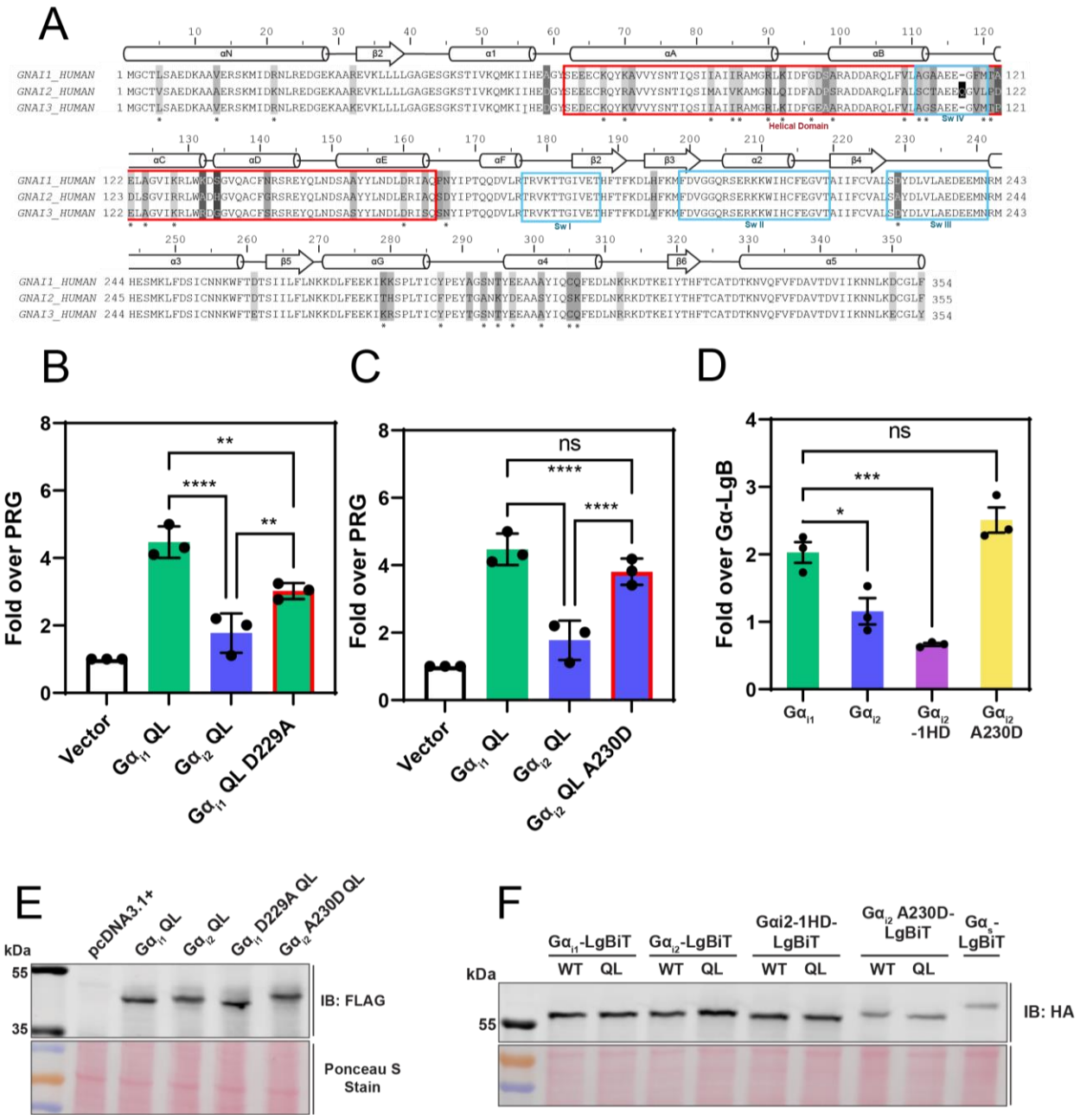
A
GNAI1_HUMAN
GNAI2_HUMAN
GNAI3_HUMAN
Helical Domain
Sw I
Sw II
Sw III
Sw IV
B
Fold over PRG
Vector
Gαi1 QL
Gαi2 QL
Gαi1 QL D229A
C
Fold over PRG
ns
Vector
Gαi1 QL
Gαi2 QL
Gαi2 QL A230D
D
Fold over Gα-LgB
ns
Gαi1
Gαi2
Gαi2 -1HD
Gαi2 A230D
E
kDa
pcDNA3.1+
Gαi1 QL
Gαi2 QL
Gαi1 D229A QL
Gαi2 A230D QL
55
35
IB: FLAG
Ponceau S Stain
F
kDa
Gαi1-LgBiT
Gαi2-LgBiT
Gαi2-1HD-LgBiT
Gαi2 A230D-LgBiT
Gαs-LgBiT
WT
QL
55
IB: HA

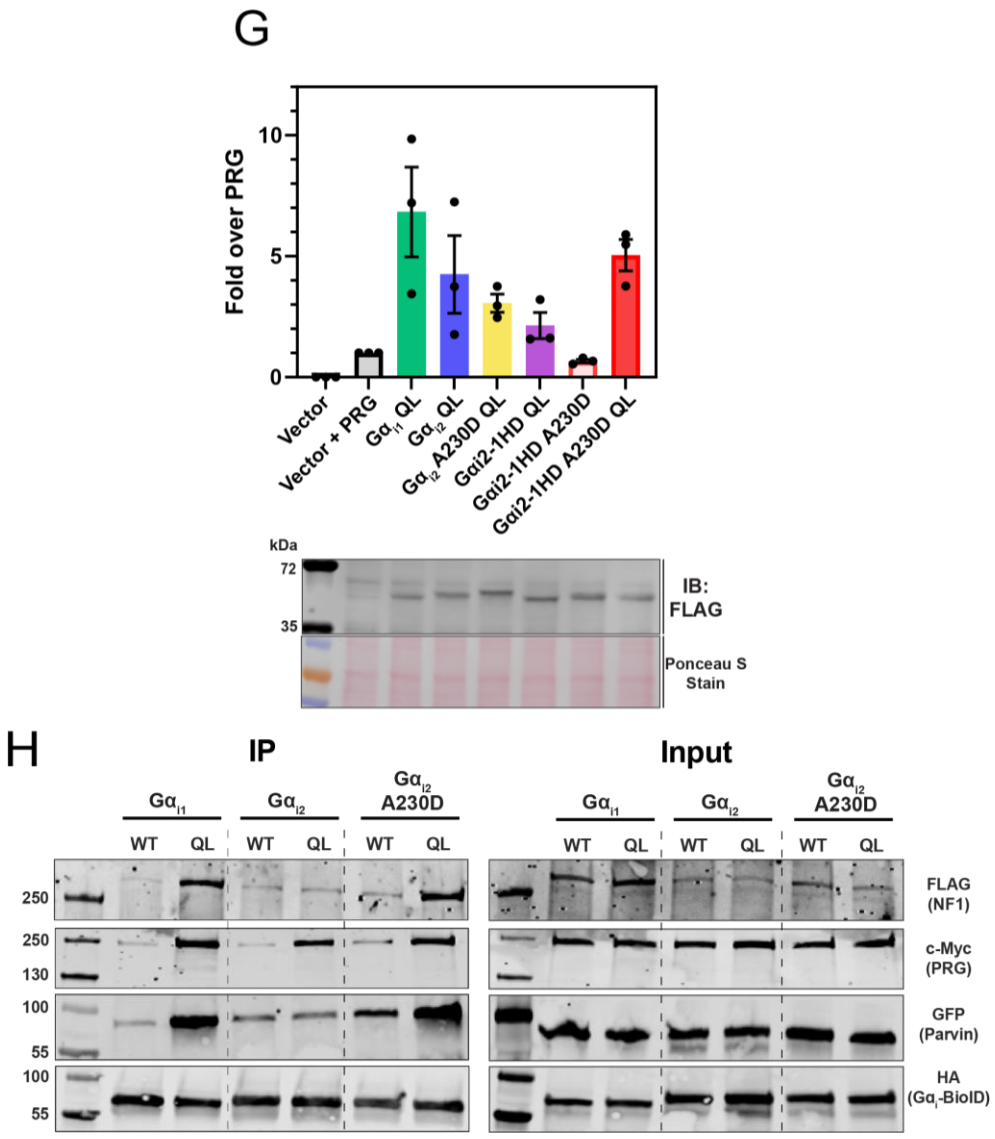

Figure 2.7: Gαi1 D229/Gαi2 A230 in the Ras-like domain is critical for differences in PRG activation.
A) Alignment of human $G\alpha_{i1}$, $G\alpha_{i2}$, and $G\alpha_{i3}$. In blue are the $G\alpha_i$ switch regions. The helical domain is boxed in red. Starred (*) amino acids are identical in $G\alpha_{i1}$ and $G\alpha_{i3}$ but different in $G\alpha_{i2}$. **B)** Mutation of $G\alpha_{i1}$ D229 to the corresponding A in $G\alpha_{i2}$ (A230) reduces the ability to activate PRG. **C)** Mutation of $G\alpha_{i2}$ A230 to the corresponding D in $G\alpha_{i1}$ (D229) enhances the ability of $G\alpha_{i2}$ to activate PRG. **D)** Mutation of $G\alpha_{i2}$ A230 to the corresponding D in $G\alpha_{i1}$ (D229) enhances interactions between $G\alpha_{i2}$-LgBiT and PRG-SmBiT in the luciferase complementation assay. **E)** Western blot analysis for transfected FLAG-$G\alpha_i$ in samples used in B) and C). **F)** Western blot for HA-Gα-LgBiT constructs transfected and expressed in samples in D). **G)** $G\alpha_{i1}$, $G\alpha_{i2}$, $G\alpha_{i2}$ A230D, Gαi2-1HD, and Gαi2-1HD A230D, each QL variants, were transfected to achieve similar protein levels to the half-maximal signal from $G\alpha_{i1}$ QL in the SRE-Luc assay. Substitution of the $G\alpha_{i1}$ HD and A230D combined in $G\alpha_{i2}$ show potent activation of PRG at this concentration, while $G\alpha_{i2}$ A230D QL or Gαi2-1HD QL alone do not. Representative western blot from assay samples showing $G\alpha_i$ expression is shown below. **H)** Mutation of $G\alpha_{i2}$ A230 to the corresponding D in $G\alpha_{i1}$ (D229) enhances interactions with other proteins in the $G\alpha_i$ proximity interactome. Shown is representative western blot for an experiment performed twice. All SRE-luc and complementation experiments were performed with 3 biological replicates performed in triplicate. Data are +/- SEM analyzed by One-way ANOVA with Šídák post-test; * $P < 0.05$, ** $P < 0.01$, *** $P < 0.001$, **** $P < 0.0001$.

2.4.7 $G\alpha_{i1}$ and $G\alpha_{i2}$ sample distinct conformations

Examination of the 3-dimensional structure of $G\alpha_{i1}$ does not clearly indicate why substitution at the D229/A230$^{s4h3.3}$ position, or substitution of the $G\alpha_{i1}$ HD, would impact binding and/or activation of target proteins. This amino acid is near the GTP binding site but is not involved in interactions with the nucleotide, and the closest residue in the HD is 6Å away (Figure 2.8A). To capture potential interactions not observable in these structures, we performed molecular dynamics simulations with GTP-bound $G\alpha_{i1}$ and $G\alpha_{i2}$ with PDB: 1CIP as starting structures. Principal component analysis was used to characterize the dynamic motions in each protein. Principle Component 1 (PC1) in both proteins is rotation of the HD and RLD relative to one another (Appendix Videos 1 and 3). Principle Component 2 (PC2) is as an "opening" motion where the HD opens relative to the RLD via the interdomain hinge region (Appendix Videos 2 and 4). This indicates that even when bound to GTP, some degree of domain opening is possible.

Plots of the two principal components show $G\alpha_{i1}$ and $G\alpha_{i2}$ having similar coordinates in the PC1 axis, but there is a large difference in PC2 between these two subunits, signifying that domain opening in the activated, GTP-bound state is more pronounced in $G\alpha_{i2}$ than in $G\alpha_{i1}$ (Figure 2.8C, top panel). When these simulations were done with $G\alpha_{i1}$ D229A, PC2 moved closer to that of $G\alpha_{i2}$. Similarly, with the A230D substitution in $G\alpha_{i2}$, PC2 moves closer to that of $G\alpha_{i1}$ (Figure 2.8C bottom panel).

To understand the inter-residue interactions responsible for the differences in domain opening between these G protein subtypes, we focused our analysis to the interdomain interface, where residue contact analysis revealed differential interactions between residues in Switch III and the αD-αE region of the HD in $G\alpha_{i1}$ compared to $G\alpha_{i2}$ (Figure 2.8D). In $G\alpha_{i1,}$ two key residues in the HD are involved in an interaction network at the HD-RLD interface, Q147$^{hdhe.2}$ and R144$^{HD.11}$.

In our simulations during dynamic rotation of the HD-RLD interface, R144$^{HD.11}$ dynamically interacts with residues D229$^{s4h3.3}$, D231$^{s4h3.5}$, L232$^{s4h3.6}$, and S228$^{s4h3.2}$ in the Switch III region of the RLD, interactions that are not evident the crystal structure (Figure 2.8A). These interactions are largely absent in $G\alpha_{i2}$. In $G\alpha_{i2}$, the cognate residue for $G\alpha_{i1}$ D229 is A230, and substitution of A230 with D partially restores many of the interdomain residue interactions with Switch III that are absent in $G\alpha_{i2}$ relative to $G\alpha_{i1}$ (Figure 2.8D). Similarly, HD residue Q147$^{hdhe.2}$ interacts more frequently with A235$^{s4h3.9}$, R242$^{H3.1}$, and V233$^{s4h3.7}$ in $G\alpha_{i1}$ than the cognate interactions in $G\alpha_{i2}$. When $G\alpha_{i2}$ A230$^{s4h3.3}$ is substituted with D interactions between Q148$^{hdhe.2}$ and V234$^{s4h3.7}$ are strengthened, with other contacts are largely unaffected. This supports the idea that $G\alpha_{i1}$ D229, while not directly interacting with Switch III, stabilizes a network of interactions between the HD and Switch III that are lost in $G\alpha_{i2}$.

As another approach, a fingerprint matrix of Switch III-HD residue contacts was constructed using data from the simulations. Bayesian Network Analysis was performed on this matrix, yielding a full Bayesian network for these contacts. Nodes were then ranked by strength to understand their cooperativity ranking within the network. This analysis shows that interactions between D229 in the RLD and R144 in the HD forms the core of a cooperativity network involving multiple contacts in Switch III (Figure 2.8F, left panel). This interaction network is disrupted in $G\alpha_{i2}$ where the D229 cognate residue is alanine ($G\alpha_{i2}$ A230) which cannot interact with the positively charged arginine ($G\alpha_{i2}$ R145$^{HD.11}$) (Figure 2.8F, center panel). Substitution of A230 with D in $G\alpha_{i2}$ restores a cooperative interaction network with Switch III (Figure 2.8F, right panel). This analysis supports the idea that in GTP-bound $G\alpha_{i1}$, D229 at the base of Switch III forms an important contact with R144 in the HD that is not observed in crystal structures of $G\alpha_{i1}$. This interaction supports network of additional interactions between the HD and multiple amino acids

in Switch III that constrain the conformation of Switch III. This network does not form in $G\alpha_{i2}$, permitting Switch III to adopt conformations other than that seen in $G\alpha_{i1}$**,** leading to lower-efficacy interactions with effectors that require Switch III for activation.

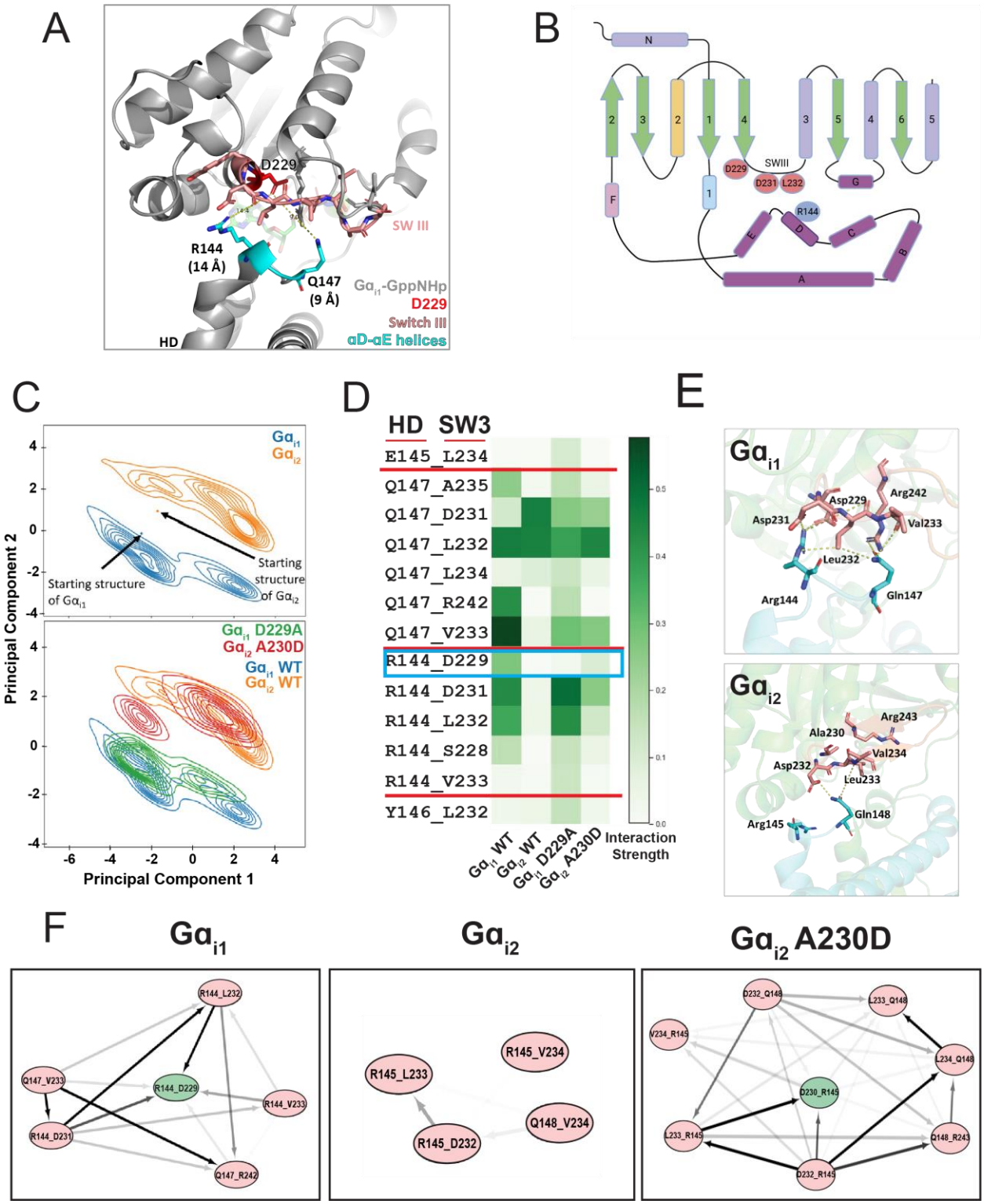
A
D229
SW III
R144
(14 Å)
Q147
(9 Å)
Gαi1-GppNHp
D229
Switch III
αD-αE helices
HD
B
N
SWIII
D229
D231
L232
R144
C
D
E
A
C
Gαi1
Gαi2
Starting structure of Gαi1
Starting structure of Gαi2
Gαi1 D229A
Gαi2 A230D
Gαi1 WT
Gαi2 WT
Principal Component 2
Principal Component 1
D
HD SW3
E145_L234
Q147_A235
Q147_D231
Q147_L232
Q147_L234
Q147_R242
Q147_V233
R144_D229
R144_D231
R144_L232
R144_S228
R144_V233
Y146_L232
Gαi1 WT
Gαi2 WT
Gαi1 D229A
Gαi2 A230D
Interaction Strength
E
Gαi1
Asp229
Arg242
Asp231
Val233
Leu232
Arg144
Gln147
Gαi2
Arg243
Ala230
Val234
Asp232
Leu233
Gln148
Arg145
F
Gαi1
Gαi2
Gαi2 A230D
R144_L232
Q147_V233
R144_D229
R144_V233
R144_D231
Q147_R242
R145_V234
R145_L233
Q148_V234
R145_D232
D232_Q148
L233_Q148
V234_R145
L234_Q148
D230_R145
L233_R145
Q148_R243
D232_R145

Figure 2.8: Molecular dynamics analysis reveals an interaction network that is not apparent in three-dimensional crystal structures in the GTP bound state.
A) Diagram of a structure of $G\alpha_{i1}$-GTP showing the distance between D229 and the nearest HD residues. **B)** Ribbon representation of Gα subunit structure highlighting key amino acids at the Switch III-helical domain interface. **C)** Principal component analysis of $G\alpha_{i1}$-GTP vs. $G\alpha_{i2}$-GTP. **D)** Interaction frequency plot of amino acid interactions between Switch III amino acids and amino acids in the HD comparing the GTP bound states of $G\alpha_{i1,}$ $G\alpha_{i2}$, $G\alpha_{i1}$ D229A, and $G\alpha_{i2}$ A230D. **E)** Diagram of interdomain interactions involving D229 in $G\alpha_{i1}$-GTP (top panel) and A230 in $G\alpha_{i2}$-GTP (bottom panel). **F)** Bayesian networks showing interdomain interactions driven by D229 and HD R144 in $G\alpha_{i1}$-GTP (left panel), In $G\alpha_{i2}$ A230 cannot interact with R145, weakening the overall interaction network (middle panel), Substitution of D for A230 in $G\alpha_{i2}$-GTP leads to interactions with R145 stabilizing the interaction network between the HD and Switch III (right panel).

2.4.8 PRG stimulation is dependent on interdomain stabilization of $G\alpha_i$ Switch III

The simulation data indicate that interaction between D229 in the RLD and R144 in the HD centers an interaction network that controls the conformation of Switch III. Based on this, we predicted that mutation of R144 to disrupt this interaction would reduce PRG activation by $G\alpha_{i1}$. $G\alpha_{i1}$ R144A reduces nucleotide-dependent PRG activation in cells, similar to that of $G\alpha_{i1}$ D229A. When alanine is substituted for both D229 and R144, the same reduction is observed (Figure 2.9A). Alanine substitution of cognate residue R145 in $G\alpha_{i2}$ does not alter nucleotide-dependent PRG activation, but completely abolishes activation of PRG conferred by A230D (Figure 2.9B). These experiments show that the D229-R144 interaction contributes to the ability of $G\alpha_{i1}$ to activate PRG, and the ability to activate PRG conferred to $G\alpha_{i2}$ by the A230D substitution is entirely dependent on D230-R145 interaction.

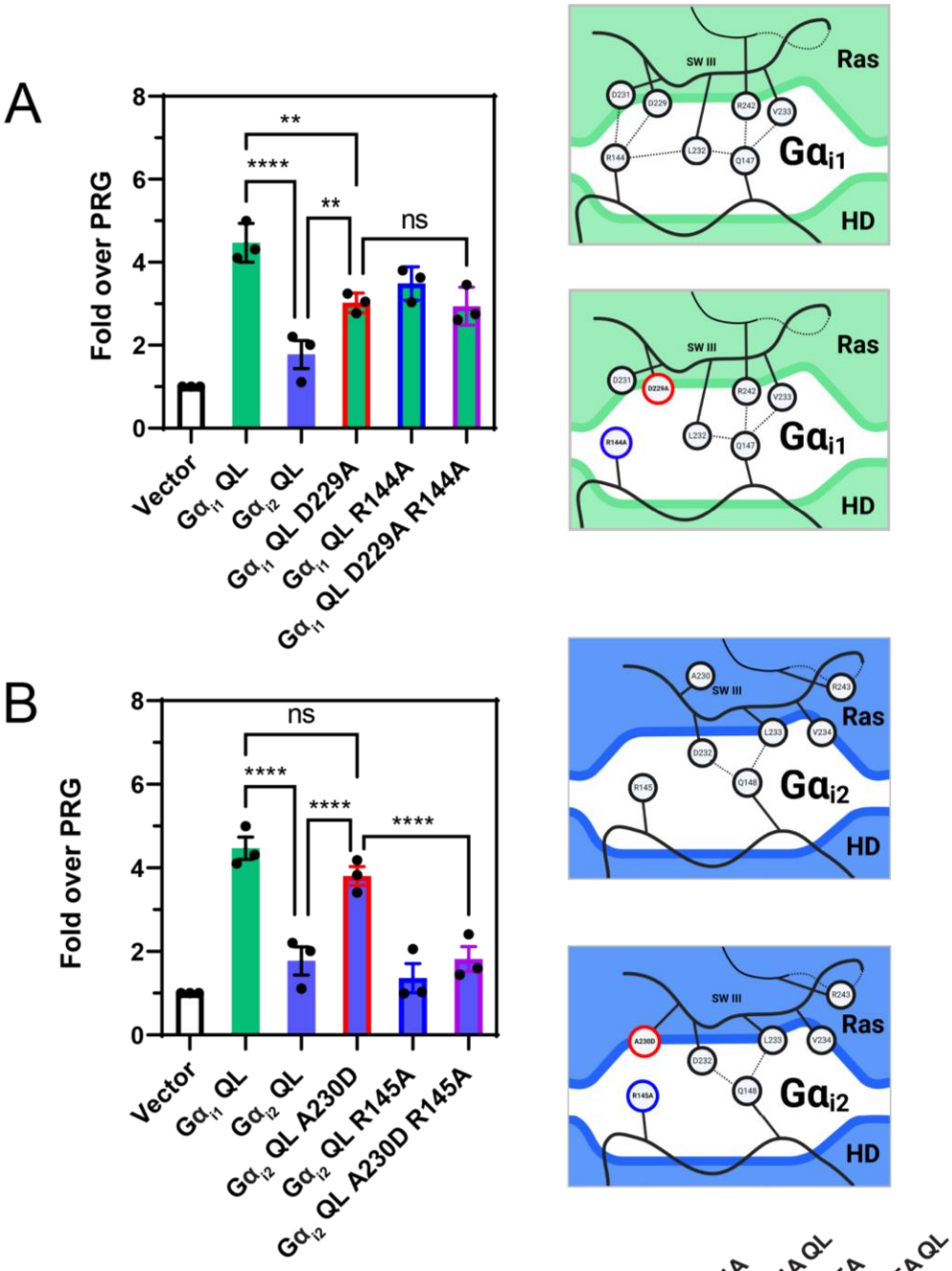
A
Fold over PRG
8
6
4
2
0
**
****
**
ns
Vector
Gαi1 QL
Gαi2 QL
Gαi1 QL D229A
Gαi1 QL R144A
Gαi1 QL D229A R144A
Ras
SW III
Gαi1
HD
B
Fold over PRG
ns
****
****
****
Vector
Gαi1 QL
Gαi2 QL
Gαi2 QL A230D
Gαi2 QL R145A
Gαi2 QL A230D R145A
Ras
SW III
Gαi2
HD
C
kDa
55
35
pcDNA3.1+
Gαi1 QL
Gαi2 QL
Gαi1 D229A QL
Gαi2 A230D QL
Gαi1 R144A QL
Gαi2 R145A QL
Gαi1 D229A / R144A
Gαi1 D229A / R144A QL
Gαi2 A230D / R145A
Gαi2 A230D / R145A QL
IB: FLAG
Ponceau S Stain

Figure 2.9: $G\alpha_{i1}$ D229/$G\alpha_{i2}$ A230 controls HD-RLD interdomain interactions.
A) SRE luciferase assay showing PRG activation by $G\alpha_{i1}$, $G\alpha_{i2}$, $G\alpha_{i1}$ D229A, $G\alpha_{i1}$ R144A, and $G\alpha_{i1}$ D229A-R144A. **B)** SRE luciferase assay showing PRG activation by $G\alpha_{i1}$, $G\alpha_{i2}$, $G\alpha_{i2}$ A230D, $G\alpha_{i2}$ R145A, and $G\alpha_{i2}$ A230D-R145A. Experiments were performed with 3 biological replicates performed in triplicate. Data are +/- SEM analyzed by One-way ANOVA with Šídák post-test; ** $P < 0.01$, **** $P < 0.0001$. Cartoons next to **A)** and **B)** display residues involved in interdomain interactions; colors for mutations matched with bar outlines in graph. **C)** Western blot showing representative expression of $G\alpha_i$ subunits transfected in **A)** and **B)**.

In the Ras-like domain are the switch regions including the Switch III loop. Switch III is critical for communication to the HD across the domain interface, and affects multiple aspects of Gα protein function, including effector recognition [148, 149] and receptor-mediated activation [53]. In the co-crystal structure of $G\alpha_{13}$ and PRG, Switch III makes multiple contacts with PRG. To test involvement of Switch III in $G\alpha_i$-dependent PRG activation, we substituted $G\alpha_{i1}$ Switch III residues D231 – A235 (DLVLA) to cognate $G\alpha_s$ residues N254 – R258 (NMVIR) ($G\alpha_{i1}$ SW3αS, Figure 2.10B). $G\alpha_{i1}$ SW3αS QL poorly activated PRG compared to $G\alpha_{i1}$ QL in the SRE luciferase assay (Figure 2.10A). The loss-of-function mutations made in Switch III along with the gain-of-function phenotype achieved by combinatory substitution of $G\alpha_{i1}$ RLD elements + HD elements provide evidence of cooperation between the RLD and HD in stabilization of Switch III, which is lost in $G\alpha_{i2}$. This is important for $G\alpha_{i1}$-mediated activation of PRG and likely other targets.

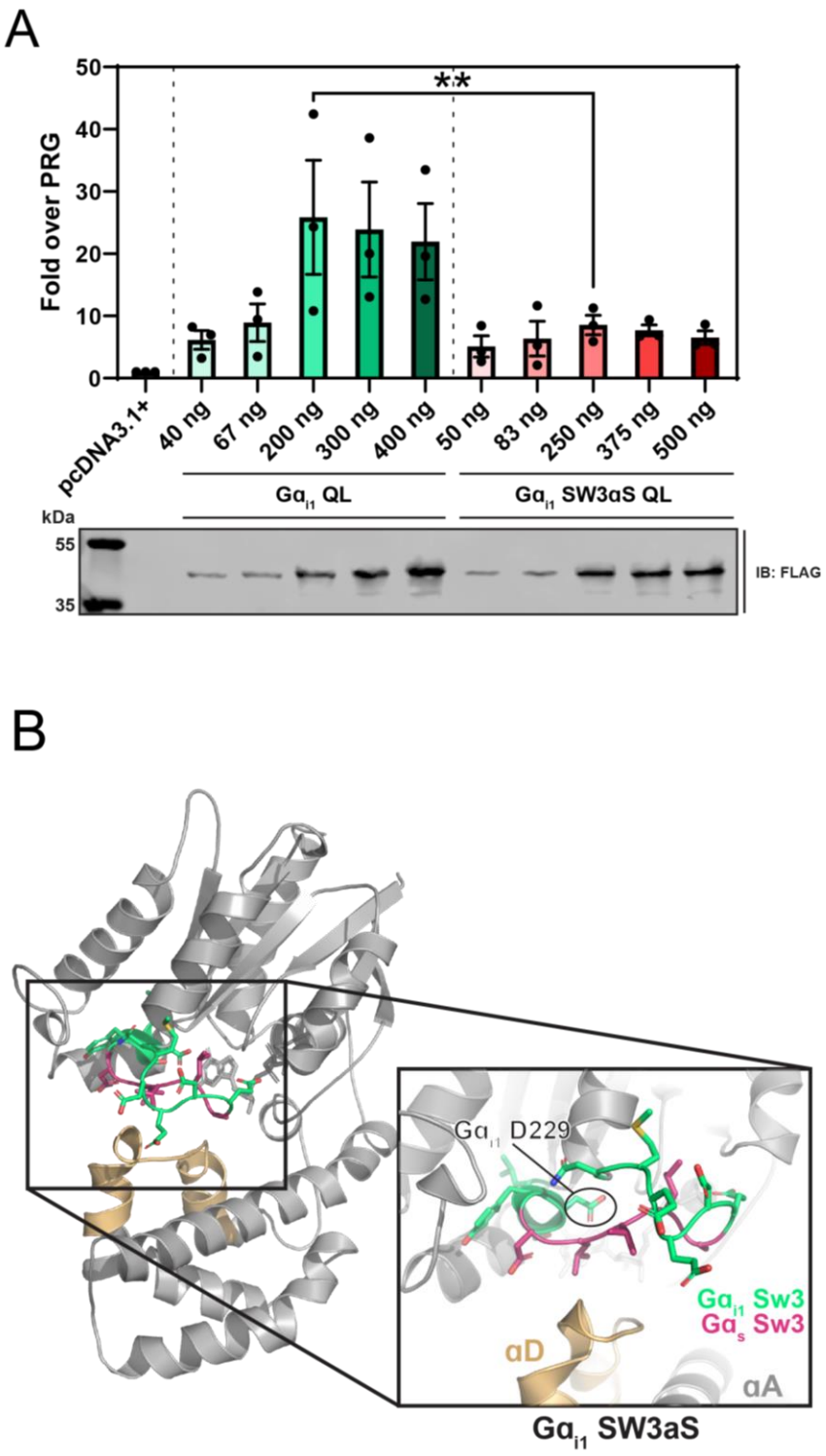

Figure 2.10: $G\alpha_{i1}$ Switch III is critical for activation of PRG.
A) Switch III amino acids in $G\alpha_{i1}$ were substituted with the cognate amino acids in $G\alpha_s$ and assayed for PRG activation using the SRE-Luc assay. Experiments were performed with 3 biological replicates performed in duplicate. Data are +/- SEM analyzed by One-way ANOVA with Šídák post-test; ** $P < 0.01$. **B)** Cartoon of active $G\alpha_{i1}$ representing $G\alpha_s$ substitutions made in $G\alpha_{i1}$ Switch III. $G\alpha_{i1}$ is grey, the αD helix is shown in tan for orientation, $G\alpha_{i1}$ Switch III residues are shown in green sticks, and the $G\alpha_{i1}$ residues mutated to corresponding residues in $G\alpha_s$ are in pink.

2.5 Discussion

A long-standing question in the function of $G\alpha_i$ proteins is one of functional redundancy: Why do three separate isoforms of $G\alpha_i$ exist, yet function so similarly? As mentioned previously, $G\alpha_{i1}$ and $G\alpha_{i3}$ have the same GDP dissociation rate, while this rate is faster in $G\alpha_{i2}$. All three isoforms have the same single-turnover GTP hydrolysis rate and they all similarly inhibit AC activity. Expression patterns for $G\alpha_{i1}$ and $G\alpha_{i3}$ show some tissue specificity in humans; $G\alpha_{i1}$ expression is favored in adipose tissue, the brain, placenta, and testes while $G\alpha_{i3}$ expression is higher in the digestive system, lymphatic system, ovaries, gall bladder, bone marrow, heart, and lungs [135]. However, there is still considerable overlap in expression of these in tissues. The expression pattern of $G\alpha_{i2}$ is unique, expressing highly relative to $G\alpha_{i1}$ and $G\alpha_{i3}$ in every system of the human body. The presence of multiple $G\alpha_i$ subtypes in these tissues is indicative of non-overlapping molecular function, as is also evidenced by several *in vivo* studies reporting differential roles for $G\alpha_{i2}$ and $G\alpha_{i3}$ in cardioprotection [108-112], cell migration [128, 129, 150, 151], calcium channel regulation [109], and platelet aggregation [114-116].

$G\alpha_{i1}$ and $G\alpha_{i3}$ have been demonstrated to identically regulate multiple signaling pathways, including IL6 signaling [152], GIRK channel function [82, 83, 137, 153], and EGFR signaling through Gab1 [87]. Among these many reports, demonstration of any unique function of these $G\alpha_i$ subtypes has remained elusive due to lack of details of specificity at the molecular level. Without knowledge of a direct effector that shows specificity downstream for $G\alpha_i$ subtypes, specificity cannot be determined. The discovery of PRG as a direct, isoform-specific effector of $G\alpha_i$ [97] has enabled the investigation of an intramolecular mechanism of specificity for effectors of $G\alpha_i$ subunits.

RLD-HD interactions have classically been understood to be a regulator of nucleotide exchange [29, 57, 64, 65, 154-156], with mutations at the interface intended to disrupt interactions leading to higher rates of GDP dissociation [57]. Specifically, mutation of residue R144 in $G\alpha_{i1}$ to an alanine is known to significantly increase the rate of GTPγS binding, presumably through the breaking of an interdomain interaction with L232 [57]. Grishina and Berlot showed in $G\alpha_s$ that substitution of residues in the Switch III loop to those of $G\alpha_{i2}$ disrupt the ability of $G\alpha_s$ to stimulate AC in response β2-AR activation. Activation can then be restored by additionally substituting the $G\alpha_s$ HD with $G\alpha_{i2}$ residues [53, 56], demonstrating the importance of Gα isoform-specific interdomain communication for effector activation. Co-crystal structures of Gα subunits in each family have shown all non-RGS effectors binding to a common cleft between the α2 (Switch II) and α3 helices [89, 146, 157-161].

In this study, we have provided evidence for a model in which $G\alpha_i$-effector interactions are dependent on the strength and frequency of interaction between Switch III residues and the HD, a new paradigm of protein effector specificity for Gα subunits. Our data suggest that $G\alpha_{i2}$ has fewer interdomain residue contacts, leading to a higher rate and extent of opening between the Ras domain and HD. Interruption of these contacts is detrimental to the ability of $G\alpha_i$ to activate PRG, and residue substitution in $G\alpha_{i2}$ to confer interdomain interactions present in $G\alpha_{i1}$ also promotes PRG activation, likely through stabilization of Switch III. While we focused on PRG stimulation as a functional indicator of $G\alpha_i$ specificity, we found in our $G\alpha_i$-BioID proximity labeling experiments that there are global differences in GTP-dependent interaction between $G\alpha_i$ subtypes and several novel targets, and that these differences can be reconciled by the same residue substitution that conferred specificity for PRG activation. This surprising result indicates that these

interdomain interactions may play an unappreciated role in the function of $G\alpha_i$ subunits, and a major role in differentiating $G\alpha_i$ subtype function.

Position s4h3.3 ($G\alpha_{i1}$ D229 and $G\alpha_{i2}$ A230) is unique for the $G\alpha_i$ subfamily in that the residue is different for each Gα family but is conserved within each family except $G\alpha_i$. Amino acids at this position for each family include Ser in $G\alpha_s$, Gly in $G\alpha_o$ and $G\alpha_z$, Ala in $G\alpha_T$, and Glu in $G\alpha_{q/11}$ and $G\alpha_{12/13}$. A similar mechanism for stabilization of Switch III through interdomain interactions is likely conserved in the $G\alpha_{q/11}$ family and also $G\alpha_{13}$, as $G\alpha_{i1}$ $R144^{HD.11}$ is conserved in these G proteins and could interact in a similar way with Glu at s4h3.3 in Switch III. $G\alpha_{i1}$ $Q147^{hdhe.2}$ is also conserved in all Gα but $G\alpha_z$ and $G\alpha_{15}$, so it is likely that the contacts made by Switch III residues shown here are highly conserved and important for Switch III stabilization. Despite the similarities to other Gα subunits at these positions, the $G\alpha_i$ subfamily seems unique in its intra-family effector specificity achieved by differentiation at s4h3.3.

The increase in activation of PRG by $G\alpha_{i2}$ A230D substitution is not met by an equal decrease in the concomitant $G\alpha_{i1}$ D229A substitution. This is supported by our molecular dynamics simulations, in which A230D substitution results in reduced interaction for only one residue pair (Q148-D232) while gaining interactions between four residue pairs across the domain interface (Figure 2.8D, Table 2.1). $G\alpha_{i1}$ D229A substitution results in a loss of interaction between five interdomain residue pairs, while increasing interaction strength between six residue pairs. Thus, there is an observed net increase of three interdomain interactions associated with A230D mutation. Where a decrease in interdomain interactions might be expected for $G\alpha_{i1}$ D229A substitution, the amount of total interactions actually increased in the area observed. Interestingly, four of the interdomain residue interactions which had reduced interaction strength involved HD residue Q147, while the associated Switch III binding partners bound to more N-terminal residues

along the αD-αE loop, indicating a relative twisting of the domains as observed in PC1 (Figure 2.8C, Appendix Video 1). This retention of interactions at the domain interface despite loss of the D229-R144 contact is reflected in our PRG activation assays performed with D229A or R144A mutations (Figure 2.9A).

$G\alpha_{i2}$ A230D		$G\alpha_{i1}$ D229A	
Loss	Gain	Loss	Gain
Q148-D232	R145-(A)D230	R144-D(A)229	R144-D231
	R145-D232		R144-L232
	R145-L233	Q147-L232	R144-V233
	Q148-V234	Q147-V233	E145-L234
		Q147-A235	Y146-L232
		Q147-R242	Q147-D231

Table 2.1: Changes in $G\alpha_i$ interdomain interactions upon $G\alpha_{i1}$ D229A or $G\alpha_{i2}$ A230D substitution
Interactions lost or gained upon substitution of A230D in $G\alpha_{i2}$ or D229A in $G\alpha_{i1}$. Interaction determined by comparing residue interaction frequencies in Fig. 2.8D. Residues on the left numbered by position in $G\alpha_{i2}$, on the right are numbered by $G\alpha_{i1}$ position.

Substitution of the whole $G\alpha_{i1}$ HD into $G\alpha_{i2}$ also confers the ability to activate PRG (Figure 2.3B) and interaction with other targets (Figure 2.3E). Since no individual secondary structure element from the $G\alpha_{i1}$ HD is able to do this, we posit that the presence of the entire $G\alpha_{i1}$ HD is crucial in positioning HD residues for interaction with Switch III residues conserved in all $G\alpha_i$ subunits. The involvement of the $G\alpha_{i1}$ D229-R144 interaction and other additional interdomain contacts in stabilization of Switch III and effector interaction are supported by multiple key results. First, the simulations discussed above show a dynamic interaction landscape where single substitutions affect the strength of other regional contacts. Second, simultaneously substituting both the $G\alpha_{i1}$ HD and A230D into $G\alpha_{i2}$ QL results in activation of PRG similar to $G\alpha_{i1}$ QL at half-maximal signal, while neither of the substitutions on their own reach this level of activation (Figure 2.7G). Finally, substitution of either the $G\alpha_{i1}$ HD or A230D in $G\alpha_{i2}$ result in increased, but not full recovery of GTP-dependent interaction with protein targets in BioID proximity labeling assays compared to $G\alpha_{i1}$ QL (Figure 2.3E and 2.7H).

While these interactions enabled by $G\alpha_{i1}$ HD substitution into $G\alpha_{i2}$ are sufficient to confer increased PRG activation and proximal interaction with some targets, this increase in interaction is not seen when observing interaction with PRG in cells (Figure 2.7D). One explanation for this disparity is that the NanoBiT complementation assay measures steady-state binding at one given time, while the SRE-luciferase assay and BioID proximity labeling assays measure an accumulation of activation or interaction signal over 24 hours. Consequently, dependent on the kinetics of interaction and assay sensitivity, interaction at a given time may not be detectable, while signal accumulation over time shows in the changes conferred by $G\alpha_{i1}$ HD substitution into $G\alpha_{i2}$. $G\alpha_{i1}$ and $G\alpha_{i3}$ are 94% identical in sequence, and both of these isoforms are able to robustly activate PRG compared to $G\alpha_{i2}$ [97]. While this study does not directly address functional differences between $G\alpha_{i3}$ and other $G\alpha_{i}$ subunits, $G\alpha_{i1}$ and $G\alpha_{i3}$ are identical through the entirety of Switch III and the αD-αE connecting loop where these interactions are observed, including at $D229^{s4h3.3}$. Their helical domains are also more similar than compared to $G\alpha_{i2}$ ($G\alpha_{i1}$ vs $G\alpha_{i2}$ 21 differences, $G\alpha_{i1}$ vs $G\alpha_{i3}$ 11 differences). Therefore, we assume that Switch III stabilization via interdomain interaction in $G\alpha_{i3}$ is more similar to $G\alpha_{i1}$ than to $G\alpha_{i2}$.

In conclusion, we describe here a previously unknown mechanism of effector specificity between $G\alpha_{i}$ subtypes. Switch III is stabilized by an interdomain interaction network with αD-αE residues in the helical domain, due in part to rearrangement of one non-conserved $G\alpha_{i}$ Switch III aspartate that contacts a conserved arginine. This stabilization of Switch III not only confers specificity for activation of $G\alpha_{i1/3}$ effector PDZ-RhoGEF, but for interaction with an array of additional protein targets, shedding light on the mystery of functional redundancy among this highly similar Gα protein family.

2.6 Contributions

Others who contributed to the work described in Chapter 2 are those listed below:

Elizaveta Mukhaleva[2], Wenyuan Wei[2], Sai Meda Venkata[1], Nagarajan Vaidehi[2], Alan V. Smrcka[1]

[1]Department of Pharmacology, University of Michigan Medical School, Ann Arbor, MI;

[2]Department of Computational and Quantitative Medicine, Beckman Research Institute of the City of Hope, Duarte, CA

EM and WW performed the MD analysis and provided data and panels for Figure 2.8. SMV performed BioID experiments for data in Figure 2.7G. NV contributed to study conceptualization and interpretation of data in MD experiments. AVS contributed to study conceptualization, data analysis, and editing and preparation of the figures and text.

Chapter 3 - Discussion and Future Directions

3.1 Significance

Our results in Chapter 2 describe the discovery of a single amino acid that can significantly alter the selectivity of $G\alpha_i$ subunits by contributing to stabilization of the Switch III loop through interaction with helical domain residues. This mechanism controls selectivity for nucleotide-dependent binding and activation of PRG, but for other novel protein interactors as well.

Critically, our mechanism of selectivity does not rely on GTP binding rate or relative amount of GTP-bound Gα subunit. There is evidence that $G\alpha_{i2}$ A230D$^{s4h3.3}$ substitution reduces single turnover GTP hydrolysis rate of $G\alpha_{i2}$ to the level of $G\alpha_{i1}$, while $G\alpha_{i1}$ D229$^{s4h3.3}$ increases this rate. However, $G\alpha_{i1}$ and $G\alpha_{i2}$ were shown to have identical affinities for GTPγS *in vitro*, and $G\alpha_{i1}$ D229A$^{s4h3.3}$ or $G\alpha_{i2}$ A230D$^{s4h3.3}$ mutation does not alter this affinity [93]. While these mutations have been shown to impact the ability of RGS19 to GAP $G\alpha_i$ subtypes, the effector interactions we observed are with GTPase-deficient QL mutants, thus eliminating any effect of altered nucleotide hydrolysis by GAPs.

While mutation at s4h3.3 can change interaction with GAPs, it could also alter interaction with receptors. Interruption of interdomain interactions in $G\alpha_s$ interrupts β2AR-dependent $G\alpha_s$ activation as measured by activation of AC, but GTPγS-stimulated cAMP generation by these mutants was still intact [53]. Since our study was entirely receptor-independent, our data regarding interactions with $G\alpha_i$ targets are unaffected by any deficiencies in receptor-mediated activation.

The control of $G\alpha_i$ subtype-effector interactions by Switch III stabilization combined with these important results from the literature clearly illustrate an essential role of interdomain

interactions in Gα function. Upstream activation by GPCRs, intrinsic nucleotide exchange, regulation of GTP hydrolysis by RGS, and now interaction with downstream signaling partners are all impacted by changes in the dynamics of this interdomain region. In this final chapter, I will discuss the larger implications of our results, important technical considerations, and possible directions for future investigation.

3.2 $G\alpha_{i2}$ as a dedicated Gβγ scaffold

While it remains untested how the selectivity differences we observed directly lead to distinct physiological roles for $G\alpha_i$ subtypes, our findings are consistent with the notion that $G\alpha_{i2}$ may act primarily as a scaffold and switch for Gβγ signaling throughout the body, whereas $G\alpha_{i1}$ or $G\alpha_{i3}$ perform this function in addition to signaling to various $G\alpha_i$-specific effectors. This is consistent with known roles for $G\alpha_{i2}$ and $G\alpha_{i3}$-mediated signaling events in neutrophils, in which presence of only $G\alpha_{i2}$ promotes cell arrest while presence of only $G\alpha_{i3}$ promotes migratory phenotypes [129]. The effects of $G\alpha_{i2}$ on arrest are similar to those found by Gβγ activation alone [125]. Eosinophils from $G\alpha_{i2}$ whole-body knockout mice display enhanced chemotactic response *in vitro***,** while leukocytes have reduced extravasation and appear to accumulate on endothelial surfaces with tight adherence [162].

The only discernable intrinsic biochemical difference between $G\alpha_i$ subunits has been rate GDP dissociation, which also affects single-turnover GTP hydrolysis. $G\alpha_{i1}$ and $G\alpha_{i3}$ have the same unstimulated GDP release rate, while $G\alpha_{i2}$ is faster [70, 71]. One might infer that this fast rate of nucleotide exchange positions $G\alpha_{i2}$ to be the $G\alpha_i$ protein best suited for rapid response to GPCR stimuli and signaling to downstream effectors. However, $G\alpha_{i2}$ is the only $G\alpha_i$ isoform not shown to interact directly with GIRK channels, which require rapid and responsive regulation for proper physiological function. Enhancement of GDP release by mutation of $G\alpha_{i2}$ interdomain residues

[57] also accelerated M2R-stimulated GIRK activation kinetics, known to be regulated by Gβγ [163]. Together, these data have brought some to hypothesize that $G\alpha_{i2}$ acts as the primary Gβγ donor for GIRK channel activation, while $G\alpha_{i1}$ and $G\alpha_{i3}$ act as direct modulators of GIRK basal activity and excitability as well as GIRK donors [84]. In murine atria, GIRK channel activity is differentially regulated by $G\alpha_{i2}$ and $G\alpha_{i1}$/$G\alpha_{i3}$. Deletion of $G\alpha_{i2}$ increases Gβγ-mediated basal and agonist-induced GIRK currents, while dual knockout of $G\alpha_{i1}$ and $G\alpha_{i3}$, which are known to bind and regulate GIRK, ablates basal and muscarinic agonist-induced GIRK activity [153]. As $G\alpha_{i2}$ is by far the most abundant and widespread of the $G\alpha_i$ isoforms [135], its main function could be that of a baseline regulator or scaffold for Gβγ throughout the body while $G\alpha_{i1}$ or $G\alpha_{i3}$ are expressed with more specificity to drive $G\alpha_i$-specific signaling.

3.3 Interdomain interaction in other Gα

In addition to the influence on effector binding we observed in $G\alpha_i$ Switch III, there are other examples of Switch III residues in other Gα which participate in interdomain interaction and impact effector binding. Despite binding via an RGS-like domain, PRG does not have GAP activity on $G\alpha_{13}$ [164, 165]. PRG-rgRGS binds to the conserved effector binding site in Gα between the α2 and α3 helices in the AlF_4^--bound and GTPγS-bound states of $G\alpha_{13}$, but also has contacts at the C-terminal "top" end of the α3 helix [146] (Figure 3.2B). Interestingly, PRG-rgRGS has an N-terminal loop that extends down into the RLD-HD interface, where its conserved IIG motif has contacts between $G\alpha_{13}$ Switch III, the αD-αE loop, and the αA helix. This binding mode has only otherwise been observed between $G\alpha_{13}$/$G\alpha_{i1}$ chimera binding to the rgRGS domain of another Dbl-family RhoGEF, P115-RhoGEF [166]. We assumed a similar binding mode of PRG to $G\alpha_{i1}$ in our study, considering these existing structures and our initial results that substituting the $G\alpha_{i1}$ HD into $G\alpha_{i2}$ conferred the ability to activate PRG. Importantly, in the co-crystal structure

of PRG-rgRGS and $G\alpha_{13}$, $R166^{HD.11}$ and $D253^{s4h3.5}$ are shown to interact. We found that altering interaction between these analogous residues in $G\alpha_i$ can impact selectivity for PRG and other protein targets. Our results and conclusions regarding the influence of $G\alpha_i$ effector interactions by Switch III stabilization in the GTP-bound state are consistent with the notion that the PRG rgRGS N-terminal segment binds to the domain interface in $G\alpha_{i1}$-GTP.

Other families of Gα also display subtype selectivity for interacting proteins. GRK2 binds via its RGS domain to $G\alpha_q$, but does not bind to $G\alpha_{16}$ of the same family. Using $G\alpha_{q/16}$ RLD/HD chimeras, this selectivity was found to depend on the RLD [167], where the GRK2 binding site was eventually found, instead of the HD [158] (Figure 3.2C). However, despite making direct contacts exclusively in the RLD, alanine substitutions in Switch III as well as in the αD-αE and αA loops disrupt GRK2 binding [168]. This dependence on Switch III is briefly mentioned in the report of this structure but is simply suggested to alter the structure and dynamics of Switch II. This may be possible but requires further investigation and this mechanism would add to the importance of Switch III in Gα-effector interactions. The mutations in the HD which impact GRK2 binding are not discussed, but the amino acids in these positions could play a role in stabilizing Switch III. Charge-charge pairs at the HD.11 and s4h3.3 positions are conserved in the $G\alpha_{q/11}$ family: HD.11 is an arginine and s4h3.3 is a glutamate residue instead of the aspartate in $G\alpha_{i1}$ (Figure 3.1). The residues before and after HD.11 and s4h3.3 are also highly conserved in the $G\alpha_{q/11}$ family.

$G\alpha_{T1}$, or transducin, binds the autoinhibitory γ subunit of cGMP phosphodiesterase (PDEγ), leading to activation of PDE, a crucial step in phototransduction. This interaction is dependent on the presence of the HD [169], however the binding site of PDEγ is not in the HD. Like all non-RGS effectors, PDEγ binds in the α2-α3 cleft [161]. Crucially, mutation of a Switch

III Glu to Leu abolishes PDE activation by $G\alpha_T$, with no effects on nucleotide binding or hydrolysis [148]. A recent cryo-EM structure of the full cGMP PDE6 αβγ complex with transducin revealed the binding of PDEγ to the outer edge of the Switch III loop as well as the previously-solved site in the α2-α3 cleft in $G\alpha_T$-GTP [2] (Figure 3.2A). The PDEγ contacts on transducin Switch III are not those found to impact PDE activity in a previous study, though this residue could impact Switch III dynamics through interaction with Switch II as suggested by Li and Cerione [148].

Disruption of $G\alpha_q$-GRK2 and $G\alpha_T$-PDEγ interactions by mutations at the domain interface, and specifically in Switch III, support the idea that Switch III dynamics control effector interaction in some capacity beyond just the $G\alpha_i$ subfamily. In conclusion, there are multiple roles for Switch III in Gα-effector interactions, some details of which have been structurally verified and some remain unclear. Stabilization of Switch III in active-state Gα is a common possible mechanism of effector selectivity in multiple Gα which has gone unappreciated despite data which support Switch III's involvement either directly or allosterically.

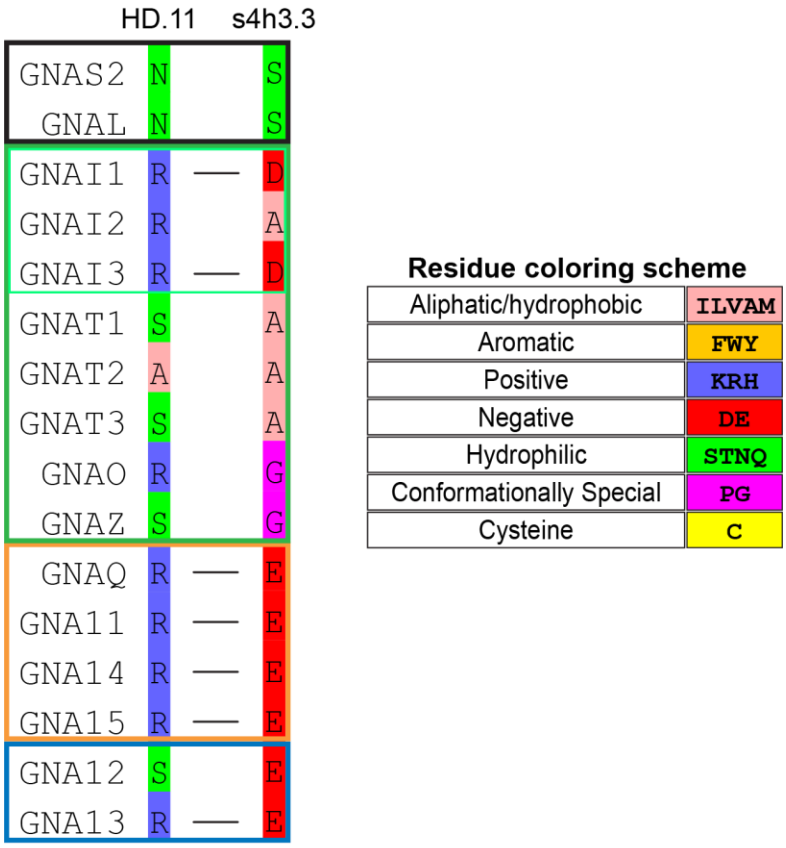

Figure 3.1: Potential for conserved HD-RLD interaction at Gα HD.11 and s4h3.3
Residues at position HD.11 and s4h3.3, or R144 and D229 in $G\alpha_{i1}$, are highlighted in a table for each human Gα. Bars between residue columns represent possible charge-charge interactions between these positions. Residues are colored according to the Zappo color scheme outlined to the right. Figure made with Jalview.

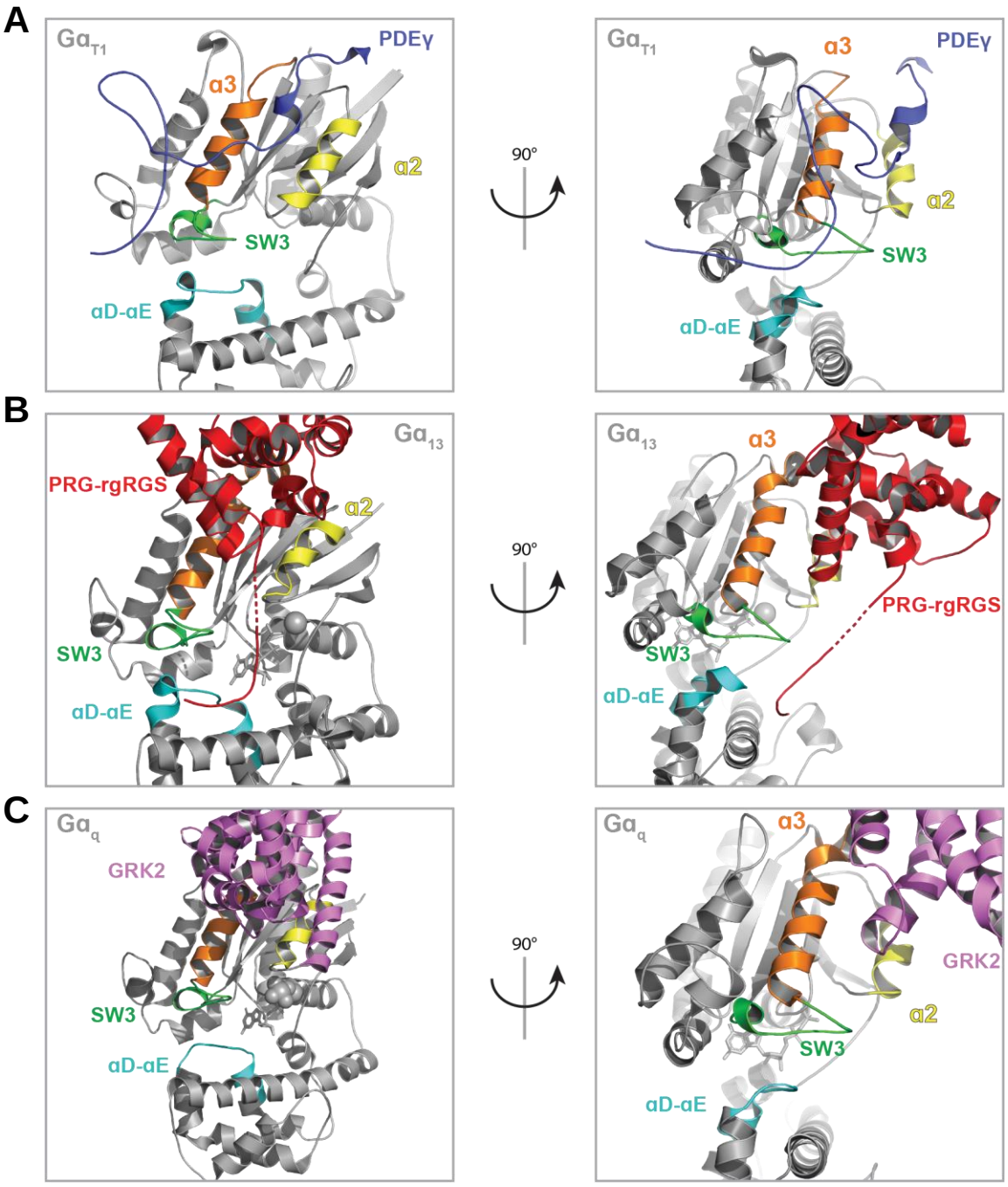

Figure 3.2: Binding modes of Gα effectors influenced by Switch III
Co-crystal structures of **A)** $G\alpha_{T1}$ with PDE6 (PDB: 7JSN) [2], **B)** $G\alpha_{13}$ with PRG-rgRGS (PDB 3CX6), and **C)** $G\alpha_q$ with GRK2 and Gβγ (PDB: 2BCJ). The PDEγ subunit (dark blue), PRG-rgRGS domain (red), and GRK2 (pink) each bind in the cleft between the parallel α2 (yellow) and α3 (orange) helices. Loops highlighted at the interdomain interface are Switch III (green) and the αD-αE loop (cyan).

3.4 Future directions

3.4.1 Expanding understanding of $G\alpha_i$-PRG interactions

To further our understanding of the mechanism described here, multiple strategies could be employed to reveal additional information. Though x-ray crystal structures offer the detail necessary to determine static binding sites with very high resolution, they are limited to capturing certain low-energy states, which may not provide key mechanistic steps. Methods such as NMR, molecular dynamics simulations as used here, or even cryo-EM can report on the dynamic states of proteins and protein complexes with enough detail to accelerate the refinement of mechanistic details. Previously solved crystal structures remain invaluable to structural biologists, as they function as a reference or starting state for other structures. Hydrogen-deuterium exchange (HDX) coupled to mass spectrometry could be used to compare Switch III dynamics in multiple G proteins and nucleotide states, including $G\alpha_{i1}$ WT and D229A, $G\alpha_{i2}$ WT and A230D, and each of them in GDP- or GTPγS-bound states. This method relies on the spontaneous exchange of hydrogen atoms with deuterium, the incorporation of which can be measured by mass spectrometry after an incubation period. Solvent-exposed residues have higher rates of exchange, and multiple states are compared to evaluate dynamics of each state. PRG could also be introduced with $G\alpha_i$ in HDX-MS analysis, which could highlight stabilization or dynamics of regions of both proteins. This strategy has been used with success to describe other Gα-effector dynamics [68, 170, 171].

While we observe enriched binding of $G\alpha_{i1}$-GTP to PRG in our NanoBiT assays, it is unclear whether $G\alpha_{i1}$ has appreciable affinity for PRG in the GDP-bound state. Using purified proteins, this could be addressed in multiple ways. Purified PRG-rgRGS is able to bind $G\alpha_{13}$-GDP, however the affinity is 10-fold weaker than PRG-rgRGS interaction with $G\alpha_{13}$-GDP-AlF_4^- or $G\alpha_{13}$-GTPγS [146]. These affinities were determined using isothermal titration calorimetry (ITC), which

measures the thermodynamics associated with binding. Using purified $G\alpha_i$ and PRG, binding could also be observed via Foerster resonance energy transfer (FRET) assays, in which protein binding partners are conjugated to donor or acceptor fluorophores. Binding is then observed through changes in fluorescence emission of the fluorophores. This can also be performed without direct labeling of proteins of interest, instead with antibodies conjugated to donor or acceptor fluorophores recognize either $G\alpha_i$ or PRG. Another label-free method in addition to ITC could be biolayer interferometry (BLI) or surface plasmon resonance (SPR), in which one protein is immobilized on a functionalized surface and direct binding of the partner protein in solution is observed via changes in reference light refraction. Gα-PRG binding in GDP-, GDP-AlF_4^-, or GTPγS-bound states could be assessed. Association and dissociation kinetics can also be captured using BLI/SPR.

Following these studies, if direct binding is observed, cryo-EM could be used to gain high-resolution structural information for the $G\alpha_i$-PRG complex. PRG is a large multidomain protein (167 kDa), which tend to be more difficult to crystallize for analysis via X-ray crystallography. Cryo-EM is more suitable for capturing larger, multiprotein complexes, as evidenced by the recent explosion of GPCR ternary complex structures solved by cryo-EM in the last decade as opposed to those solved with traditional X-ray crystallography [172, 173]. Additionally, the $G\alpha_{i1}$-PRG interaction may be dependent on co-localization at a lipid membrane. Lipid nanodiscs have recently enabled the solving of many membrane-embedded and membrane-associated proteins and complexes via cryo-EM. Information gained from these studies could verify the binding mode of PRG to Gα and further our understanding of $G\alpha_i$ subfamily selectivity for PRG and possibly other effectors.

Importantly, binding does not infer the ability of one protein to activate another. To gain insight on $G\alpha_i$ activation of PRG, *in vitro* reconstitution experiments could be performed. Reconstituted RhoGEF activity assays have been developed, which use purified RhoA and fluorophore-labeled GTP to measure GTP binding to RhoA via FRET [174, 175]. Activation of PRG by $G\alpha_i$ would be determined by the subsequent activation of RhoA by active PRG. Based on our results in cells with SRE-Luc reporter assays and NanoBiT complementation assays, we would expect to see GTP-dependent binding and activation of PRG by $G\alpha_{i1}$, but not by $G\alpha_{i2}$. Furthermore, we would expect that $G\alpha_{i2}$ A230D would behave similarly to $G\alpha_{i1}$, but perhaps less potently.

Beyond PRG, details on $G\alpha_i$ nucleotide-dependent and subtype-selective interactions could be probed in many of the ways listed above. NanoBiT complementation assays would test direct interaction with $G\alpha_i$ in cells, while FRET or BLI/SPR could be used to gauge interaction with $G\alpha_i$ *in vitro*.

3.4.2 Studies of the Gα interactome in physiology

Studies on the relative physiological roles of the different $G\alpha_i$ subunits rely almost exclusively on murine global $G\alpha_i$ subunit knockout models. While these investigations have undoubtedly been useful in determining the impact of $G\alpha_i$ family signaling in physiology, findings regarding subtype selectivity for certain functions are often complicated by the increase in levels of remaining $G\alpha_i$ after knockout of one or two other $G\alpha_i$ subtypes [109, 152]. Additionally, especially in the case of $G\alpha_{i2}$, it is likely that significant alterations in basal $G\beta\gamma$ signaling occur with significant loss of $G\alpha_i$ protein. Since $G\beta\gamma$ does not function via an active/inactive state, only bound or free, any reduction in the levels of $G\beta\gamma$-scavenging $G\alpha_i$-GDP could result in loss of spatiotemporal regulation of $G\beta\gamma$ signaling. Additionally, even if levels of each $G\alpha_i$ remain the

same, many studies have not attempted to differentiate $G\alpha_i$-specific signaling from the complimentary signaling of Gβγ downstream of Gi-coupled receptors.

RGS-insensitive $G\alpha_{i2}$ has been used to study its specific *in vivo* effects [118, 119, 130, 131, 176]. This strategy is well-designed to better probe roles of $G\alpha_{i2}$ *in vivo*, but in some cases has given similar results to knockout studies [114, 119]. One consistent possibility here is that by either knocking out $G\alpha_{i2}$ and increasing the lifetime of active $G\alpha_{i2}$-GTP, the concentration of free, signaling-competent Gβγ would be higher than in WT animals.

Methods which can uncouple $G\alpha_{i/o}$ signaling from Gβγ signaling will be critical to defining roles for $G_{i/o}$ α subunits in pathophysiology. To achieve this, the method must keep $G\alpha_{i/o}$ intact to properly regulate Gβγ, $G\alpha_{i/o}$ must retain their full function, and ideally the signal is completely bioorthogonal. Pertussis toxin-insensitive $G\alpha_{i/o}$ have been used, however the signal is restricted to one defined readout. Affinity purification mass spectrometry, whereby $G\alpha_{i/o}$ is co-precipitated with proteins of interest and proteomic analysis is performed, can identify binders of $G\alpha_{i/o}$. However, the stringency of purification must be adequately calibrated so as to eliminate nonspecific binders without washing away real binders. This also is biased toward robust interactions and cannot capture transient binding, which are characteristic of many G protein-effector interactions.

In our studies in Chapter 2, we opted to use BioID, which covalently and nonspecifically labels proximity interacting partners of transfected $G\alpha_i$-BioID subunits with biotin, a somewhat inert biomolecule. Although we used this method in an adherent, immortalized cell line for simplicity and proof of concept, proximity labeling using biotin can take place either before or after isolation of proximity labeling enzyme-expressing tissues. In *ex vivo* contexts, biotin can be exogenously applied to cultured cells. In whole animals, biotin can be administered directly via

injection or system-wide through dietary incorporation. In either system, disease state models can be utilized to probe the interactomes of disease-relevant proteins.

As an example, we planned a proteomic interaction screen for $G\alpha_{i2}$ and $G\alpha_{i3}$ interactors in isolated neonatal rat cardiomyocytes (NRVMs). Primary cells were prepared from WT animals and transduced with adenoviruses encoding one of $G\alpha_{i2}$-BioID2, $G\alpha_{i3}$-BioID2, or their QL variants and treated with biotin (Figure 3.3). Cardiomyocytes would be cultured in normal media or media containing endothelin 1 (ET1) to induce pathological cardiac hypertrophy, a key step in the progression of heart failure and an accepted *ex vivo* model. Twenty-four hours after biotin addition, samples of labeled proteins would then be prepared and sent for proteomic tandem mass spectrometry as in the screen in Chapter 2. The interactomes of $G\alpha_{i2}$ and $G\alpha_{i3}$ in their active and inactive states would be compared in both untreated cells and in hypertrophic cardiomyocytes with the intent to expand our knowledge of $G\alpha_{i}$ subtype-specific signaling in heart failure. Similar investigations could be performed downstream of activated GPCRs to capture physiologically-relevant signaling of Gα proteins. Since there is evidence of differential roles for $G\alpha_{i2}$ and $G\alpha_{i3}$ in heart failure but no molecular details of these interactions, studies like this one will likely be of great value in understanding the pathophysiology of heart failure and other conditions.

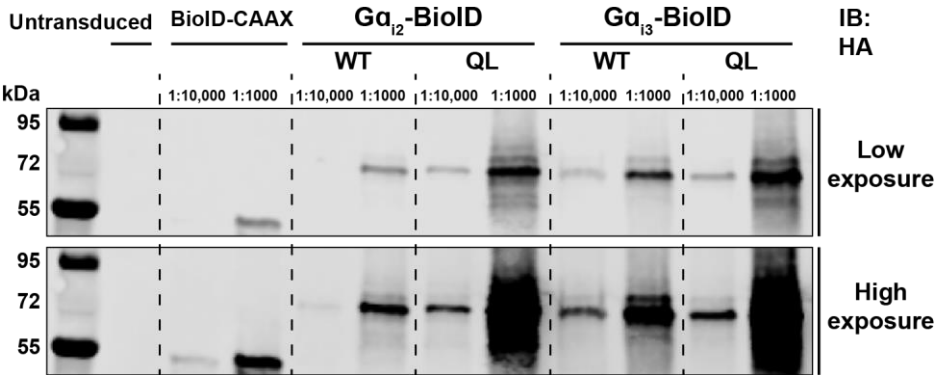

Figure 3.3: Expression of Gαi-BioID in primary neonatal rat cardiomyocytes via adenoviral transduction
Western blot for expression of Gαi-BioID-HA constructs from cultured primary cardiomyocytes. Concentrated supernatant from viral amplification in HEK293 cells was added to primary cultured neonatal rat cardiomyocytes at either a 1:1000 or 1:10,000 dilution factor relative to culture media as denoted above the blot. Viral transduction was performed for 48 hours. Cells were then harvested, and samples were prepared for SDS-PAGE and western blotting.

3.4.3 The need for active-state Gαi inhibitors

The availability of inhibitors for $G\alpha_i$ would rapidly advance studies in $G\alpha_i$ subtype specificity. Inhibitors currently exist for the G_s [177], $G_{q/11}$ [178-181], and $G_{i/o}$ [182, 183] families of Gα. However, since pertussis toxin (PTX) prevents interaction of G_i heterotrimers with GPCRs, blockade of $G\alpha_i$ signaling via PTX simultaneously inhibits a significant amount of Gβγ signaling. This is useful in determining the role of the whole of $G_{i/o}$ signaling in a given cell or tissue, however it occludes the dissection of signaling pathways downstream of $G_{i/o}$-coupled GPCRs. A reliable direct inhibitor which selectively binds $G\alpha_i$-GTP and blocks effector interaction would allow for such elucidation, as it would allow for receptor activation of Gβγ signaling but would block $G\alpha_i$-specific pathways. Separation of free Gβγ signaling from $G\alpha_i$ signaling is currently possible with tools such as the small molecule 12155, discovered by our laboratory to displace Gβγ from Gα without inducing nucleotide exchange [124]. Gβγ blockers are also available in the form of peptides and small molecules [184-189].

Compared to PTX, the $G\alpha_{q/11}$ and $G\alpha_s$ family inhibitors were discovered recently. $G\alpha_{q/11}$ family members are inhibited by two very structurally related cyclic peptides, YM254890 (YM) and FR900359 (FR), which act as GDIs. YM [190], and presumably FR [178], bind at the interdomain interface between Switch I and Linker 1, directly leading to their GDI activity. YM and FR are natural products first isolated from a bacterium [180, 181] and ornamental plant [179], respectively.

The $G\alpha_s$ cyclic peptides were discovered very recently by screening a generated library of over one trillion macrocyclic peptides against different nucleotide binding states of $G\alpha_s$. This yielded two separate macrocyclic inhibitors: GN13, which binds to GTP-bound $G\alpha_s$, and GD20, which binds to GDP-bound $G\alpha_s$. Both bind to the conserved α2-α3 effector binding site in the RLD. GD20 acts as a GDI, while GN13 inhibits $G\alpha_s$-GTP interaction with effectors by competition. YM and FR have been revolutionary tools to study $G\alpha_{q/11}$ signaling in biology, and GN13 and GD20 have promising cell-permeable analogs which perform similarly. Considering the structural homology and functional similarities among Gα proteins, development of cyclic peptide inhibitors for $G\alpha_{i/o}$ or $G\alpha_{12/13}$ could be achieved in much a similar manner as the $G\alpha_s$ inhibitors. A full suite of these molecules for each Gα as tools in experimental biology would significantly accelerate research progress and may even offer a path to potential therapeutics targeting Gα proteins and their interactions with signaling partners.

3.4.4 Closing Remarks

Gα subunits function through a grand symphony of interconnected movements, each subtype's sequence leading to minute variations on a theme of allosteric interaction. The mechanisms which contribute to these proteins' functional states have been intensely studied for nearly four decades, building our understanding of nucleotide binding and hydrolysis, as well as

how these guanine nucleotides position Gα for interaction with receptors and downstream targets. Advances in our understanding of the complexity of Gα subunits will only be revealed by methods which capture the dynamics of these proteins, where additional states can be observed and defined. The results from the studies above describe a previously unknown mechanism which determines the differential selectivity of $G\alpha_i$ subtypes for downstream effector proteins through stabilization of Switch III at the domain interface. It is also possible that this mechanism extends to other Gα subtypes, which requires further investigation.

The convergence of over 800 GPCRs on just 16 Gα subunits spells the significance of G proteins as both signal transducers and signal integrators in human pathophysiology. Changes in their functional dynamics can be reflected in signal amplification, leading to significant dysregulation of pathways downstream of GPCRs. Understanding how these changes or differences affect signaling is of great therapeutic importance.

Appendix

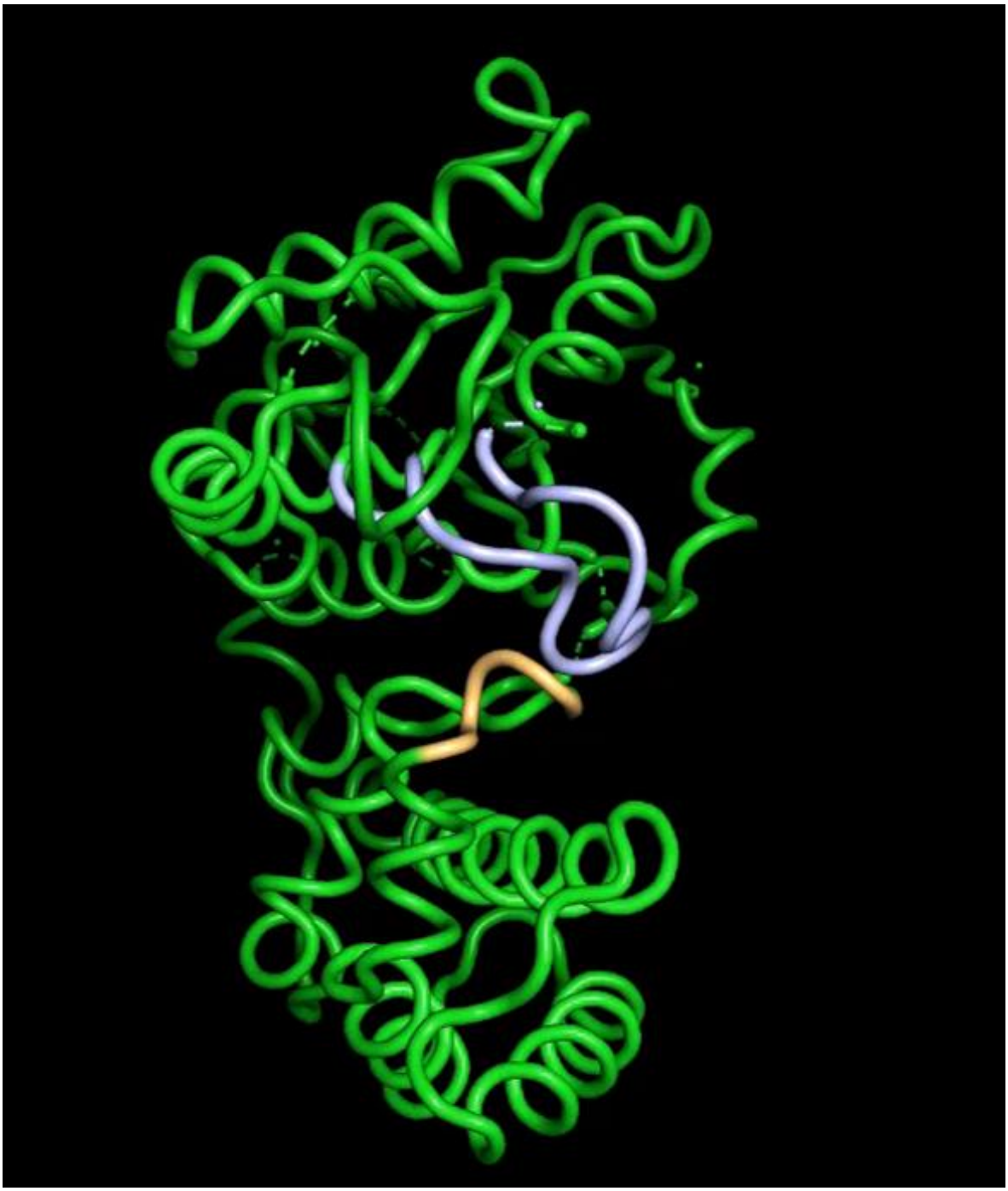

Appendix Video 1: $G\alpha_{i1}$ Principle Component 1
Video of the "turning" movement that comprises PC1 in $G\alpha_{i1}$-GTP. Ras-like domain is on top, while the helical domain is on the bottom. Switch III is in purple, while the αD-αE loop is tan.

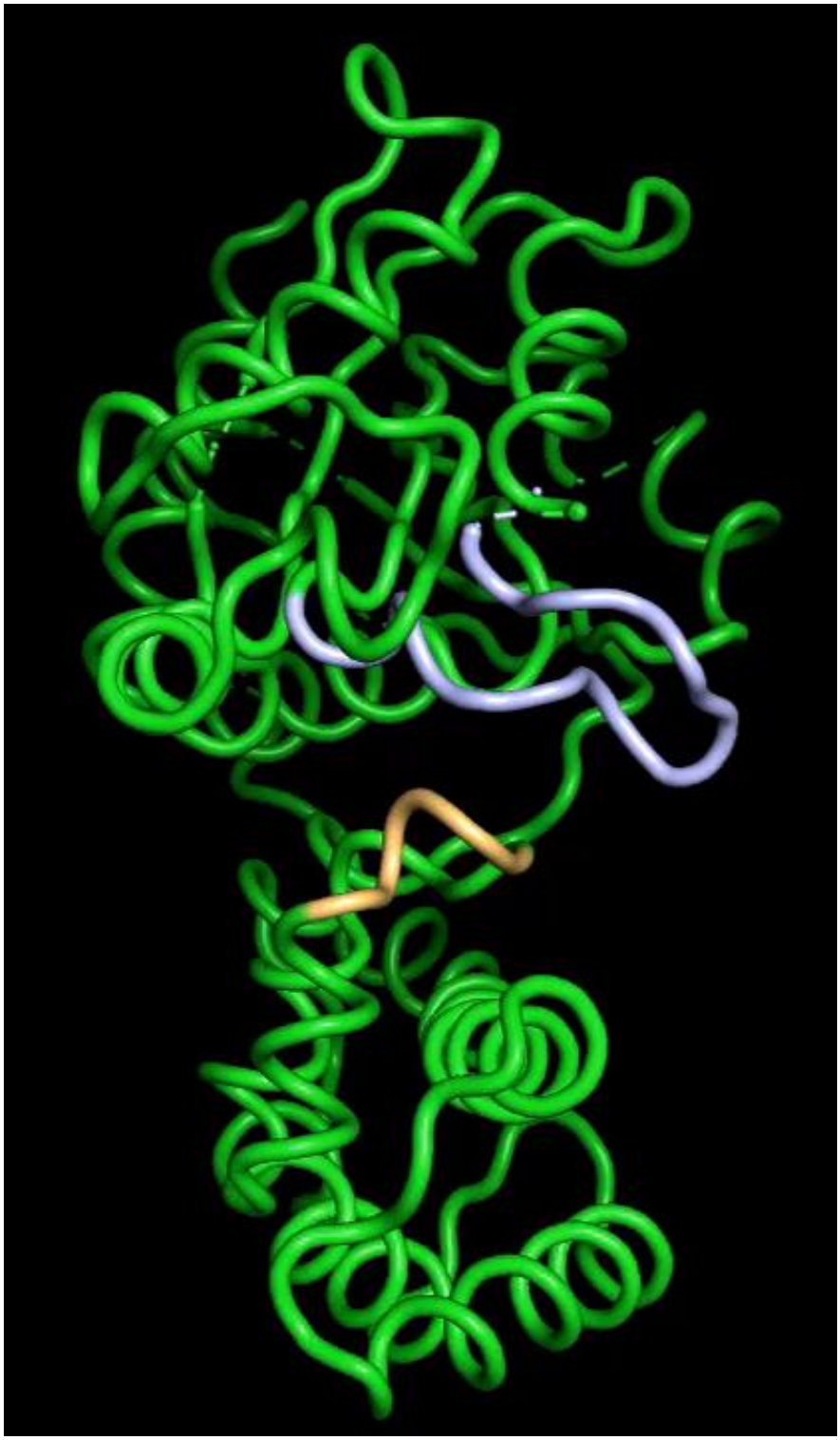

Appendix Video 2: $G\alpha_{i1}$ Principle Component 2
Video of the "opening" movement that comprises PC2 in $G\alpha_{i1}$-GTP. Ras-like domain is on top, while the helical domain is on the bottom. Switch III is in purple, while the αD-αE loop is tan.

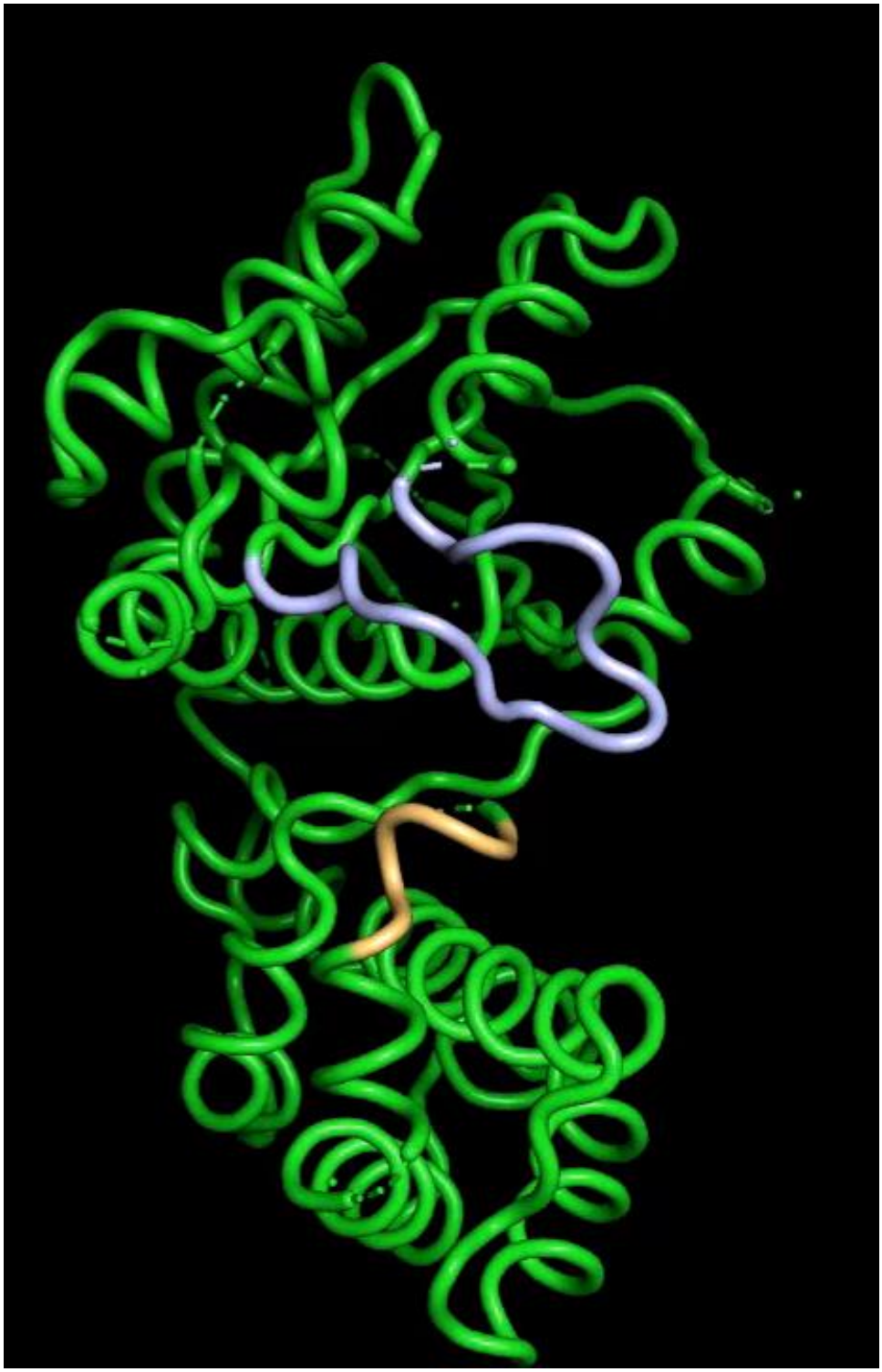

Appendix Video 3: $G\alpha_{i2}$ Principle Component 1
Video of the "opening" movement that comprises PC1 in $G\alpha_{i2}$-GTP. Ras-like domain is on top, while the helical domain is on the bottom. Switch III is in purple, while the αD-αE loop is tan.

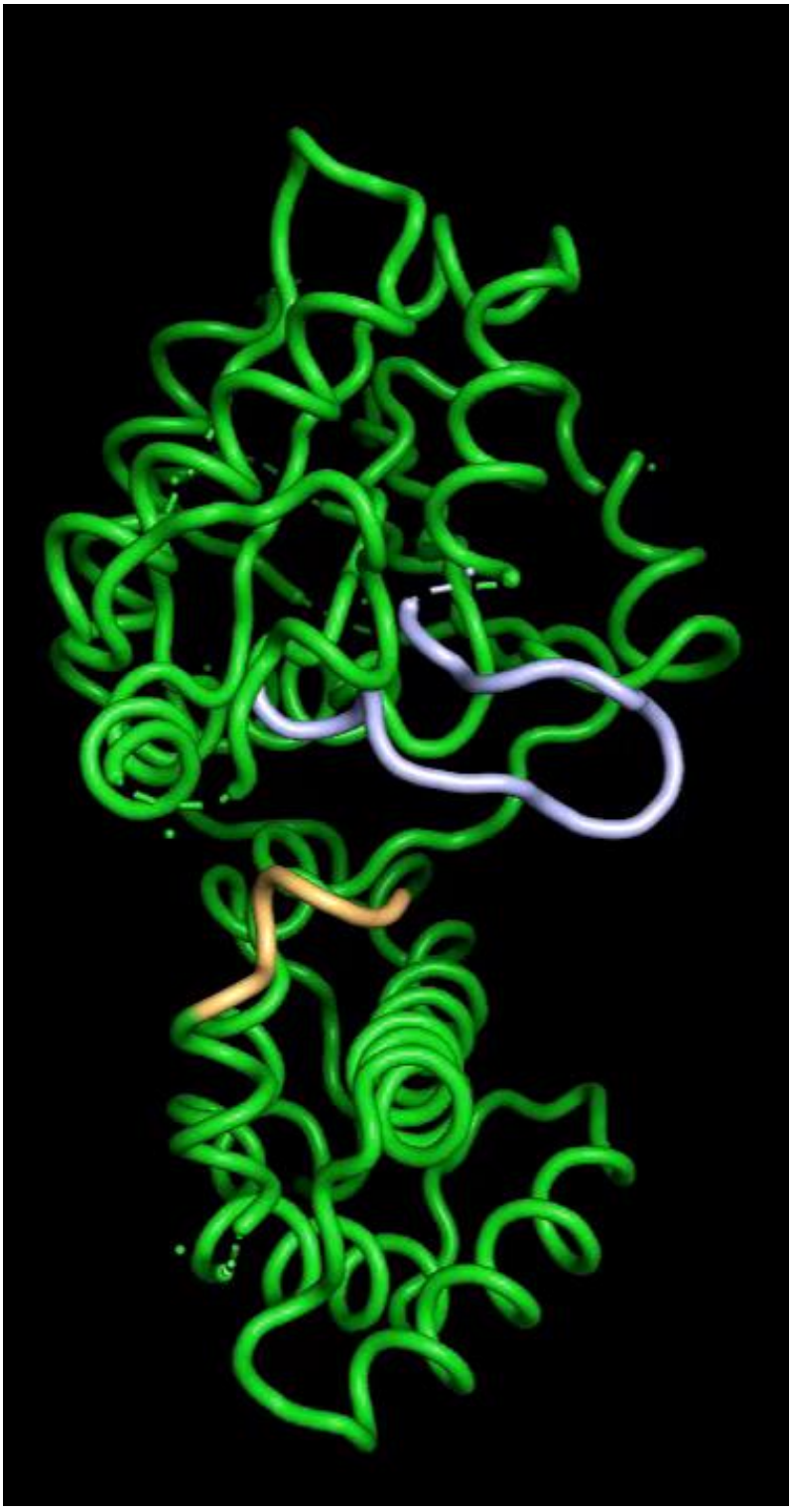

Appendix Video 4: $G\alpha_{i2}$ Principle Component 2
Video of the "opening" movement that comprises PC2 in $G\alpha_{i2}$-GTP. Ras-like domain is on top, while the helical domain is on the bottom. Switch III is in purple, while the αD-αE loop is tan.

Bibliography

1. Hepler, J.R. and A.G. Gilman, *G proteins.* Trends in Biochemical Sciences, 1992. **17**(10): p. 383-387.

2. Gao, Y., et al., *Structure of the Visual Signaling Complex between Transducin and Phosphodiesterase 6.* Molecular Cell, 2020. **80**(2): p. 237-245.e4.

3. Jiang, H., et al., *G protein-coupled receptor signaling: transducers and effectors.* American Journal of Physiology-Cell Physiology, 2022. **323**(3): p. C731-C748.

4. Oldham, W.M. and H.E. Hamm, *Heterotrimeric G protein activation by G-protein-coupled receptors.* Nature Reviews Molecular Cell Biology, 2008. **9**(1): p. 60-71.

5. Hauser, A.S., et al., *Trends in GPCR drug discovery: new agents, targets and indications.* Nature Reviews Drug Discovery, 2017. **16**(12): p. 829-842.

6. Sriram, K. and P.A. Insel, *G Protein-Coupled Receptors as Targets for Approved Drugs: How Many Targets and How Many Drugs?* Molecular Pharmacology, 2018. **93**(4): p. 251-258.

7. Wold, E.A., et al., *Allosteric Modulation of Class A GPCRs: Targets, Agents, and Emerging Concepts.* Journal of Medicinal Chemistry, 2019. **62**(1): p. 88-127.

8. Vilardaga, J.-P., *Theme and variations on kinetics of GPCR activation/deactivation.* Journal of Receptors and Signal Transduction, 2010. **30**(5): p. 304-312.

9. Lohse, M.J., et al., *Kinetics of G-protein-coupled receptor signals in intact cells.* British Journal of Pharmacology, 2008. **153**(S1): p. S125-S132.

10. Kunselman, J.M., J. Lott, and M.A. Puthenveedu, *Mechanisms of selective G protein–coupled receptor localization and trafficking.* Current Opinion in Cell Biology, 2021. **71**: p. 158-165.

11. Crilly, S.E. and M.A. Puthenveedu, *Compartmentalized GPCR Signaling from Intracellular Membranes.* The Journal of Membrane Biology, 2021. **254**(3): p. 259-271.

12. Irannejad, R., et al., *Conformational biosensors reveal GPCR signalling from endosomes.* Nature, 2013. **495**(7442): p. 534-538.

13. Plouffe, B., A.R.B. Thomsen, and R. Irannejad, *Emerging Role of Compartmentalized G Protein-Coupled Receptor Signaling in the Cardiovascular Field.* ACS Pharmacology & Translational Science, 2020. **3**(2): p. 221-236.

14. Puri, N.M., et al., *The organic cation transporter 2 regulates dopamine D1 receptor signaling at the Golgi apparatus.* eLife, 2022. **11**.

15. Kwon, Y., et al., *Non-canonical β-adrenergic activation of ERK at endosomes.* Nature, 2022. **611**(7934): p. 173-179.

16. Nash, C.A., et al., *Compartmentalized cyclic nucleotides have opposing effects on regulation of hypertrophic phospholipase Cε signaling in cardiac myocytes.* J Mol Cell Cardiol, 2018. **121**: p. 51-59.

17. Nash, C.A., et al., *Golgi localized β1-adrenergic receptors stimulate Golgi PI4P hydrolysis by PLCε to regulate cardiac hypertrophy.* eLife, 2019. **8**.

18. Cabrera, J.L., et al., *Identification of the Gbeta5-RGS7 protein complex in the retina.* Biochem Biophys Res Commun, 1998. **249**(3): p. 898-902.

19. Jeong, E., et al., *Structure of the class C orphan GPCR GPR158 in complex with RGS7-Gβ5.* Nature Communications, 2021. **12**(1).

20. Patil, D.N., et al., *Cryo-EM structure of human GPR158 receptor coupled to the RGS7-Gβ5 signaling complex.* Science, 2022. **375**(6576): p. 86-91.

21. Akgoz, M., V. Kalyanaraman, and N. Gautam, *G protein βγ complex translocation from plasma membrane to Golgi complex is influenced by receptor γ subunit interaction.* Cellular Signalling, 2006. **18**(10): p. 1758-1768.

22. O'Neill, P.R., et al., *G-protein signaling leverages subunit-dependent membrane affinity to differentially control βγ translocation to intracellular membranes.* Proceedings of the National Academy of Sciences, 2012. **109**(51): p. E3568-E3577.

23. Masuho, I., et al., *Diversity of the Gβγ complexes defines spatial and temporal bias of GPCR signaling.* Cell Systems, 2021. **12**(4): p. 324-337.e5.

24. Smrcka, A.V. and I. Fisher, *G-protein βγ subunits as multi-functional scaffolds and transducers in G-protein-coupled receptor signaling.* Cellular and Molecular Life Sciences, 2019. **76**(22): p. 4447-4459.

25. Smrcka, A.V., *G protein βγ subunits: Central mediators of G protein-coupled receptor signaling.* Cellular and Molecular Life Sciences, 2008. **65**(14): p. 2191-2214.

26. Campbell, A.P. and A.V. Smrcka, *Targeting G protein-coupled receptor signalling by blocking G proteins.* Nature Reviews Drug Discovery, 2018.

27. Touhara, K.K. and R. MacKinnon, *Molecular basis of signaling specificity between GIRK channels and GPCRs.* eLife, 2018. **7**: p. e42908.

28. Gilman, A.G., *G PROTEINS: TRANSDUCERS OF RECEPTOR-GENERATED SIGNALS.* Annual Review of Biochemistry, 1987. **56**(1): p. 615-649.

29. Noel, J.P., H.E. Hamm, and P.B. Sigler, *The 2.2 Å crystal structure of transducin-α complexed with GTPγS.* Nature, 1993. **366**(6456): p. 654-663.

30. Coleman, D.E., et al., *Structures of active conformations of Gi alpha 1 and the mechanism of GTP hydrolysis.* Science, 1994. **265**(5177): p. 1405-12.

31. Linder, M.E., et al., *Lipid modifications of G proteins: alpha subunits are palmitoylated.* Proceedings of the National Academy of Sciences, 1993. **90**(8): p. 3675-3679.

32. Wedegaertner, P.B., *Lipid Modifications and Membrane Targeting of G<sub>α</sub&gt.* Neurosignals, 1998. **7**(2): p. 125-135.

33. Conklin, B.R., et al., *Substitution of three amino acids switches receptor specificity of Gqα to that of Giα.* Nature, 1993. **363**(6426): p. 274-276.

34. Flock, T., et al., *Selectivity determinants of GPCR–G-protein binding.* Nature, 2017. **545**(7654): p. 317-322.

35. Okashah, N., et al., *Variable G protein determinants of GPCR coupling selectivity.* Proceedings of the National Academy of Sciences, 2019. **116**(24): p. 12054-12059.

36. Siderovski, D.P., M.a.A. Diversé-Pierluissi, and L. De Vries, *The GoLoco motif: a Gαi/o binding motif and potential guanine-nucleotide exchange factor.* Trends in Biochemical Sciences, 1999. **24**(9): p. 340-341.

37. Cismowski, M.J., et al., *Activation of Heterotrimeric G-protein Signaling by a Ras-related Protein.* Journal of Biological Chemistry, 2000. **275**(31): p. 23421-23424.

38. Takesono, A., et al., *Receptor-independent Activators of Heterotrimeric G-protein Signaling Pathways.* Journal of Biological Chemistry, 1999. **274**(47): p. 33202-33205.

39. Blumer, J.B., et al., *AGS proteins: receptor-independent activators of G-protein signaling.* Trends in Pharmacological Sciences, 2005. **26**(9): p. 470-476.

40. Gabay, M., et al., *Ric-8 Proteins Are Molecular Chaperones That Direct Nascent G Protein α Subunit Membrane Association.* Science Signaling, 2011. **4**(200): p. ra79-ra79.

41. Papasergi-Scott, M.M., et al., *Dual phosphorylation of Ric-8A enhances its ability to mediate G protein α subunit folding and to stimulate guanine nucleotide exchange.* Sci Signal, 2018. **11**(532).

42. Chan, P., et al., *Molecular chaperoning function of Ric-8 is to fold nascent heterotrimeric G protein α subunits.* Proceedings of the National Academy of Sciences, 2013. **110**(10): p. 3794-3799.

43. Tall, G.G., *Ric-8 regulation of heterotrimeric G proteins.* Journal of Receptors and Signal Transduction, 2013. **33**(3): p. 139-143.

44. Johnston, C.A., et al., *A bifunctional Gαi/Gαs modulatory peptide that attenuates adenylyl cyclase activity.* FEBS Letters, 2005. **579**(25): p. 5746-5750.

45. Garcia-Marcos, M., P. Ghosh, and M.G. Farquhar, *GIV is a nonreceptor GEF for Gαi with a unique motif that regulates Akt signaling.* Proceedings of the National Academy of Sciences, 2009. **106**(9): p. 3178-3183.

46. Ghosh, P., P. Rangamani, and I. Kufareva, *The GAPs, GEFs, GDIs and…now, GEMs: New kids on the heterotrimeric G protein signaling block.* Cell Cycle, 2017. **16**(7): p. 607-612.

47. Tesmer, J.J.G., et al., *Structure of RGS4 Bound to AlF4−-Activated Giα1: Stabilization of the Transition State for GTP Hydrolysis.* Cell, 1997. **89**(2): p. 251-261.

48. Masuho, I., et al., *A Global Map of G Protein Signaling Regulation by RGS Proteins.* Cell, 2020. **183**(2): p. 503-521.e19.

49. Kozasa, T., et al., *p115 RhoGEF, a GTPase activating protein for Galpha12 and Galpha13.* Science, 1998. **280**(5372): p. 2109-11.

50. Suzuki, N., et al., *Gα12 activates Rho GTPase through tyrosine-phosphorylated leukemia-associated RhoGEF*. Proceedings of the National Academy of Sciences, 2003. **100**(2): p. 733-738.

51. Sprang, S.R., *G PROTEIN MECHANISMS: Insights from Structural Analysis.* Annual Review of Biochemistry, 1997. **66**(1): p. 639-678.

52. Knight, K.M., et al., *A universal allosteric mechanism for G protein activation.* Molecular Cell, 2021. **81**(7): p. 1384-1396.e6.

53. Grishina, G. and C.H. Berlot, *Mutations at the Domain Interface of Gsα Impair Receptor-mediated Activation by Altering Receptor and Guanine Nucleotide Binding.* Journal of Biological Chemistry, 1998. **273**(24): p. 15053-15060.

54. Grishina, G. and C.H. Berlot, *A surface-exposed region of G(salpha) in which substitutions decrease receptor-mediated activation and increase receptor affinity.* Mol Pharmacol, 2000. **57**(6): p. 1081-92.

55. Grishina, G. and C.H. Berlot, *Identification of Common and Distinct Residues Involved in the Interaction of αi2 and αs with Adenylyl Cyclase.* Journal of Biological Chemistry, 1997. **272**(33): p. 20619-20626.

56. Marsh, S.R., et al., *Receptor-Mediated Activation of Gsα: Evidence for Intramolecular Signal Transduction.* Molecular Pharmacology, 1998. **53**(6): p. 981-990.

57. Remmers, A.E., et al., *Interdomain Interactions Regulate GDP Release from Heterotrimeric G Proteins.* Biochemistry, 1999. **38**(42): p. 13795-13800.

58. Mixon, M.B., et al., *Tertiary and quaternary structural changes in Gi alpha 1 induced by GTP hydrolysis.* Science, 1995. **270**(5238): p. 954-60.

59. Hong, J.X., et al., *Isolation and characterization of a novel B cell activation gene.* J Immunol, 1993. **150**(9): p. 3895-904.

60. Siderovski, D.P., S.P. Heximer, and D.R. Forsdyke, *A human gene encoding a putative basic helix-loop-helix phosphoprotein whose mRNA increases rapidly in cycloheximide-treated blood mononuclear cells.* DNA Cell Biol, 1994. **13**(2): p. 125-47.

61. De Vries, L., et al., *GAIP, a protein that specifically interacts with the trimeric G protein G alpha i3, is a member of a protein family with a highly conserved core domain.* Proceedings of the National Academy of Sciences, 1995. **92**(25): p. 11916-11920.

62. Conklin, B.R. and H.R. Bourne, *Structural elements of Gα subunits that interact with Gβγ, receptors, and effectors.* Cell, 1993. **73**(4): p. 631-641.

63. Markby, D.W., R. Onrust, and H.R. Bourne, *Separate GTP binding and GTPase activating domains of a G alpha subunit.* Science, 1993. **262**(5141): p. 1895-901.

64. Codina, J. and L. Birnbaumer, *Requirement for intramolecular domain interaction in activation of G protein alpha subunit by aluminum fluoride and GDP but not by GTP gamma S.* Journal of Biological Chemistry, 1994. **269**(47): p. 29339-29342.

65. Kim, H.R., et al., *Effect of α-helical domain of Gi/o α subunit on GDP/GTP turnover.* Biochemical Journal, 2022. **479**(17): p. 1843-1855.

66. Rasmussen, S.G.F., et al., *Crystal structure of the β2 adrenergic receptor–Gs protein complex.* Nature, 2011. **477**(7366): p. 549-555.

67. Westfield, G.H., et al., *Structural flexibility of the Gαs α-helical domain in the β2-adrenoceptor Gs complex.* Proceedings of the National Academy of Sciences, 2011. **108**(38): p. 16086-16091.

68. Chung, K.Y., et al., *Conformational changes in the G protein Gs induced by the β2 adrenergic receptor.* Nature, 2011. **477**(7366): p. 611-615.

69. Dror, R.O., et al., *Structural basis for nucleotide exchange in heterotrimeric G proteins.* Science, 2015. **348**(6241): p. 1361-1365.

70. Linder, M.E., et al., *Purification and characterization of Go alpha and three types of Gi alpha after expression in Escherichia coli.* Journal of Biological Chemistry, 1990. **265**(14): p. 8243-8251.

71. Carty, D.J., et al., *Distinct guanine nucleotide binding and release properties of the three Gi proteins.* Journal of Biological Chemistry, 1990. **265**(11): p. 6268-6273.

72. Taussig, R., et al., *Distinct patterns of bidirectional regulation of mammalian adenylyl cyclases.* Journal of Biological Chemistry, 1994. **269**(8): p. 6093-6100.

73. Draper-Joyce, C.J., et al., *Structure of the adenosine-bound human adenosine A1 receptor–Gi complex.* Nature, 2018. **558**(7711): p. 559-563.

74. Draper-Joyce, C.J., et al., *Positive allosteric mechanisms of adenosine A1 receptor-mediated analgesia.* Nature, 2021. **597**(7877): p. 571-576.

75. Zhu, Y., et al., *Structural basis of FPR2 in recognition of Aβ42 and neuroprotection by humanin.* Nature Communications, 2022. **13**(1).

76. Zhang, X., et al., *Structures of the human cholecystokinin receptors bound to agonists and antagonists.* Nature Chemical Biology, 2021. **17**(12): p. 1230-1237.

77. Yang, X., et al., *Molecular mechanism of allosteric modulation for the cannabinoid receptor CB1.* Nature Chemical Biology, 2022. **18**(8): p. 831-840.

78. Soundararajan, M., et al., *Structural diversity in the RGS domain and its interaction with heterotrimeric G protein α-subunits.* Proceedings of the National Academy of Sciences, 2008. **105**(17): p. 6457-6462.

79. Kimple, A.J., et al., *Structural Determinants of G-protein α Subunit Selectivity by Regulator of G-protein Signaling 2 (RGS2).* Journal of Biological Chemistry, 2009. **284**(29): p. 19402-19411.

80. Kalogriopoulos, N.A., et al., *Structural basis for GPCR-independent activation of heterotrimeric Gi proteins.* Proceedings of the National Academy of Sciences, 2019. **116**(33): p. 16394-16403.

81. Berlin, S., et al., *Two Distinct Aspects of Coupling between Gαi Protein and G Protein-activated K+ Channel (GIRK) Revealed by Fluorescently Labeled Gαi3 Protein Subunits.* Journal of Biological Chemistry, 2011. **286**(38): p. 33223-33235.

82. Rubinstein, M., et al., *Divergent regulation of GIRK1 and GIRK2 subunits of the neuronal G protein gated K+ channel by GαiGDP and Gβγ.* The Journal of Physiology, 2009. **587**(14): p. 3473-3491.

83. Rubinstein, M., et al., *Gαi3 primes the G protein-activated K+ channels for activation by coexpressed Gβγ in intact Xenopus oocytes.* The Journal of Physiology, 2007. **581**(1): p. 17-32.

84. Ivanina, T., et al., *Gαi1 and Gαi3 Differentially Interact with, and Regulate, the G Protein-activated K+ Channel.* Journal of Biological Chemistry, 2004. **279**(17): p. 17260-17268.

85. Mase, Y., et al., *Structural Basis for Modulation of Gating Property of G Protein-gated Inwardly Rectifying Potassium Ion Channel (GIRK) by i/o-family G Protein α Subunit (Gαi/o).* Journal of Biological Chemistry, 2012. **287**(23): p. 19537-19549.

86. Kano, H., et al., *Structural mechanism underlying G protein family-specific regulation of G protein-gated inwardly rectifying potassium channel.* Nature Communications, 2019. **10**(1): p. 2008.

87. Cao, C., et al., *Gαi1 and Gαi3 Are Required for Epidermal Growth Factor-Mediated Activation of the Akt-mTORC1 Pathway.* Science Signaling, 2009. **2**(68): p. ra17-ra17.

88. Kalogriopoulos, N.A., et al., *Receptor tyrosine kinases activate heterotrimeric G proteins via phosphorylation within the interdomain cleft of Gαi.* Proceedings of the National Academy of Sciences, 2020. **117**(46): p. 28763-28774.

89. Kimple, R.J., et al., *Structural determinants for GoLoco-induced inhibition of nucleotide release by Gα subunits.* Nature, 2002. **416**(6883): p. 878-881.

90. Shu, F.-j., et al., *Selective interactions between Giα1 and Giα3 and the GoLoco/GPR domain of RGS14 influence its dynamic subcellular localization.* Cellular Signalling, 2007. **19**(1): p. 163-176.

91. Mittal, V. and M.E. Linder, *The RGS14 GoLoco Domain Discriminates among Gαi Isoforms.* Journal of Biological Chemistry, 2004. **279**(45): p. 46772-46778.

92. De Vries, L., et al., *GAIP is membrane-anchored by palmitoylation and interacts with the activated (GTP-bound) form of Gαi subunits.* Proceedings of the National Academy of Sciences, 1996. **93**(26): p. 15203-15208.

93. Woulfe, D.S. and J.M. Stadel, *Structural Basis for the Selectivity of the RGS Protein, GAIP, for Gαi Family Members.* Journal of Biological Chemistry, 1999. **274**(25): p. 17718-17724.

94. Gazi, L., S.A. Nickolls, and P.G. Strange, *Functional coupling of the human dopamine D2 receptor with Gαi1 , Gαi2 , Gαi3 and Gαo G proteins: evidence for agonist regulation of G protein selectivity.* British Journal of Pharmacology, 2003. **138**(5): p. 775-786.

95. Senogles, S.E., et al., *Specificity of receptor-G protein interactions. Discrimination of Gi subtypes by the D2 dopamine receptor in a reconstituted system.* Journal of Biological Chemistry, 1990. **265**(8): p. 4507-4514.

96. Sternweis, P.C., et al., *Regulation of Rho Guanine Nucleotide Exchange Factors by G Proteins*, in *Advances in Protein Chemistry*. 2007, Academic Press. p. 189-228.

97. Chandan, N.R., et al., *A network of Gαi signaling partners is revealed by proximity labeling proteomics analysis and includes PDZ-RhoGEF.* Science Signaling, 2022. **15**(717): p. eabi9869.

98. Lucia, C.d., A. Eguchi, and W.J. Koch, *New Insights in Cardiac β-Adrenergic Signaling During Heart Failure and Aging.* 2018. **9**(904).

99. Rockman, H.A., W.J. Koch, and R.J. Lefkowitz, *Seven-transmembrane-spanning receptors and heart function.* Nature, 2002. **415**(6868): p. 206-212.

100. Xiao, R.-P., et al., *Coupling of β2-Adrenoceptor to Gi Proteins and Its Physiological Relevance in Murine Cardiac Myocytes.* 1999. **84**(1): p. 43-52.

101. Xiao, R.P., X. Ji, and E.G. Lakatta, *Functional coupling of the β2-adrenoceptor to a pertussis toxin-sensitive G protein in cardiac myocytes.* Mol Pharmacol, 1995. **47**(2): p. 322-9.

102. Abramson, S.N., et al., *Interaction of beta-adrenergic receptors with the inhibitory guanine nucleotide-binding protein of adenylate cyclase in membranes prepared from cyc- S49 lymphoma cells.* Biochem Pharmacol, 1988. **37**(22): p. 4289-97.

103. Daaka, Y., L.M. Luttrell, and R.J. Lefkowitz, *Switching of the coupling of the beta2-adrenergic receptor to different G proteins by protein kinase A.* Nature, 1997. **390**(6655): p. 88-91.

104. Devic, E., et al., *β-Adrenergic Receptor Subtype-Specific Signaling in Cardiac Myocytes from β1 and β2 Adrenoceptor Knockout Mice.* 2001. **60**(3): p. 577-583.

105. Strohman, M.J., et al., *Local membrane charge regulates β(2) adrenergic receptor coupling to G(i3).* Nat Commun, 2019. **10**(1): p. 2234.

106. Jiang, M., et al., *Mouse Gene Knockout Knockin Strategies in Application to α Subunits of Gi/Go Family of G Proteins*, in *Methods in Enzymology*, R. Iyengar and J.D. Hildebrandt, Editors. 2002, Academic Press. p. 277-298.

107. Rudolph, U., et al., *Ulcerative colitis and adenocarcinoma of the colon in Gαi2-deficient mice.* Nature Genetics, 1995. **10**(2): p. 143-150.

108. Foerster, K., et al., *Cardioprotection specific for the G protein Gi2 in chronic adrenergic signaling through β2-adrenoceptors.* 2003. **100**(24): p. 14475-14480.

109. Dizayee, S., et al., *Galphai2- and Galphai3-specific regulation of voltage-dependent L-type calcium channels in cardiomyocytes.* PLoS One, 2011. **6**(9): p. e24979.

110. Kaur, K., et al., *Gαi2 signaling: friend or foe in cardiac injury and heart failure?* Naunyn Schmiedebergs Arch Pharmacol, 2012. **385**(5): p. 443-53.

111. Köhler, D., et al., *Gαi2- and Gαi3-Deficient Mice Display Opposite Severity of Myocardial Ischemia Reperfusion Injury.* PLOS ONE, 2014. **9**(5): p. e98325.

112. DeGeorge, B.R., Jr., et al., *Targeted inhibition of cardiomyocyte Gi signaling enhances susceptibility to apoptotic cell death in response to ischemic stress.* Circulation, 2008. **117**(11): p. 1378-87.

113. Bauer, A., et al., *Inhibitory G Protein Overexpression Provides Physiologically Relevant Heart Rate Control in Persistent Atrial Fibrillation.* Circulation, 2004. **110**(19): p. 3115-3120.

114. Woulfe, D., et al., *Activation of Rap1B by Gi Family Members in Platelets.* Journal of Biological Chemistry, 2002. **277**(26): p. 23382-23390.

115. Yang, J., et al., *Signaling through Gi Family Members in Platelets: REDUNDANCY AND SPECIFICITY IN THE REGULATION OF ADENYLYL CYCLASE AND OTHER EFFECTORS.* Journal of Biological Chemistry, 2002. **277**(48): p. 46035-46042.

116. Devanathan, V., et al., *Platelet Gi protein Gαi2 is an essential mediator of thrombo-inflammatory organ damage in mice.* Proceedings of the National Academy of Sciences, 2015. **112**(20): p. 6491-6496.

117. Lan, K.-L., et al., *A Point Mutation in Gαo and Gαi1Blocks Interaction with Regulator of G Protein Signaling Proteins.* Journal of Biological Chemistry, 1998. **273**(21): p. 12794-12797.

118. Fu, Y., et al., *RGS-Insensitive G-Protein Mutations to Study the Role of Endogenous RGS Proteins*, in *Methods in Enzymology*. 2004, Academic Press. p. 229-243.

119. Signarvic, R.S., et al., *RGS/Gi2α interactions modulate platelet accumulation and thrombus formation at sites of vascular injury.* Blood, 2010. **116**(26): p. 6092-6100.

120. Arai, H., C.-L. Tsou, and I.F. Charo, *Chemotaxis in a lymphocyte cell line transfected with C-C chemokine receptor 2B: Evidence that directed migration is mediated by βγ dimers released by activation of Gαi-coupled receptors.* Proceedings of the National Academy of Sciences, 1997. **94**(26): p. 14495-14499.

121. Thelen, M., *Dancing to the tune of chemokines.* Nature Immunology, 2001. **2**(2): p. 129-134.

122. Neptune, E.R. and H.R. Bourne, *Receptors induce chemotaxis by releasing the βγ subunit of Gi, not by activating Gq or Gs.* Proceedings of the National Academy of Sciences, 1997. **94**(26): p. 14489-14494.

123. Lehmann, D.M., A.M. Seneviratne, and A.V. Smrcka, *Small molecule disruption of G protein beta gamma subunit signaling inhibits neutrophil chemotaxis and inflammation.* Mol Pharmacol, 2008. **73**(2): p. 410-8.

124. Surve, C.R., D. Lehmann, and A.V. Smrcka, *A chemical biology approach demonstrates G protein betagamma subunits are sufficient to mediate directional neutrophil chemotaxis.* J Biol Chem, 2014. **289**(25): p. 17791-801.

125. Surve, C.R., et al., *Dynamic regulation of neutrophil polarity and migration by the heterotrimeric G protein subunits Galphai-GTP and Gbetagamma.* Sci Signal, 2016. **9**(416): p. ra22.

126. To, J.Y. and A.V. Smrcka, *Activated heterotrimeric G protein αi subunits inhibit Rap-dependent cell adhesion and promote cell migration.* Journal of Biological Chemistry, 2018. **293**(5): p. 1570-1578.

127. Zarbock, A., et al., *Gαi2 is required for chemokine-induced neutrophil arrest.* Blood, 2007. **110**(10): p. 3773-3779.

128. Thompson, B.D., et al., *Inhibition of Gαi2 Activation by Gαi3 in CXCR3-mediated Signaling.* Journal of Biological Chemistry, 2007. **282**(13): p. 9547-9555.

129. Kuwano, Y., et al., *Gαi2 and Gαi3 Differentially Regulate Arrest from Flow and Chemotaxis in Mouse Neutrophils.* The Journal of Immunology, 2016. **196**(9): p. 3828-3833.

130. Hwang, I.-Y., et al., *An Essential Role for RGS Protein/Gαi2 Interactions in B Lymphocyte–Directed Cell Migration and Trafficking.* The Journal of Immunology, 2015. **194**(5): p. 2128-2139.

131. Cho, H., et al., *The Loss of RGS Protein-Gαi2 Interactions Results in Markedly Impaired Mouse Neutrophil Trafficking to Inflammatory Sites.* Molecular and Cellular Biology, 2012. **32**(22): p. 4561-4571.

132. Li, H., et al., *Association between Gαi2 and ELMO1/Dock180 connects chemokine signalling with Rac activation and metastasis.* Nature Communications, 2013. **4**(1): p. 1706.

133. Wang, Y., H. Li, and F. Li, *ELMO2 association with Gαi2 regulates pancreatic cancer cell chemotaxis and metastasis.* PeerJ, 2020. **8**: p. e8910.

134. Kamakura, S., et al., *The Cell Polarity Protein mInsc Regulates Neutrophil Chemotaxis via a Noncanonical G Protein Signaling Pathway.* Developmental Cell, 2013. **26**(3): p. 292-302.

135. Wang, D., et al. *A deep proteome and transcriptome abundance atlas of 29 healthy human tissues*. Molecular systems biology, 2019. **15**, e8503 DOI: 10.15252/msb.20188503.

136. Itoh, H., et al., *Presence of three distinct molecular species of Gi protein alpha subunit. Structure of rat cDNAs and human genomic DNAs.* Journal of Biological Chemistry, 1988. **263**(14): p. 6656-6664.

137. Peleg, S., et al., *Gαi Controls the Gating of the G Protein-Activated K+ Channel, GIRK.* Neuron, 2002. **33**(1): p. 87-99.

138. Mumby, S.M. and A.G. Gilman, *Synthetic peptide antisera with determined specificity for G protein alpha or beta subunits.* Methods Enzymol, 1991. **195**: p. 215-33.

139. McAlister, G.C., et al., *MultiNotch MS3 Enables Accurate, Sensitive, and Multiplexed Detection of Differential Expression across Cancer Cell Line Proteomes.* Analytical Chemistry, 2014. **86**(14): p. 7150-7158.

140. Masters, S.B., et al., *Mutations in the GTP-binding site of GSα alter stimulation of adenylyl cyclase.* Journal of Biological Chemistry, 1989. **264**(26): p. 15467-15474.

141. Graziano, M.P. and A.G. Gilman, *Synthesis in Escherichia coli of GTPase-deficient mutants of Gsα.* Journal of Biological Chemistry, 1989. **264**(26): p. 15475-15482.

142. Wong, Y.H., et al., *Mutant α subunits of Gi2 inhibit cyclic AMP accumulation.* Nature, 1991. **351**(6321): p. 63-65.

143. Dixon, A.S., et al., *NanoLuc Complementation Reporter Optimized for Accurate Measurement of Protein Interactions in Cells.* ACS Chemical Biology, 2016. **11**(2): p. 400-408.

144. Laschet, C., N. Dupuis, and J. Hanson, *A dynamic and screening-compatible nanoluciferase-based complementation assay enables profiling of individual GPCR–G protein interactions.* Journal of Biological Chemistry, 2019. **294**(11): p. 4079-4090.

145. Kim, D.I., et al., *An improved smaller biotin ligase for BioID proximity labeling.* Molecular Biology of the Cell, 2016. **27**(8): p. 1188-1196.

146. Chen, Z., et al., *Recognition of the activated states of Galpha13 by the rgRGS domain of PDZRhoGEF*. Structure, 2008. **16**(10): p. 1532-43.

147. Flock, T., et al., *Universal allosteric mechanism for Gα activation by GPCRs.* Nature, 2015. **524**(7564): p. 173-179.

148. Li, Q. and R.A. Cerione, *Communication between Switch II and Switch III of the Transducin α Subunit Is Essential for Target Activation.* Journal of Biological Chemistry, 1997. **272**(35): p. 21673-21676.

149. Pereira, R. and R.A. Cerione, *A Switch 3 Point Mutation in the α Subunit of Transducin Yields a Unique Dominant-negative Inhibitor.* Journal of Biological Chemistry, 2005. **280**(42): p. 35696-35703.

150. Wiege, K., et al., *Gαi2 Is the Essential Gαi Protein in Immune Complex–Induced Lung Disease.* The Journal of Immunology, 2013. **190**(1): p. 324-333.

151. Pero, R.S., et al., *Gαi2 -mediated signaling events in the endothelium are involved in controlling leukocyte extravasation.* Proceedings of the National Academy of Sciences, 2007. **104**(11): p. 4371-4376.

152. Li, Z.-W., et al., *GNAI1 and GNAI3 Reduce Colitis-Associated Tumorigenesis in Mice by Blocking IL6 Signaling and Down-regulating Expression of GNAI2.* Gastroenterology, 2019. **156**(8): p. 2297-2312.

153. Nobles, M., et al., *Differential effects of inhibitory G protein isoforms on G protein-gated inwardly rectifying K+ currents in adult murine atria.* American Journal of Physiology-Cell Physiology, 2018. **314**(5): p. C616-C626.

154. Jones, J.C., et al., *Differences in intradomain and interdomain motion confer distinct activation properties to structurally similar Gα proteins.* Proceedings of the National Academy of Sciences, 2012. **109**(19): p. 7275-7279.

155. Marin, E.P., et al., *The Function of Interdomain Interactions in Controlling Nucleotide Exchange Rates in Transducin.* Journal of Biological Chemistry, 2001. **276**(26): p. 23873-23880.

156. Toyama, Y., et al., *Dynamic regulation of GDP binding to G proteins revealed by magnetic field-dependent NMR relaxation analyses.* Nature Communications, 2017. **8**(1): p. 14523.

157. Tesmer, J.J.G., et al., *Crystal Structure of the Catalytic Domains of Adenylyl Cyclase in a Complex with Gsα-GTPγS.* Science, 1997. **278**(5345): p. 1907-1916.

158. Tesmer, V.M., et al., *Snapshot of Activated G Proteins at the Membrane: The Gαq-GRK2-Gβγ Complex.* Science, 2005. **310**(5754): p. 1686-1690.

159. Lyon, A.M., et al., *Full-length Gαq–phospholipase C-β3 structure reveals interfaces of the C-terminal coiled-coil domain.* Nature Structural & Molecular Biology, 2013. **20**(3): p. 355-362.

160. Hajicek, N., et al., *Identification of critical residues in G(alpha)13 for stimulation of p115RhoGEF activity and the structure of the G(alpha)13-p115RhoGEF regulator of G protein signaling homology (RH) domain complex.* J Biol Chem, 2011. **286**(23): p. 20625-36.

161. Slep, K.C., et al., *Structural determinants for regulation of phosphodiesterase by a G protein at 2.0 Å.* Nature, 2001. **409**(6823): p. 1071-1077.

162. Pero, R.S., et al., *Gα_{i2}-mediated signaling events in the endothelium are involved in controlling leukocyte extravasation.* Proceedings of the National Academy of Sciences, 2007. **104**(11): p. 4371-4376.

163. Zhang, Q., A. Dickson, and C.A. Doupnik, *Gβγ-activated Inwardly Rectifying K+ (GIRK) Channel Activation Kinetics via Gαi and Gαo-coupled Receptors Are Determined by Gα-specific Interdomain Interactions That Affect GDP Release Rates.* Journal of Biological Chemistry, 2004. **279**(28): p. 29787-29796.

164. Wells, C.D., et al., *Mechanisms for Reversible Regulation between G13 and Rho Exchange Factors.* Journal of Biological Chemistry, 2002. **277**(2): p. 1174-1181.

165. Jackson, M., et al., *Modulation of the neuronal glutamate transporter EAAT4 by two interacting proteins.* Nature, 2001. **410**(6824): p. 89-93.

166. Chen, Z., et al., *Structure of the p115RhoGEF rgRGS domain–Gα13/i1 chimera complex suggests convergent evolution of a GTPase activator.* Nature Structural & Molecular Biology, 2005. **12**(2): p. 191-197.

167. Day, P.W., et al., *Differential Interaction of GRK2 with Members of the Gαq Family.* Biochemistry, 2003. **42**(30): p. 9176-9184.

168. Day, P.W., et al., *Characterization of the GRK2 Binding Site of Gαq.* Journal of Biological Chemistry, 2004. **279**(51): p. 53643-53652.

169. Liu, W. and J.K. Northup, *The helical domain of a G protein α subunit is a regulator of its effector.* Proceedings of the National Academy of Sciences, 1998. **95**(22): p. 12878-12883.

170. Fisher, I.J., et al., *Activation of Phospholipase C β by Gβγ and Gαq Involves C-Terminal Rearrangement to Release Autoinhibition.* Structure, 2020. **28**(7): p. 810-819.e5.

171. Kant, R., et al., *Ric-8A, a G protein chaperone with nucleotide exchange activity induces long-range secondary structure changes in Gα.* eLife, 2016. **5**.

172. Zhang, X., et al., *Evolving cryo-EM structural approaches for GPCR drug discovery.* Structure, 2021. **29**(9): p. 963-974.e6.

173. García-Nafría, J. and C.G. Tate, *Structure determination of GPCRs: cryo-EM compared with X-ray crystallography.* Biochemical Society Transactions, 2021. **49**(5): p. 2345-2355.

174. Brecht, M., et al., *The use of surface plasmon resonance (SPR) and fluorescence resonance energy transfer (FRET) to monitor the interaction of the plant G-proteins Ms-Rac1 and Ms-Rac4 with GTP.* Journal of Biotechnology, 2004. **112**(1): p. 151-164.

175. Bandekar, S.J., et al., *Structural/functional studies of Trio provide insights into its configuration and show that conserved linker elements enhance its activity for Rac1.* Journal of Biological Chemistry, 2022. **298**(8): p. 102209.

176. Kehrl, J.H., *The impact of RGS and other G-protein regulatory proteins on Gαi-mediated signaling in immunity.* Biochemical Pharmacology, 2016. **114**: p. 40-52.

177. Dai, S.A., et al., *State-selective modulation of heterotrimeric Gαs signaling with macrocyclic peptides.* Cell, 2022. **185**(21): p. 3950-3965.e25.

178. Schrage, R., et al., *The experimental power of FR900359 to study Gq-regulated biological processes.* Nature Communications, 2015. **6**(1): p. 10156.

179. Fujioka, M., et al., *Structure of FR900359, a cyclic depsipeptide from Ardisia crenata sims.* The Journal of Organic Chemistry, 1988. **53**(12): p. 2820-2825.

180. Taniguchi, M., et al., *Antithrombotic and thrombolytic efficacy of YM-254890, a Gq/11 inhibitor, in a rat model of arterial thrombosis.* Thrombosis and Haemostasis, 2003. **90**(09): p. 406-413.

181. Takasaki, J., et al., *A Novel Gαq/11-selective Inhibitor.* Journal of Biological Chemistry, 2004. **279**(46): p. 47438-47445.

182. Katada, T. and M. Ui, *Slow interaction of islet-activating protein with pancreatic islets during primary culture to cause reversal of alpha-adrenergic inhibition of insulin secretion.* Journal of Biological Chemistry, 1980. **255**(20): p. 9580-8.

183. West, R.E., Jr., et al., *Pertussis toxin-catalyzed ADP-ribosylation of transducin. Cysteine 347 is the ADP-ribose acceptor site.* J Biol Chem, 1985. **260**(27): p. 14428-30.

184. Scott, J.K., et al., *Evidence that a protein-protein interaction 'hot spot' on heterotrimeric G protein βγ subunits is used for recognition of a subclass of effectors.* The EMBO Journal, 2001. **20**(4): p. 767-776.

185. Davis, T.L., et al., *Structural and molecular characterization of a preferred protein interaction surface on G protein beta gamma subunits.* Biochemistry, 2005. **44**(31): p. 10593-604.

186. Mathews, J.L., A.V. Smrcka, and J.M. Bidlack, *A Novel Gβγ-Subunit Inhibitor Selectively Modulates μ-Opioid-Dependent Antinociception and Attenuates Acute Morphine-Induced Antinociceptive Tolerance and Dependence.* The Journal of Neuroscience, 2008. **28**(47): p. 12183-12189.

187. Mathews, J.L., A.V. Smrcka, and J.M. Bidlack, *A novel Gbetagamma-subunit inhibitor selectively modulates mu-opioid-dependent antinociception and attenuates acute morphine-induced antinociceptive tolerance and dependence.* The Journal of neuroscience : the official journal of the Society for Neuroscience, 2008. **28**(47): p. 12183-12189.

188. Seneviratne, A.M., et al., *Direct-reversible binding of small molecules to G protein betagamma subunits.* Biochim Biophys Acta, 2011. **1814**(9): p. 1210-8.

189. Smrcka, A.V., *Molecular targeting of Gα and Gβγ subunits: a potential approach for cancer therapeutics.* Trends in Pharmacological Sciences, 2013. **34**(5): p. 290-298.

190. Nishimura, A., et al., *Structural basis for the specific inhibition of heterotrimeric Gq protein by a small molecule.* Proceedings of the National Academy of Sciences, 2010. **107**(31): p. 13666-13671.